

Ligand-controlled and nanoconfinement-boosted luminescence employing Pt(II) and Pd(II) complexes: From color-tunable aggregation-enhanced dual emitters towards self-referenced oxygen reporters

Iván Maisuls^{a,b,†}, Cui Wang^{c,d,†}, Matias E. Gutierrez Suburu^{a,b}, Sebastian Wilde^{a,b}, Constantin-Gabriel Daniliuc^e, Dana Brünink^f, Nikos L. Doltsinis^f, Stefan Ostendorp^g, Gerhard Wilde^g, Jutta Kösters^b, Ute Resch-Genger^{c*} and Cristian A. Strassert^{a,b*}

^a Institut für Anorganische und Analytische Chemie, Westfälische Wilhelms-Universität Münster, Corrensstraße 28/30, D-48149 Münster, Germany.

^b CeNTech, CiMIC, SoN, Westfälische Wilhelms-Universität Münster, Heisenbergstraße 11, D-48149 Münster, Germany. ca.s@wwu.de

^c Division Biophotonics, Federal Institute for Materials Research and Testing (BAM), Richard-Willstaetter-Straße 11, 12489 Berlin, Germany

^d Institute of Chemistry and Biochemistry, Freie Universität Berlin, Arnimallee 22, 14195 Berlin, Germany

^e Organisch-Chemisches Institut, Westfälische Wilhelms-Universität Münster, Corrensstraße 40, D-48149 Münster, Germany

^f Institut für Festkörpertheorie and Center for Multiscale Theory and Computation, Westfälische Wilhelms-Universität Münster, Wilhelm-Klemm-Straße 10, D-48149 Münster, Germany

^g Institut für Materialphysik and CeNTech, Westfälische Wilhelms-Universität Münster, Wilhelm-Klemm-Straße 10, D-48149 Münster, Germany

[†]These authors contributed equally to this work

Table of contents

| | |
|--|-----------|
| Section S1: Materials and methods | 3 |
| S1.1 Single crystal X-ray diffractometry | 3 |
| S1.2 Photophysical characterization of the complexes | 3 |
| S1.3 Structural characterization of the nanoparticles | 4 |
| S1.4 Photophysical characterization of the nanoparticles and oxygen sensing | 4 |
| Section S2: Synthesis and characterization of PtLH, PtLF, PdLH and PdLF | 6 |
| Section S3: X-ray diffractometric analysis of PtLH, PtLF, PdLH and PdLF | 27 |
| Section S4: Photophysical characterization of PtLH, PtLF, PdLH and PdLF | 41 |
| Section S5: Quantum chemistry of PtLH, PtLF, PdLH and PdLF | 49 |
| Section S6: Synthesis and characterization of the loaded nanoparticles | 56 |
| S6.1 Preparation of the Pt(II)- and Pd(II)-complex loaded nanoparticles | 56 |
| S6.2 Surface and structural characterization of the nanoparticles | 57 |
| S6.3 Leaking experiments | 62 |
| S6.4 Determination of the loading with PtLF | 62 |
| S6.5 Photophysical studies of nanoparticles loaded with the complexes | 63 |
| S6.6 Stern-Volmer studies of PSNPs loaded with the complexes | 69 |
| References | 71 |

Section S1: Materials and methods

All reagents were analytical grade and used as received. Column chromatography was performed with silica gel 60 (particle size 35-70 μm , 230-400 mesh, Merck). NMR and mass spectra were measured by the Department of Organic Chemistry, University of Münster. NMR spectra were recorded on an DPX/Avance 300 or an Avance 400 from Bruker Analytische Messtechnik for the precursor and on an DD2 500 and DD2 600 from Agilent for the Pt(II) complexes. The ^1H -NMR and ^{13}C -NMR chemical shifts (δ) of the signals are given in parts per million and referenced to residual protons in the deuterated solvent: DMSO- d_6 (2.50 ppm and 39.5 ppm). The ^{19}F NMR chemical shifts are referenced to CFCl_3 as an internal standard. The signal multiplicities are abbreviated as follows: s, singlet; d, doublet; t, triplet; q, quartet; m, multiplet. All coupling constants (J) are given in Hertz. Exact mass (EM) determination by mass spectrometry (MS) was carried out at the Organisch-Chemisches Institut in Münster (WWU) using a LTQ Orbitap LTQ XL (Thermo-Fisher Scientific, Bremen) with electron spray injection (ESI).

S1.1 Single crystal X-ray diffractometry

Data sets for compound **PdLF** were collected on Bruker Quazar diffractometer with MoK_α radiation. The collection method involved ω scans. Data reduction was carried out using the program SAINT^{+1,2}. The crystal structures were solved by Direct Methods using SHELXTL^{3,4}. Non-hydrogen atoms were first refined isotropically followed by anisotropic refinement by full matrix least-squares calculation based on F2 using SHELXTL. Hydrogen atoms were positioned geometrically and allowed to ride on their respective parent atoms. Data sets for compounds **PtLH**, **PtLF** and **PdLH** were collected with graphite-monochromated Mo $\text{K}\alpha$ radiation ($\lambda = 0.71073 \text{ \AA}$) on a Bruker Quazar diffractometer. The structures solved by Direct Methods and refined by full-matrix least squares on F2 by using the programs SHELXTL and SHELX197.

S1.2 Photophysical characterization of the complexes

Absorption spectra were measured on a Varian Cary 100 double-beam UV-Vis-NIR spectrometer and baseline-corrected. Steady-state excitation and emission spectra were recorded on a FluoTime 300 spectrometer from PicoQuant equipped with a 300 W ozone-free Xe lamp (250 - 900 nm), a 10 W Xe flash-lamp (250-900 nm, pulse width $< 10 \mu\text{s}$) with repetition rates of 0.1 - 300 Hz, an excitation monochromator (Czerny-Turner 2.7 nm/mm dispersion, 1200 grooves/mm, blazed at 300 nm), diode lasers (pulse width $< 80 \text{ ps}$) operated by a computer-controlled laser driver PDL-820 (repetition rate up to 80 MHz, burst mode for slow and weak decays), two emission monochromators (Czerny-Turner, selectable gratings blazed at 500 nm with 2.7 nm/mm dispersion and 1200 grooves/mm, or blazed at 1250 nm with 5.4 nm/mm dispersion and 600 grooves/mm), Glan-Thompson polarizers for excitation (Xe-lamps) and emission, a

Peltier-thermostated sample holder from Quantum Northwest (-40 °C – 105 °C), and two detectors, namely a PMA Hybrid 40 (transit time spread FWHM < 120 ps, 300 – 720 nm) and a R5509-42 NIR-photomultiplier tube (transit time spread FWHM 1.5 ns, 300-1400 nm) with external cooling (-80 °C) from Hamamatsu. Steady-state and fluorescence lifetimes were recorded in TCSPC mode by a PicoHarp 300 (minimum base resolution 4 ps). Emission and excitation spectra were corrected for source intensity (lamp and grating) by standard correction curves. Lifetime analysis was performed using the commercial FluoFit software. The quality of the fit was assessed by minimizing the reduced chi squared function (χ^2) and visual inspection of the weighted residuals and their autocorrelation. Luminescence quantum yields were measured with a Hamamatsu Photonics absolute PL quantum yield measurement system (C9920-02) equipped with a L9799-01 CW Xenon light source (150 W), monochromator, C7473 photonic multi-channel analyzer, integrating sphere and employing U6039-05 PLQY measurement software (Hamamatsu Photonics, Ltd., Shizuoka, Japan). All solvents used were of spectrometric grade (Uvasol®). Phosphorescence Lifetime Imaging Microscopy (PLIM) Measurements and photoluminescence images were acquired using a time-resolved confocal Fluorescence Microscopy (MicroTime 200, Picoquant®), using as excitation source a $\lambda = 375$ nm laser (for PLIM) and a Xe lamp with BP360-370 and BA520IF filters (fluorescence images). Single Photon Avalanche Diodes (SPAD) were used as detectors. A TimeHarp 260 (PicoQuant) was used as Time-Correlated Single Photon Counting (TCSPC). Sepia II® software was used for data acquisition. Phosphorescence lifetimes were recorded by a NanoHarp 250 (minimum base resolution 32 ns) in Multi-Channel Scaling MCS mode

S1.3 Structural characterization of the nanoparticles

TEM experiments were performed using a Thermo Fisher Scientific (previously FEI) Themis G3 60-300 transmission electron microscope (TEM) equipped with a high-brightness field emission gun (XFEG), a monochromator, an image Cs-corrector, a quadrupole energy-dispersive X-ray (EDX) system (Super-X EDX detector), a high-angle annular dark-field (HAADF) detector (Fischione Model 3000), and a fast CMOS camera (Ceta, 4k × 4k). For the measurements, the microscope was operated at an acceleration voltage of either 60 or 300 kV. The size distribution of the PS nanoparticles (1 mg/mL dispersed in H₂O) were determined by dynamic light scattering (DLS) with a Zetasizer Nano ZS from Malvern Panalytical.

S1.4 Photophysical characterization of the nanoparticles and oxygen sensing

Absorption spectra of the metal complexes and of stained PS dispersions were obtained with a calibrated Cary 5000 spectrometer from Agilent. The amount of encapsulated metal complex was obtained from the absorption spectra of stained particle samples disrupted in DMF employing the species' molar absorption coefficients (which were previously determined by absorption measurements of concentration series of the emitters, with DMF containing dissolved PS nanoparticles as the solvent, see Section S6.4, Figure S92 and

Table S14). Luminescence spectra and decay kinetics were measured with the calibrated spectrofluorometers FSP 920 and FLS 920 from Edinburgh Instruments. For the measurement of the emission spectra, a continuous xenon lamp was applied as excitation light source on FSP 920 and FLS 920, while the time-resolved luminescence measurements were completed with a μs xenon flashlamp on FSP 920 and an EPLED laser (375 nm) on FLS 920 with both detectors in a multi-channel scaling mode. The luminescence decays were analysed by fitting the obtained decay curves exponentially with the program FAST (Fluorescence Analysis Software Technology, Edinburgh Instruments Ltd.). Absolute luminescence quantum yields were obtained with the commercial integrating sphere setup Quantaury-QY C11347-11 from Hamamatsu and special long neck cuvettes from the instrument manufacturer (1x1 cm, quartz). The standard deviations of luminescence quantum yield measurements were estimated to be $\pm 2\%$. All luminescence measurements were performed in these long neck quartz cuvettes with precision seal rubber septa (Sigma-Aldrich) at room temperature, if not otherwise stated. The oxygen concentration was varied for Stern-Volmer studies by purging the stained PS nanoparticle dispersion with Ar in a sealed long neck cuvette. The oxygen partial pressure was determined with a commercial fiber-optic oxygen meter Firesting O₂ from PyroScience and a solvent-resistant oxygen probe tip (OXSOVPT).

Section S2: Synthesis and characterization of PtLH, PtLF, PdLH and PtLF

Synthesis of N,N-di(2-bromopyrid-6-yl)-4-methoxyaniline (1): 2,6-Dibromopyridine (4.930 g, 20.8 mmol), Pd₂(dba)₃ (0.154 g, 0.168 mmol), 4-methoxyaniline (1.064 g, 8.62 mmol) and NaOtBu (2.323 g, 23.20 mmol), 1,1'-bis(diphenylphosphino)ferrocene (0.196 g, 0.354 mmol) were combined in toluene (100 mL) under Ar atmosphere. The reaction mixture was degassed during the heating process and reacted at 110°C for 12 - 14 h to yield a dark brown solution. Once at room temperature, the solution was filtered and poured into water (100 mL), the residue was washed with ethyl acetate (EtOAc). The aqueous phase was extracted with EtOAc (3 times 50 mL). The combined organic phases were washed with water (25 mL) and brine (25 mL), dried with MgSO₄, filtered, concentrated and the crude compound was adsorbed onto silica gel. This was loaded onto a column packed with silica gel to perform a column chromatography separation with cyclohexane/EtOAc (9:1) to yield a yellow solid (1.269 g). Yield: 34 %.

¹H NMR (300 MHz, DCM-d₂): δ = 7.41 (dd, *J* = 8.2, 7.6 Hz, 2H), 7.16 – 7.12 (m, 2H), 7.10 (dd, *J* = 7.6, 0.7 Hz, 2H), 7.01 – 6.92 (m, 4H), 3.84 (s, 3H).

¹³C NMR (75 MHz, Methylene Chloride-*d*₂): δ = 159.0, 157.8, 140.1, 139.9, 136.5, 130.0, 122.2, 115.6, 115.1, 56.0.

HRMS (ESI+, MeOH, *m/z*): calcd. for [M + H]⁺ 435.94777, found 435.94785; calcd. for [M + Na]⁺ 457.92971, found 457.92979; calcd. for [M + K]⁺ 473.90365, found 473.90340.

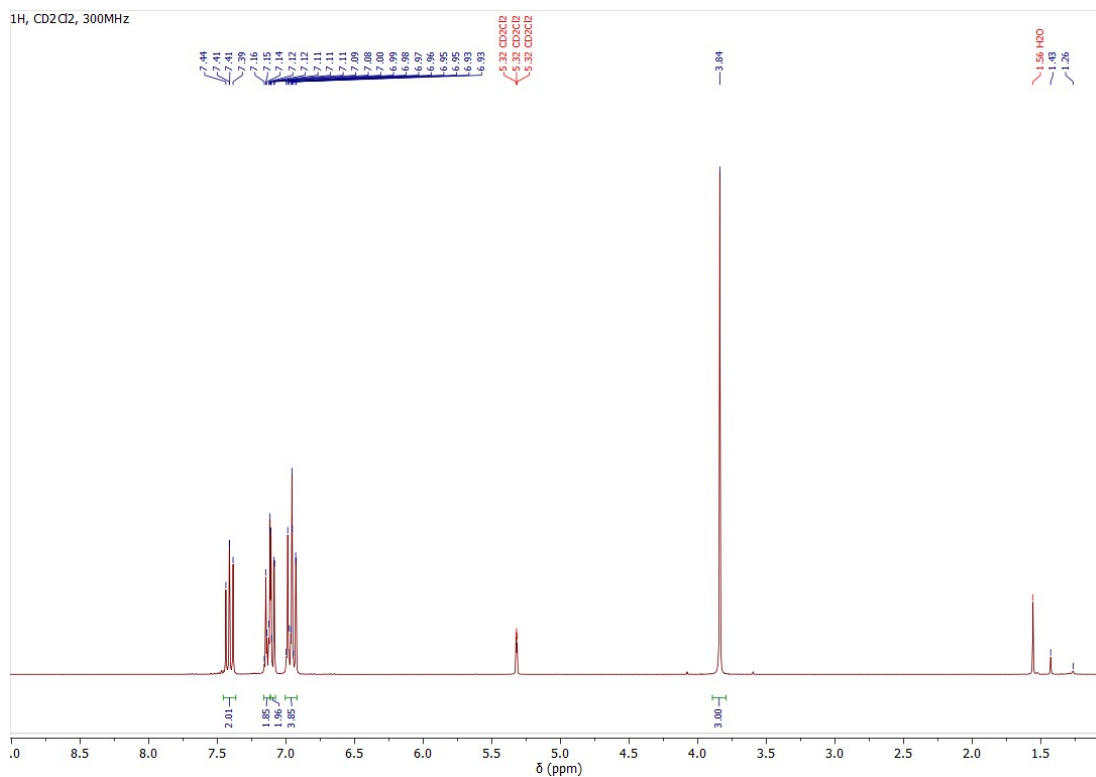


Figure S1. ¹H-NMR spectrum (300 MHz, DCM-d₂) of **1**.

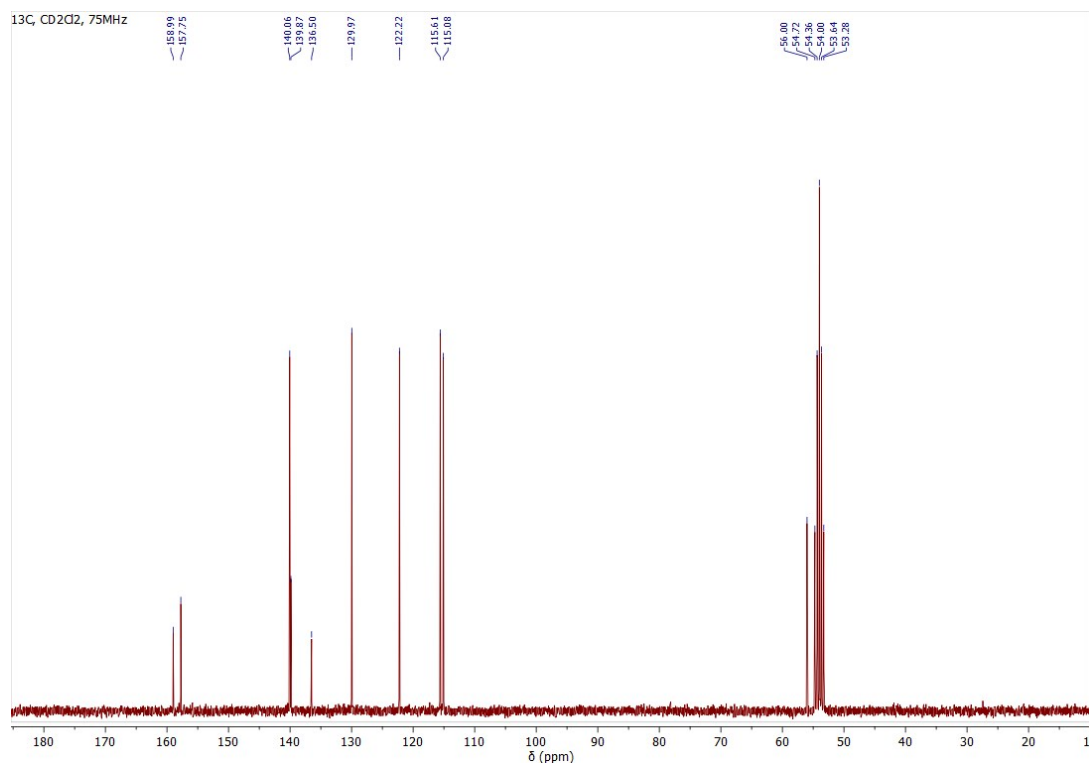


Figure S2. ^{13}C - $\{^1\text{H}\}$ -NMR spectrum (75 MHz, DCM-d_2) of **1**.

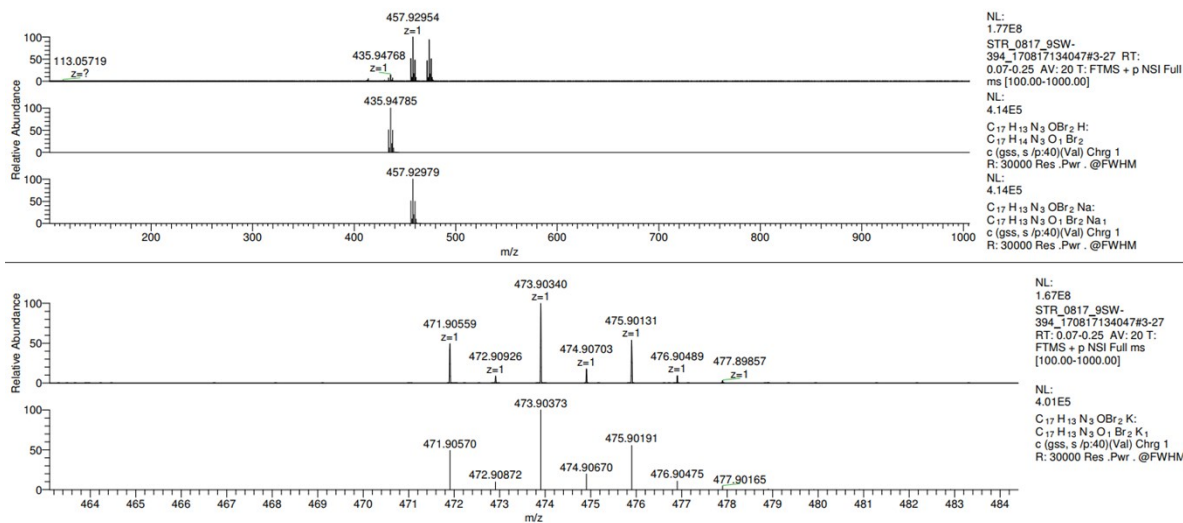


Figure S3. ESI-MS (MeOH) of **1**.

Synthesis of N,N-di(2-phenylpyrid-6-yl)-3,5-dimethoxyaniline (LH): 1 (323 mg, 0.74 mmol), $\text{Pd}(\text{PPh}_3)_4$ (109 mg, 0.0094 mmol) and the corresponding phenylboronic acid (236 mg, 1.94 mmol) were combined in THF (50 mL) and degassed by bubbling with Ar. The solution was heated up to reflux and aqueous K_2CO_3 (2M, 3 ml) were added under Ar flux. The reaction mixture was refluxed for 12 h to yield a yellow solution. Afterwards, THF was removed under reduced pressure and the precipitate was dissolved in EtOAc (50 ml)

and the solution washed with water (50 ml) and brine (50 ml). The organic phase was dried with MgSO_4 , filtered, concentrated and the crude compound was adsorbed onto silica gel. This was loaded onto a column packed with silica gel to perform a column chromatographic separation with cyclohexane/EtOAc as eluent (20:1) to yield a white solid (238 mg). Yield: 75 %.

^1H NMR (400 MHz, Methylene Chloride- d_2): δ = 7.81 – 7.75 (m, 4H), 7.55 (dd, J = 8.2, 7.6 Hz, 2H), 7.33 – 7.22 (m, 8H), 7.19 – 7.15 (m, 2H), 6.96 (dd, J = 8.3, 0.7 Hz, 2H), 6.93 – 6.88 (m, 2H), 3.76 (s, 3H).

HRMS (ESI+, MeOH, m/z): calcd. for $[\text{M} + \text{H}]^+$ 430.19139, found, 430.19108; calcd. for $[\text{M} + \text{Na}]^+$ 452.172, found, 452.17290; calcd. for $[2\text{M} + \text{Na}]^+$ 881.35745, found, 881.35786.

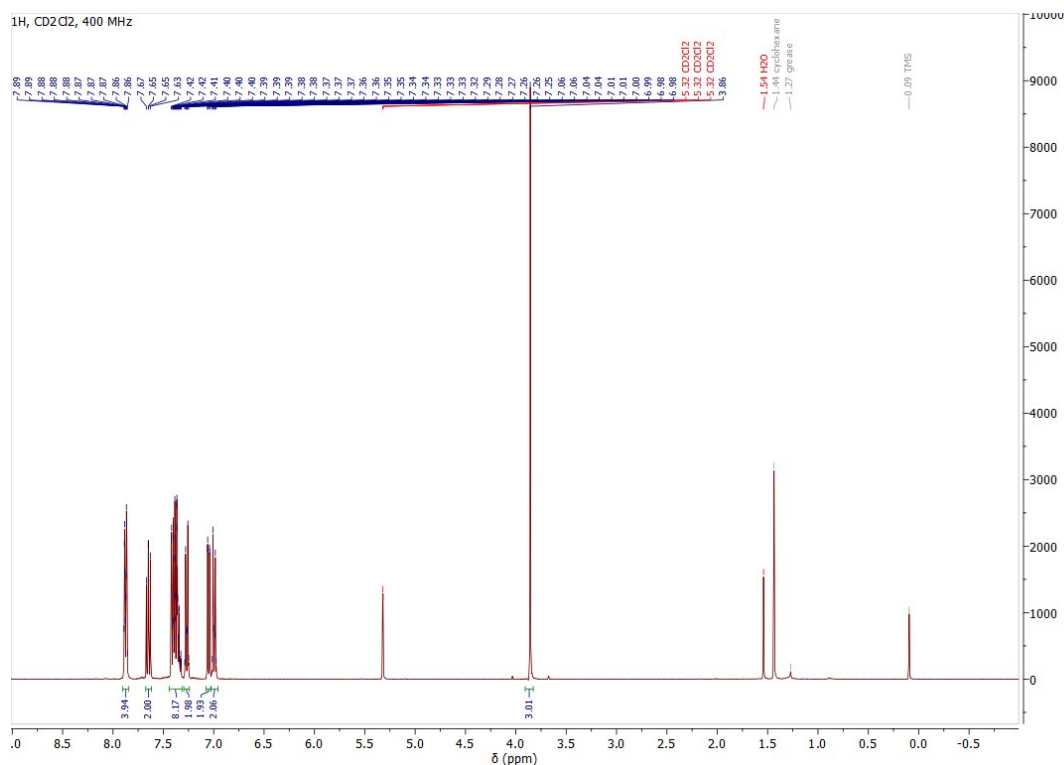


Figure S4. ^1H -NMR spectrum (400 MHz, DCM-d_2) of LH.

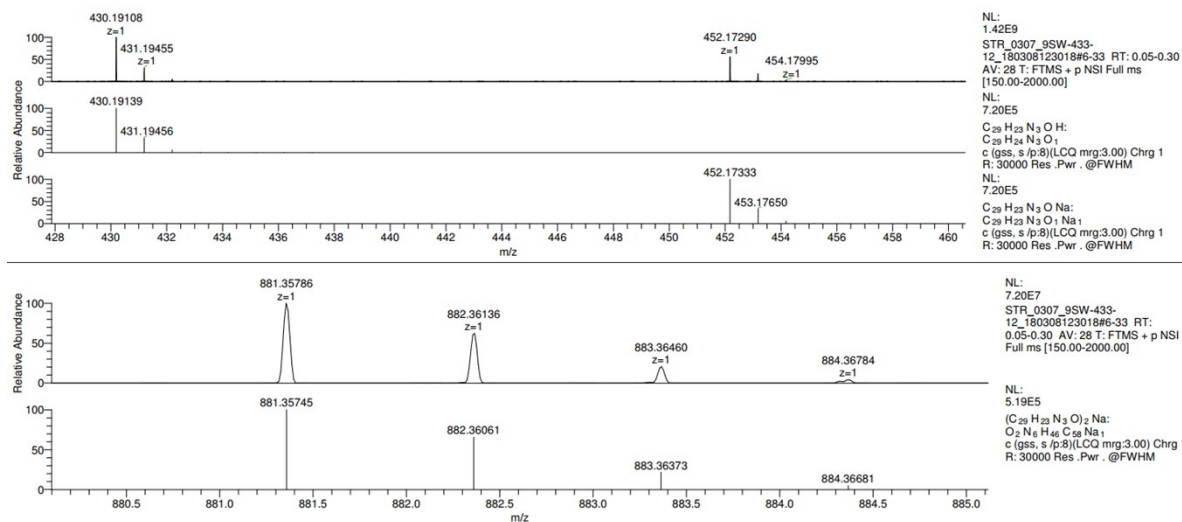


Figure S5. ESI-MS (MeOH) of **LH**.

Synthesis of N,N-di(2-(2,4-difluorophenyl)pyrid-6-yl)-4-methoxyaniline (LF): The same procedure described for **LH** was adapted. Column chromatography was performed on silica with cyclohexane/ethyl acetate (100:1) as an eluent, yielding a yellow solid. Yield: 84 %.

¹H NMR (300 MHz, DMSO-d₆): δ = 7.74 – 7.64 (m, 2H), 7.56 (t, *J* = 7.9 Hz, 2H), 7.34 (ddd, *J* = 7.6, 2.4, 0.8 Hz, 2H), 7.18 – 7.11 (m, 2H), 6.97 – 6.87 (m, 3H), 6.86 – 6.76 (m, 3H), 3.76 (s, 3H).

¹⁹F NMR (282 MHz, DMSO-d₆): δ = 113.46 (d, *J* = 8.3 Hz), -115.08 (d, *J* = 8.5 Hz).

HRMS (ESI+, MeOH, m/z): calcd. for [M + H]⁺ 502.15370, found 502.15392; calcd. for [M + Na]⁺ 524.13565, found 524.13546.

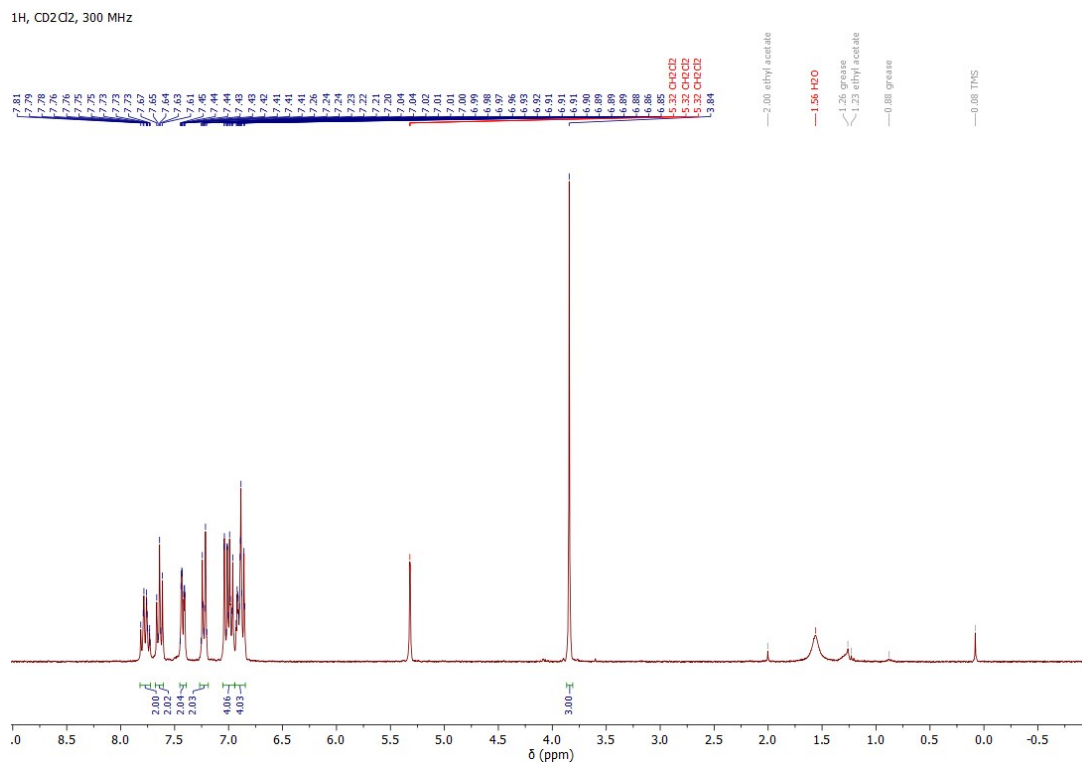


Figure S6. ¹H-NMR spectrum (300 MHz, DCM-d₂) of LF.

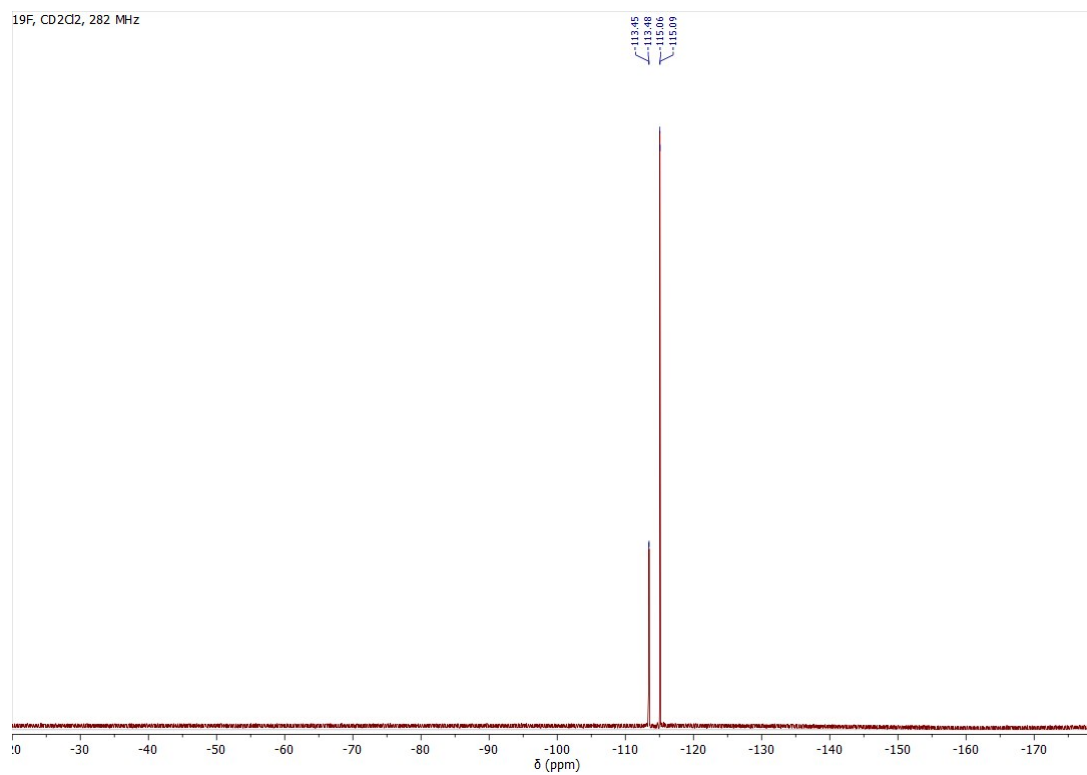


Figure S7. ¹⁹F-¹H-NMR (282 MHz, DCM-d₂) of LF.

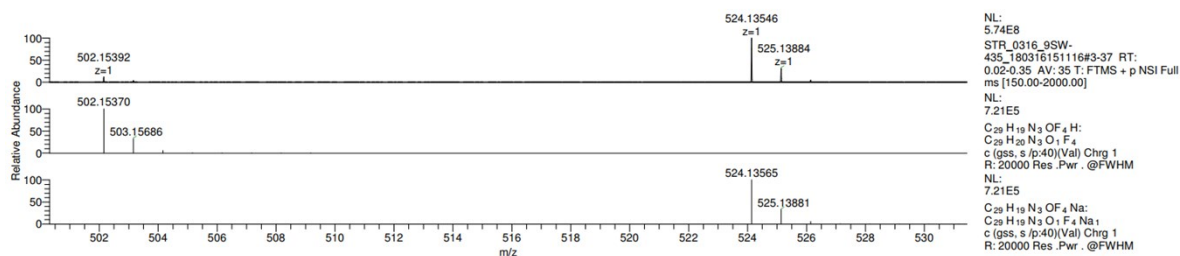


Figure S8. ESI-MS (MeOH) of LF.

Synthesis of PtLH: A mixture of the tetradentate ligand precursor **LH** (100 mg, 0.233 mmol), K_2PtCl_4 (106 mg, 0.256 mmol) and NBu_4Cl (10 mg, 0.034 mmol) were refluxed in glacial acetic acid (15 mL) for 48–60 h. After cooling down the orange solution to room temperature, the solvent was removed to a minimum, red-orange precipitates were formed which were filtered off and washed several times with water to give the complex **PtLH**. This was loaded onto a column packed with silica gel to perform a column chromatography separation with DCM as eluent to yield yellow solid (84 mg) Yield: 58 %.

1H NMR (600 MHz, $DMSO-d_6$): δ = 8.20 (d, J = 7.0 Hz, 2H), 8.02 (dd, J = 8.7, 7.6 Hz, 2H), 7.96 (dd, J = 8.0, 1.4 Hz, 2H), 7.96 (d, J = 6.6 Hz, 2H), 7.92 (d, J = 7.3 Hz, 1H), 7.56 (m, 2H), 7.36 (td, J = 7.3, 1.4 Hz, 2H), 7.32 (m, 2H), 7.17 (td, J = 7.5, 1.2 Hz, 2H), 6.62 (dd, J = 8.7, 0.9 Hz, 2H), 3.92 (s, 3H).

^{13}C NMR (150 MHz, $DMSO-d_6$): δ = 163.2, 160.6 – 159.3 (m), 149.6, 149.0, 147.4, 138.3, 135.8, 131.8, 129.3, 124.9 – 123.9 (m), 123.4, 117.2, 114.8, 56.1.

HRMS (ESI+, MeOH, m/z) calcd. for $[M + H]^+$ 623.14077, found 623.14122.

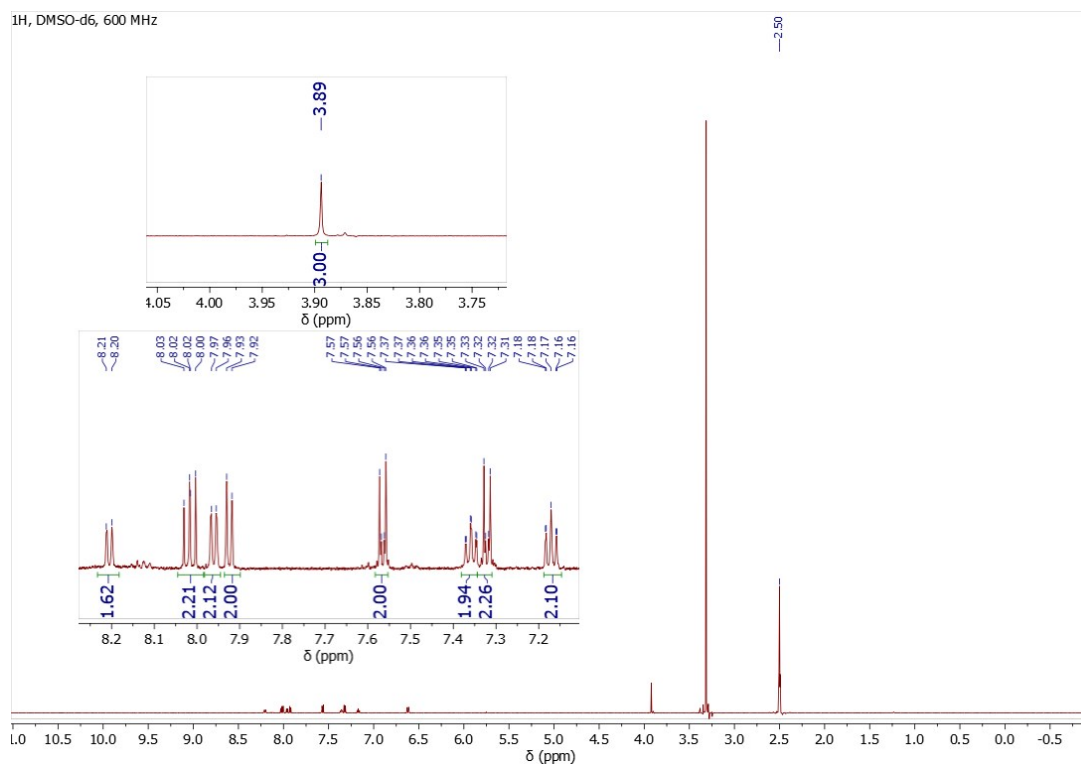


Figure S9. ¹H-NMR spectrum (600 MHz, DMSO-d₆) of PtLH.

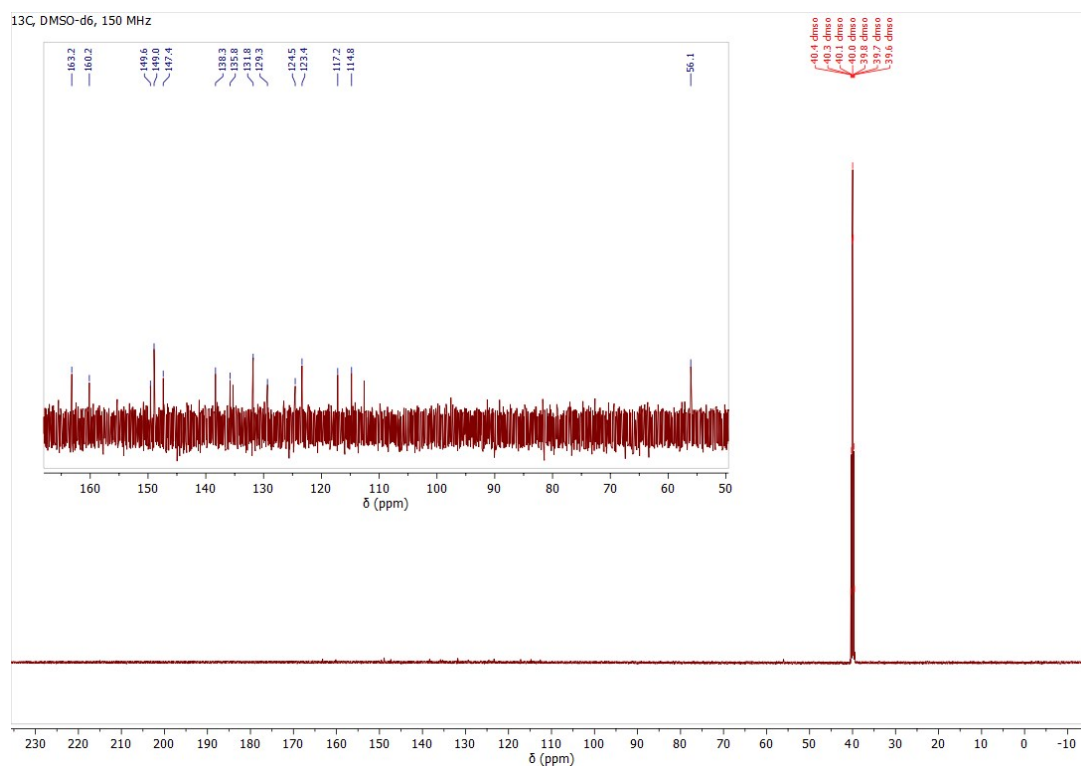


Figure S10. ¹³C-¹H-NMR spectrum (150 MHz, DMSO-d₆) of PtLH.

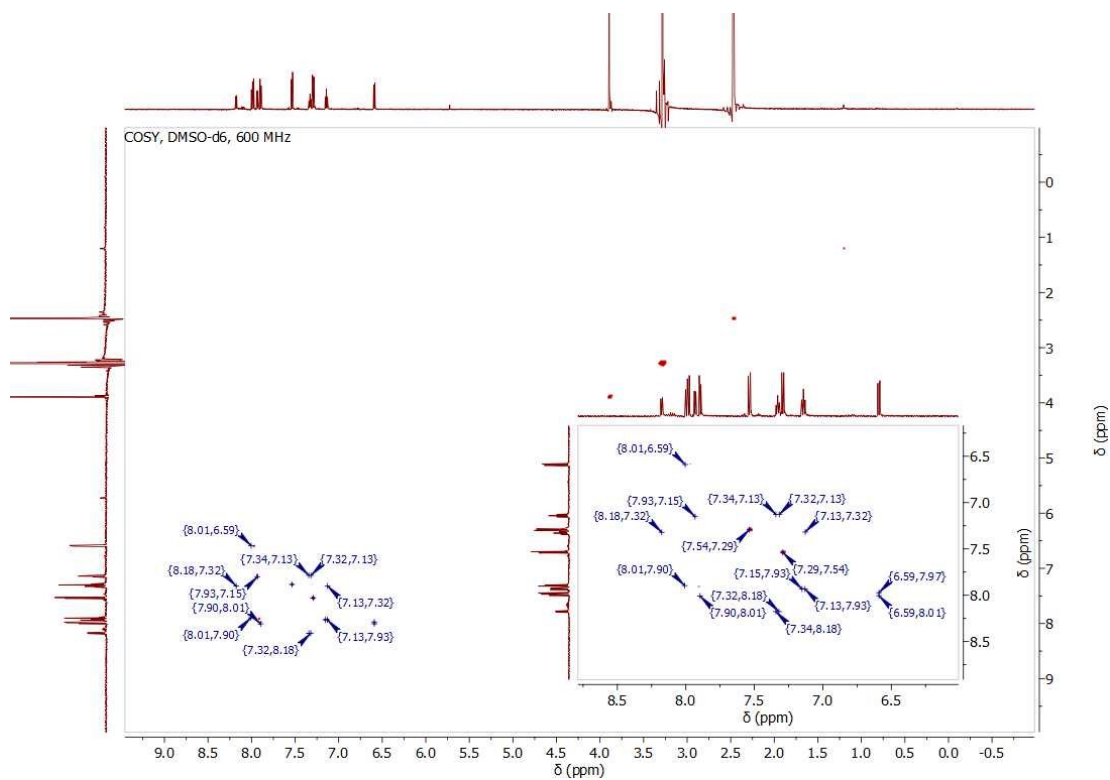


Figure S11. $^1\text{H}/^1\text{H}$ -COSY-NMR spectrum (600 MHz/600 MHz, DMSO-d₆) of PtLH.

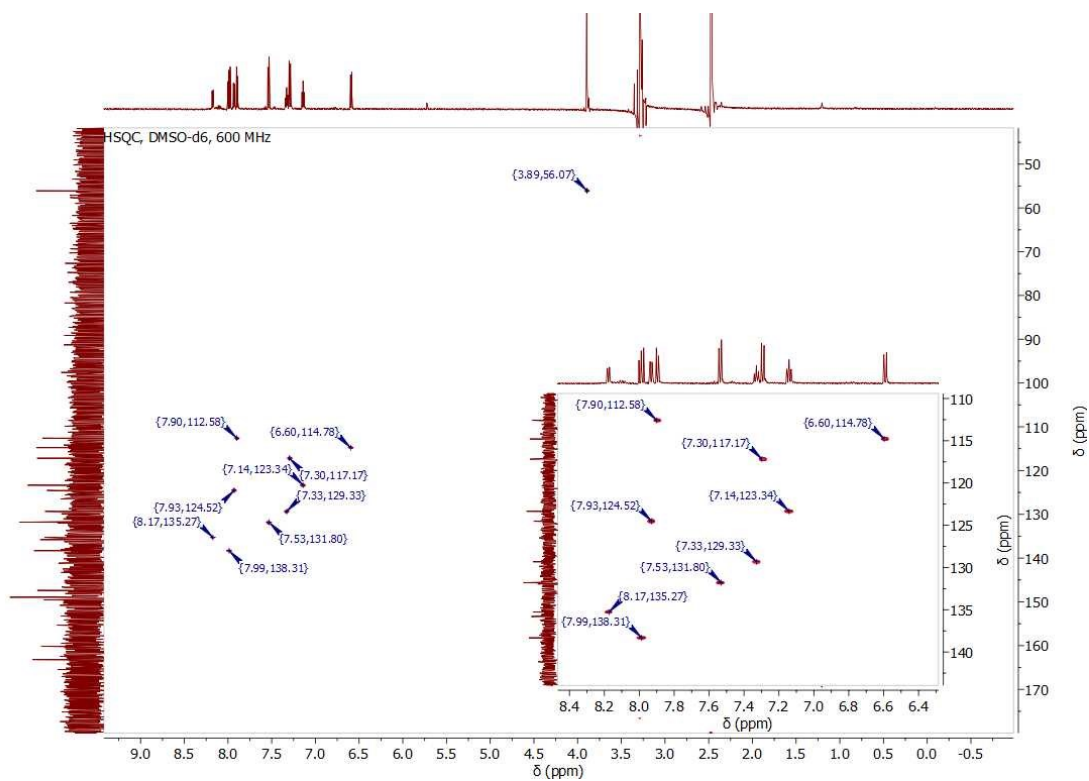


Figure S12. $^1\text{H}/^{13}\text{C}$ -gHSQC-NMR spectrum (600 MHz/150 MHz, DMSO-d₆) of PtLH.

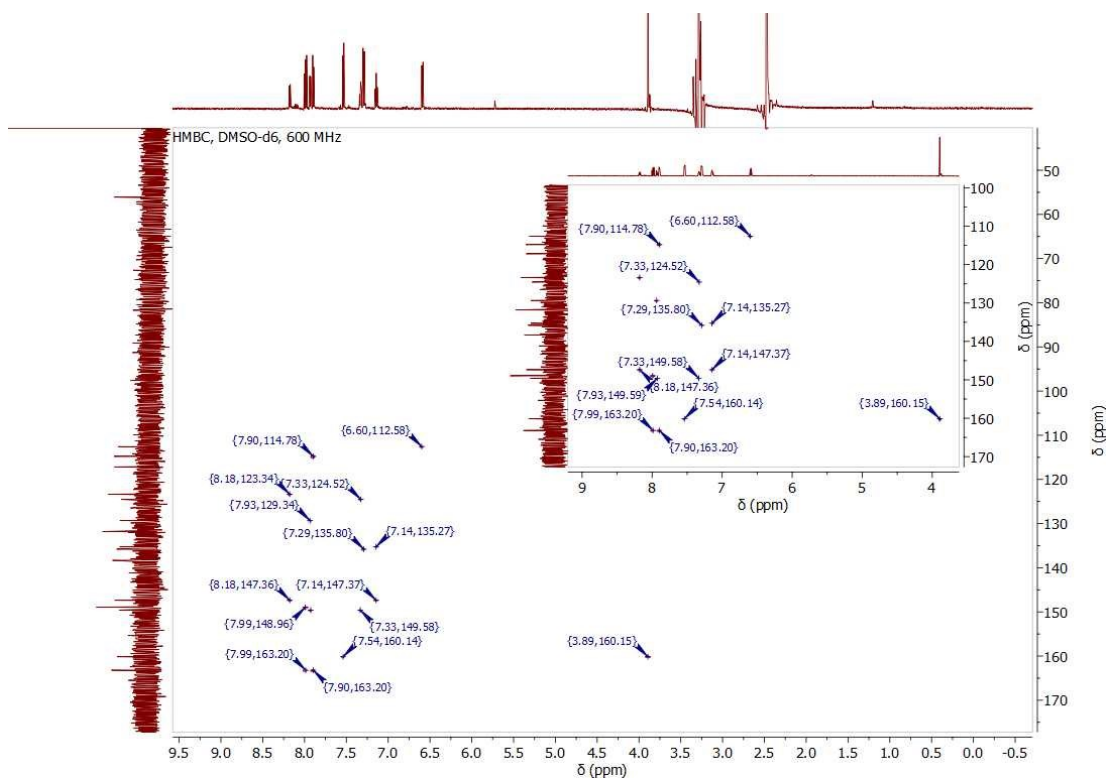


Figure S13. $^1\text{H}/^{13}\text{C}$ -gHMBC-NMR spectrum (600 MHz/150 MHz, $\text{DMSO}-d_6$) of **PtLH**.

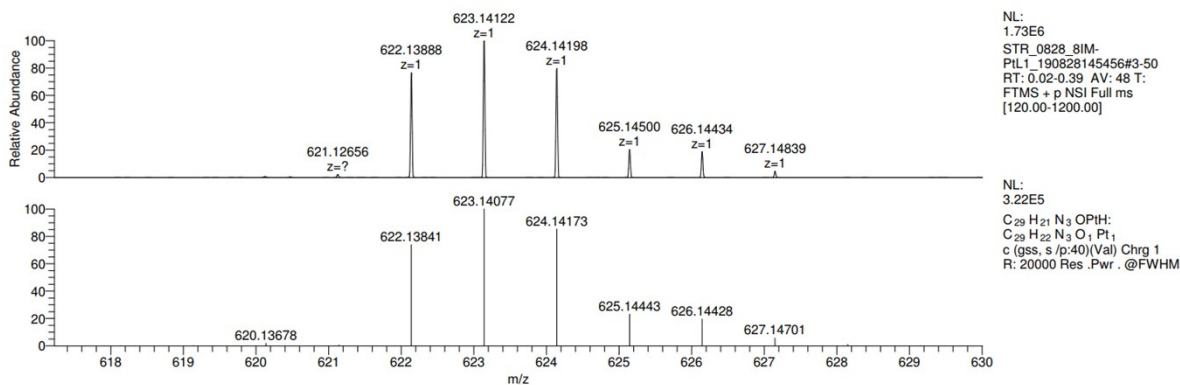


Figure S14. ESI+MS (MeOH) of **PtLH**.

Synthesis of PtLF: The same procedure described for **PtLH** was adapted. Column chromatography was performed on silica with DCM as eluent yielding a yellow-orange solid. Yield: 55 %.

^1H NMR (500 MHz, $\text{DMSO}-d_6$): δ = 8.07 (dd, J = 8.8, 7.7 Hz, 2H), 7.97 (dt, J = 7.9, 1.1 Hz, 2H), 7.59 (dd, J = 9.3, 2.5 Hz, 2H), 7.56 – 7.52 (m, 2H), 7.32 – 7.29 (m, 2H), 6.96 (ddd, J = 12.9, 9.2, 2.4 Hz, 2H), 6.75 (dd, J = 8.7, 0.9 Hz, 2H), 3.94 (s, 3H).

^{13}C NMR (125 MHz, $\text{DMSO}-d_6$): δ = 162.7, 160.3, 160.3, 158.9, 154.83, 149.2, 139.3, 135.6, 131.7, 130.2, 117.3, 116.8, 116.1, 115.4, 99.3, 56.1.

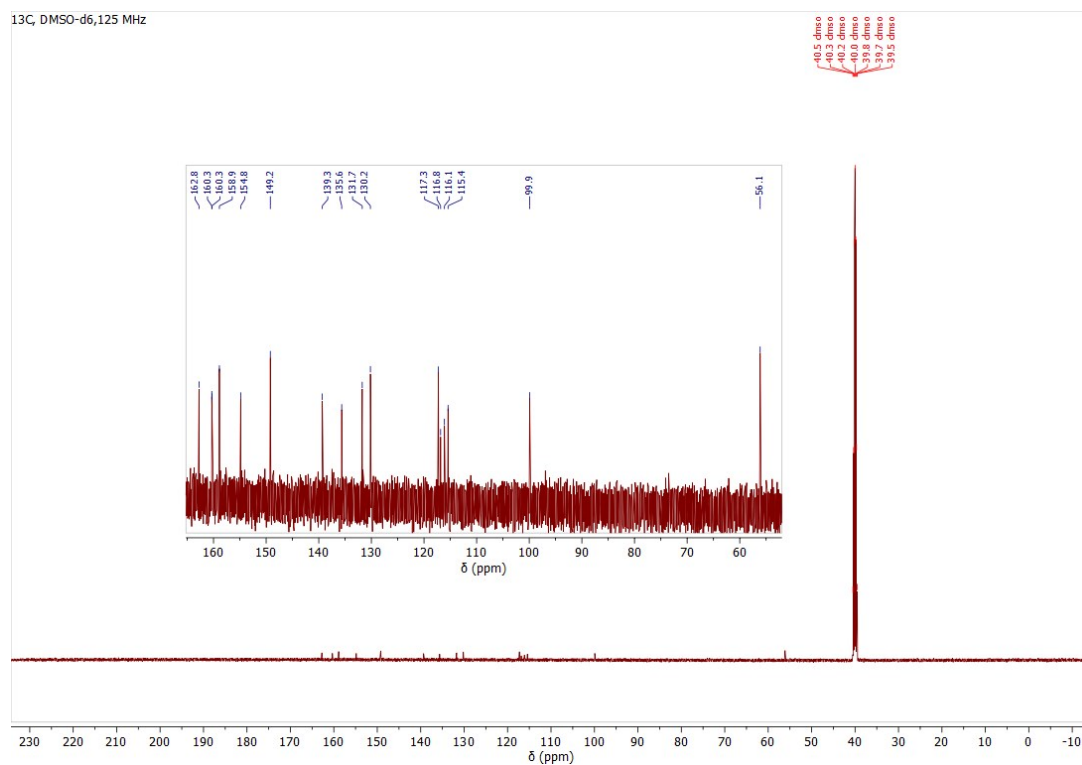


Figure S16. ^{13}C - $\{^1\text{H}\}$ -NMR spectrum (125 MHz, DMSO-d_6) of PtLF.

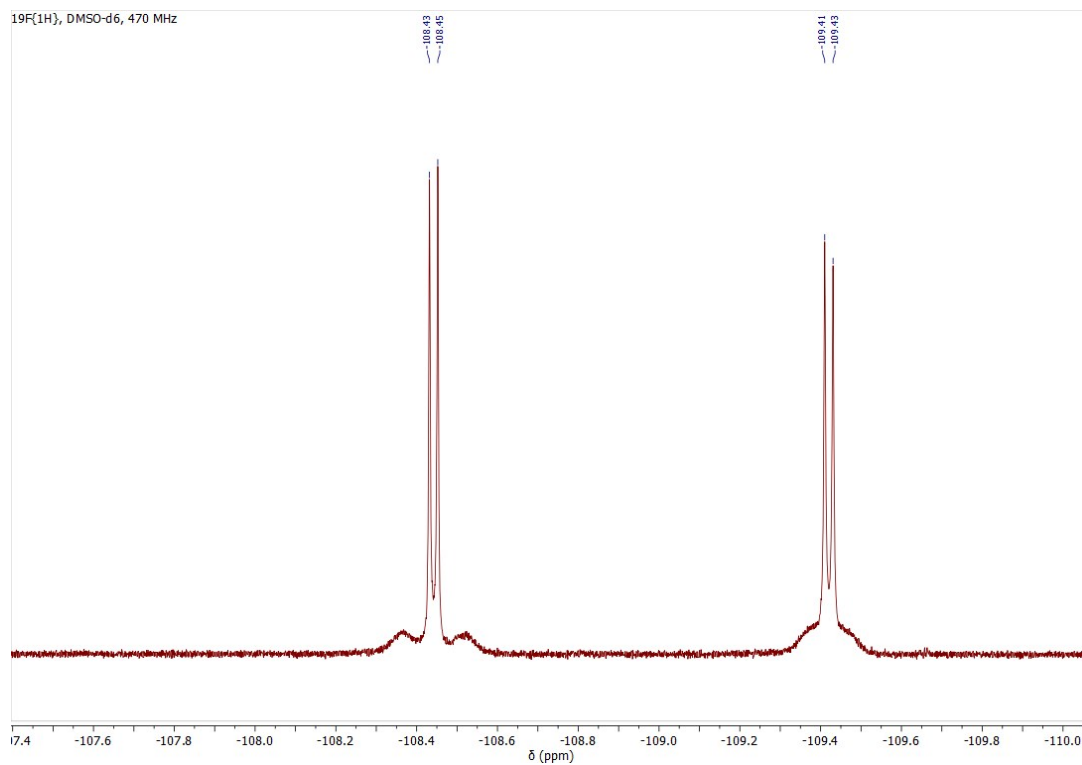


Figure S17. ^{19}F - $\{^1\text{H}\}$ -NMR spectrum (470 MHz, DMSO-d_6) of PtLF.

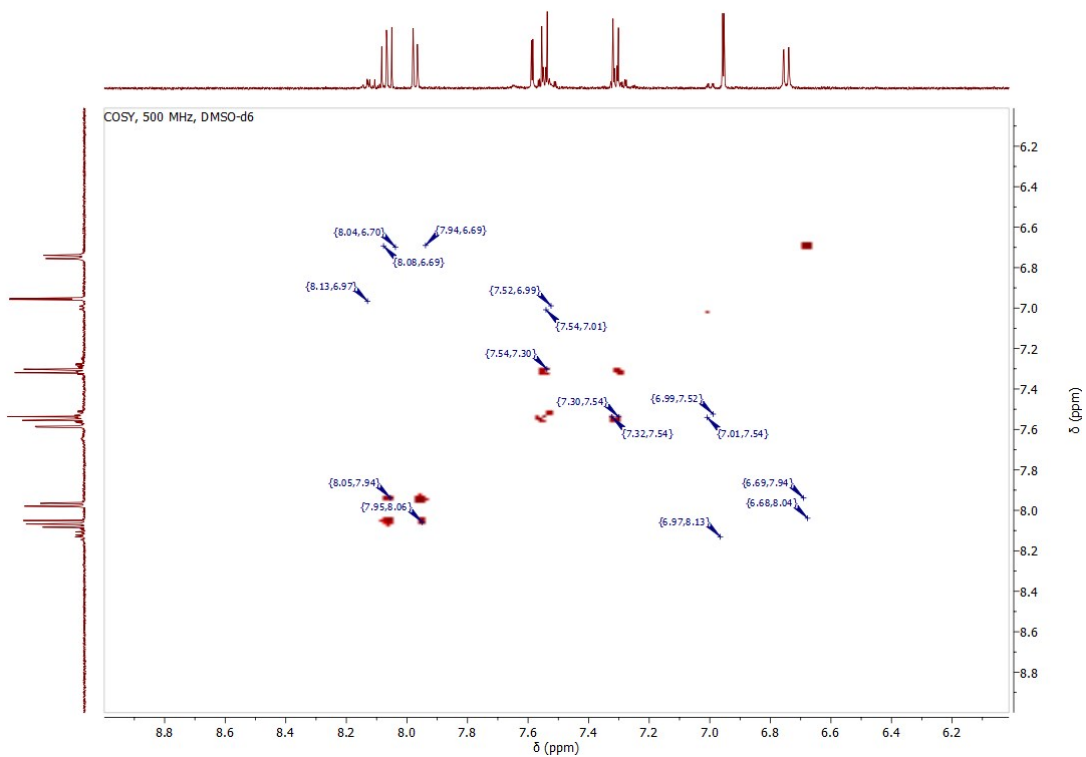


Figure S18. $^1\text{H}/^1\text{H}$ -COSY-NMR spectrum (600 MHz/600 MHz, DMSO- d_6) of PtLF.

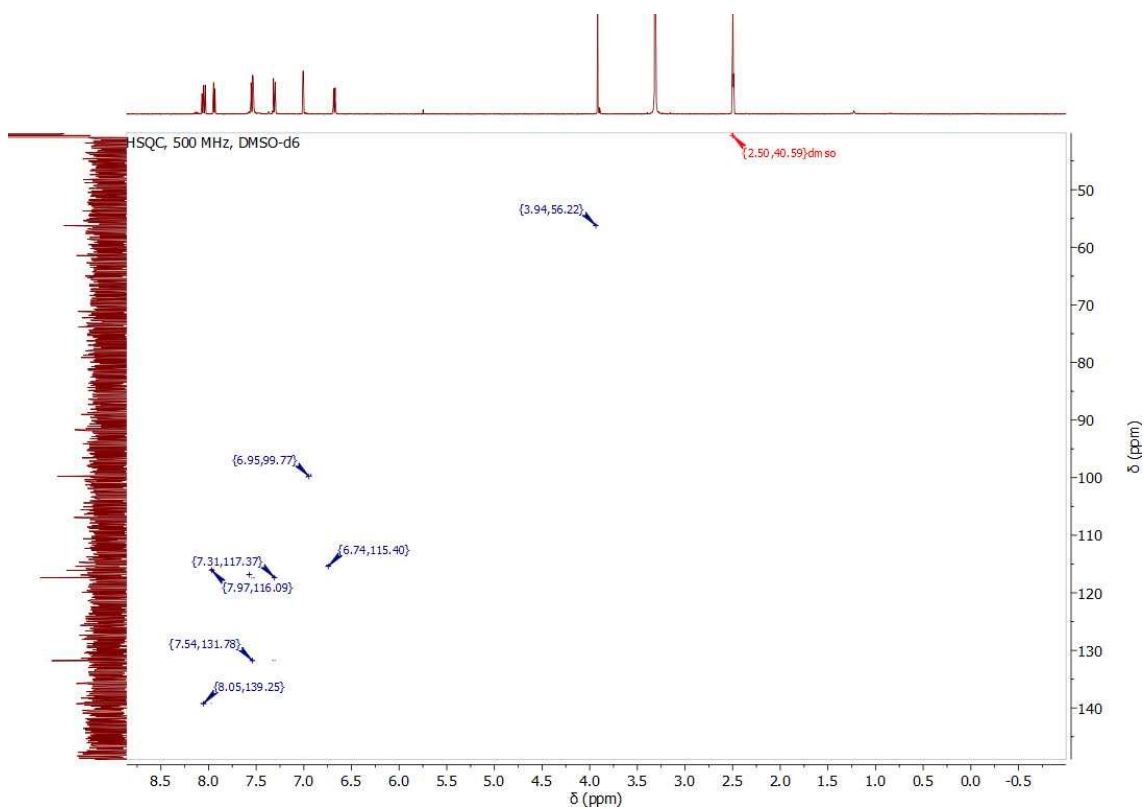


Figure S19. $^1\text{H}/^{13}\text{C}$ -gHSQC-NMR spectrum (600 MHz/150 MHz, DMSO- d_6) of PtLF.

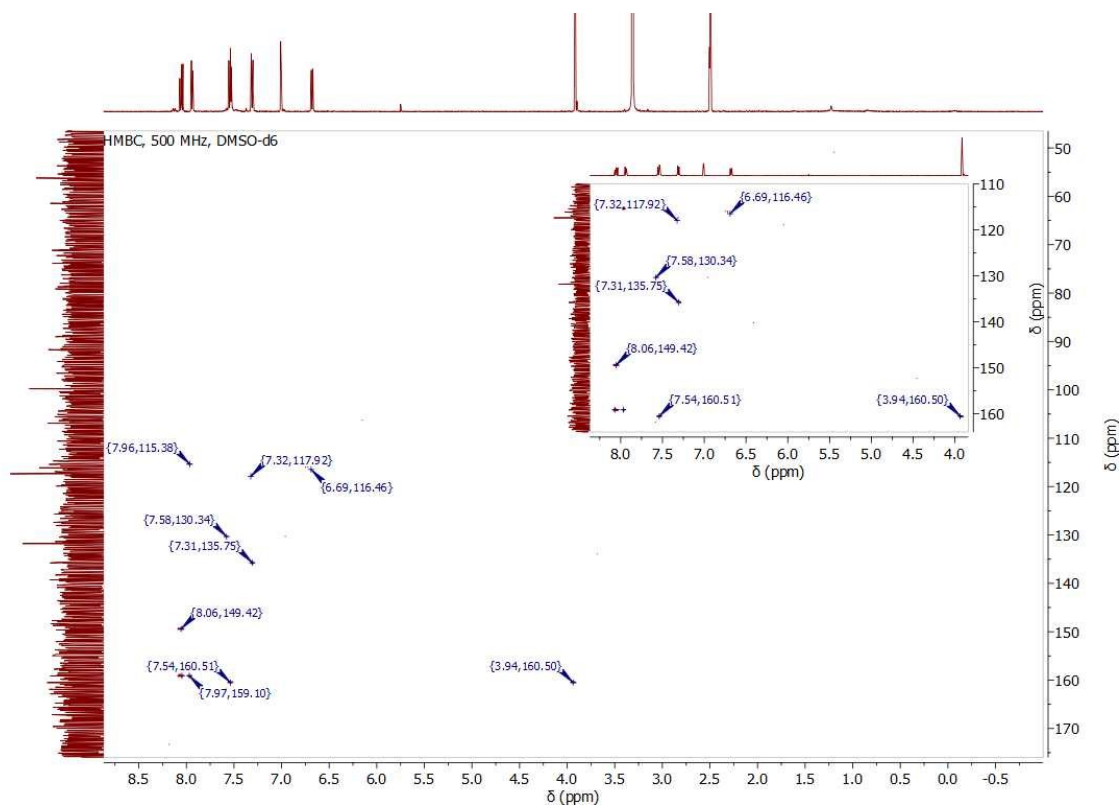


Figure S20. $^1\text{H}/^{13}\text{C}$ -gHMBC-NMR spectrum (600 MHz/150 MHz, DMSO-d_6) of PtLF.

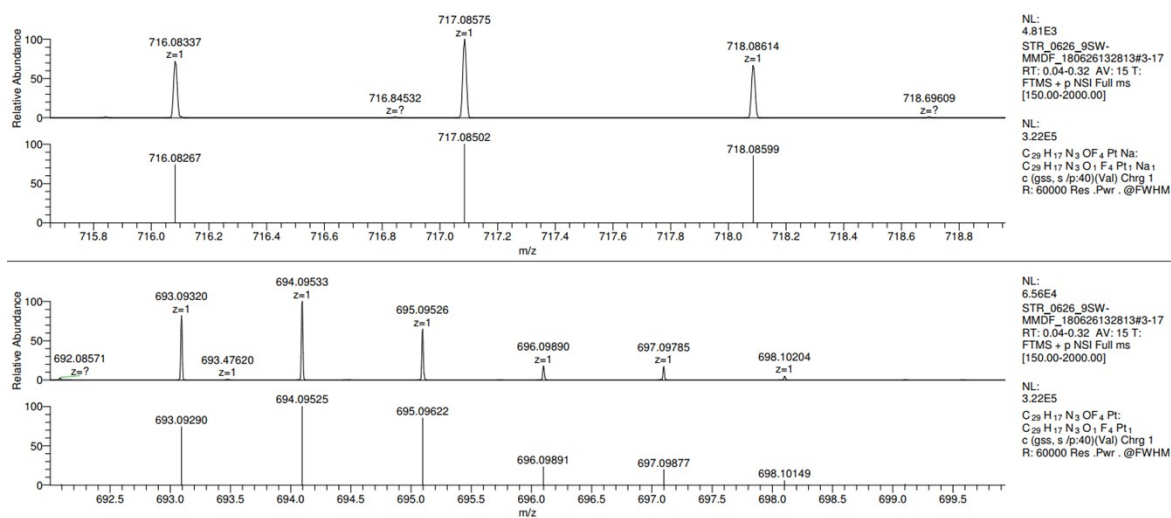


Figure S21. ESI-MS (MeOH) of PtLF.

Synthesis of PdLH: A mixture of the tetradentate ligand precursor **LH** (100 mg, 0.233 mmol) and palladium(II) acetate (54 mg, 0.239 mmol) were heated in glacial acetic acid (15 mL) for 72 h and refluxed afterwards at 130 °C for 12 h. After cooling down to room temperature, the solvent was removed. The crude

product was loaded onto a column packed with silica gel to perform a column chromatography separation with DCM as eluent to yield yellow solid (7 mg). Yield: 6%.

^1H NMR (500 MHz, $\text{DMSO-}d_6$): δ = 8.05 (dd, J = 7.7, 1.3 Hz, 2H), 7.91 (dd, J = 7.8, 1.4 Hz, 2H), 7.90 – 7.86 (m, 4H), 7.52 (d, J = 8.8 Hz, 2H), 7.32 (dd, J = 7.4, 1.3 Hz, 2H), 7.29 (d, J = 8.8 Hz, 2H), 7.19 – 7.14 (m, 2H), 6.46 (dd, J = 6.7, 2.8 Hz, 2H), 3.91 (s, 3H).

^{13}C NMR (125 MHz, $\text{DMSO-}d_6$): δ = 162.5, 161.4, 160.1, 151.6, 148.0, 139.5, 135.7, 135.5, 131.8, 129.2, 124.6, 124.0, 117.2, 114.4, 112.5, 56.1.

HRMS (ESI+, MeOH, m/z): calcd. for $[\text{M} + \text{H}]^+$ 534.08033, found 534.07960.

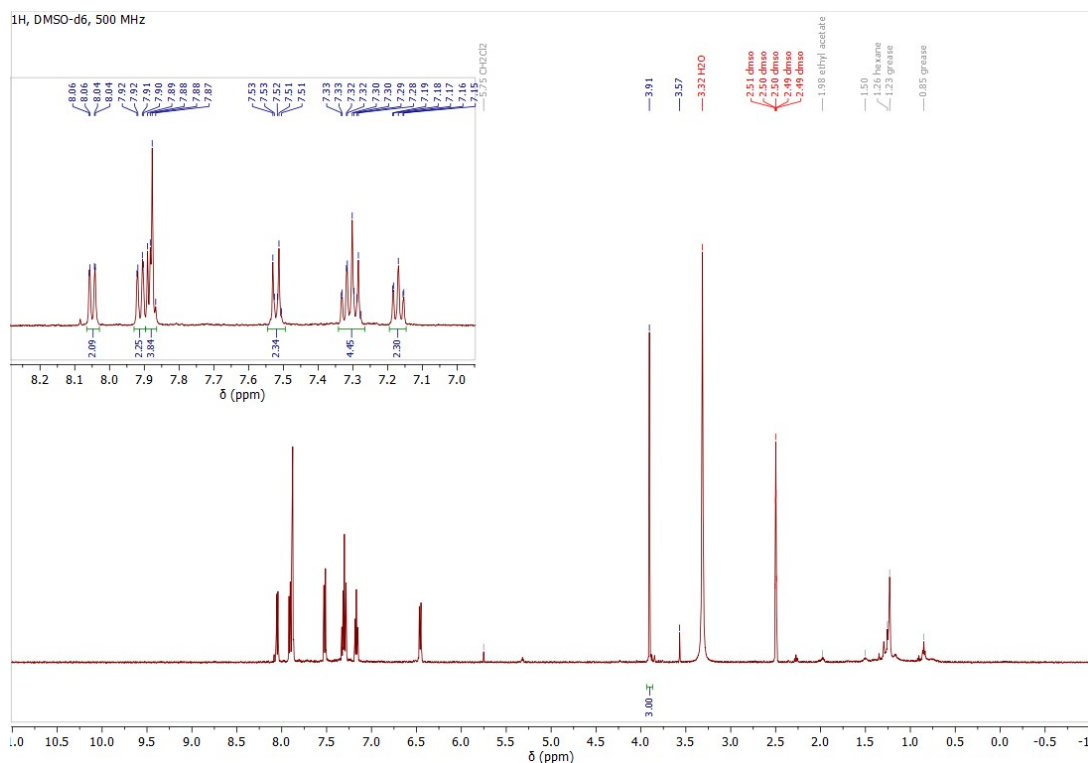


Figure S22. ^1H -NMR spectrum (500 MHz, $\text{DMSO-}d_6$) of PdLH.

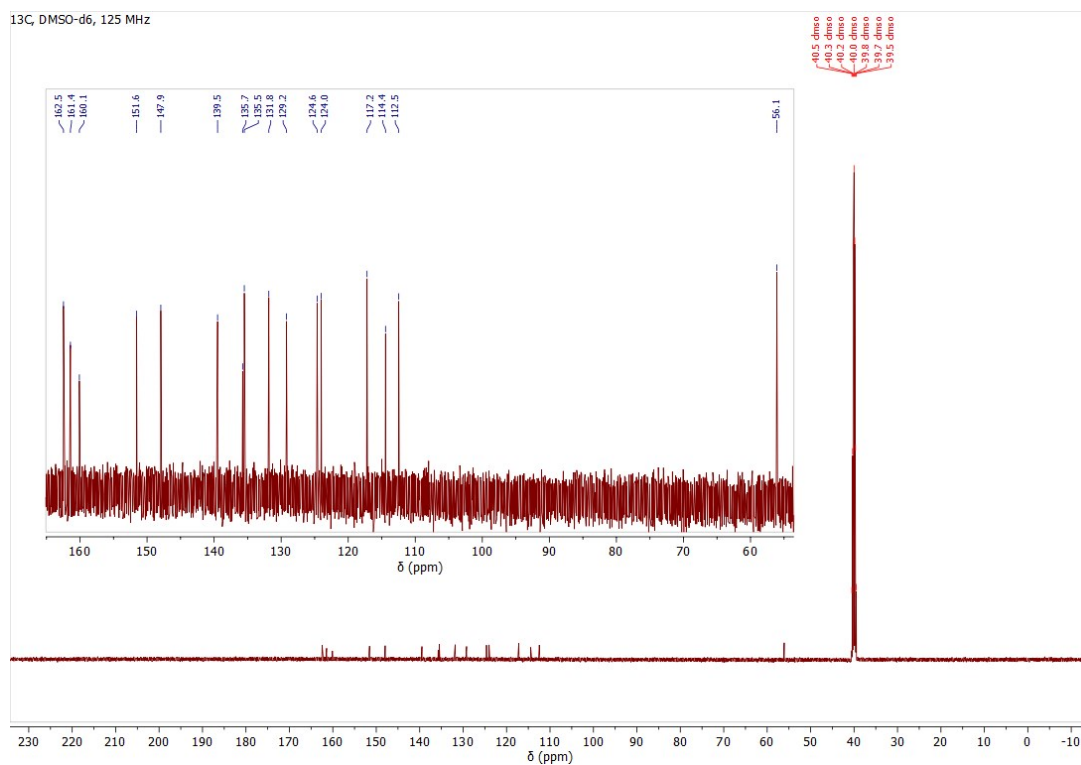


Figure S23. ¹³C-¹H-NMR spectrum (125 MHz, DMSO-d₆) of PdLH.

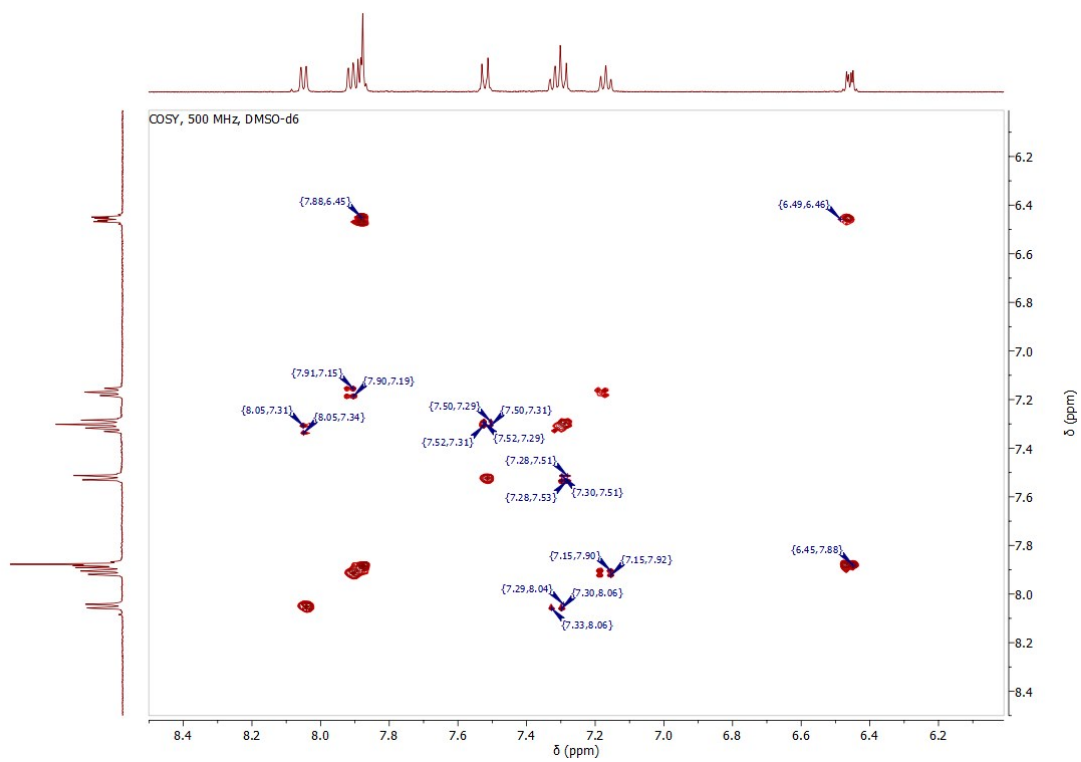


Figure S24. ¹H/¹H-COSY-NMR spectrum (600 MHz/600 MHz, DMSO-d₆) of PdLH.

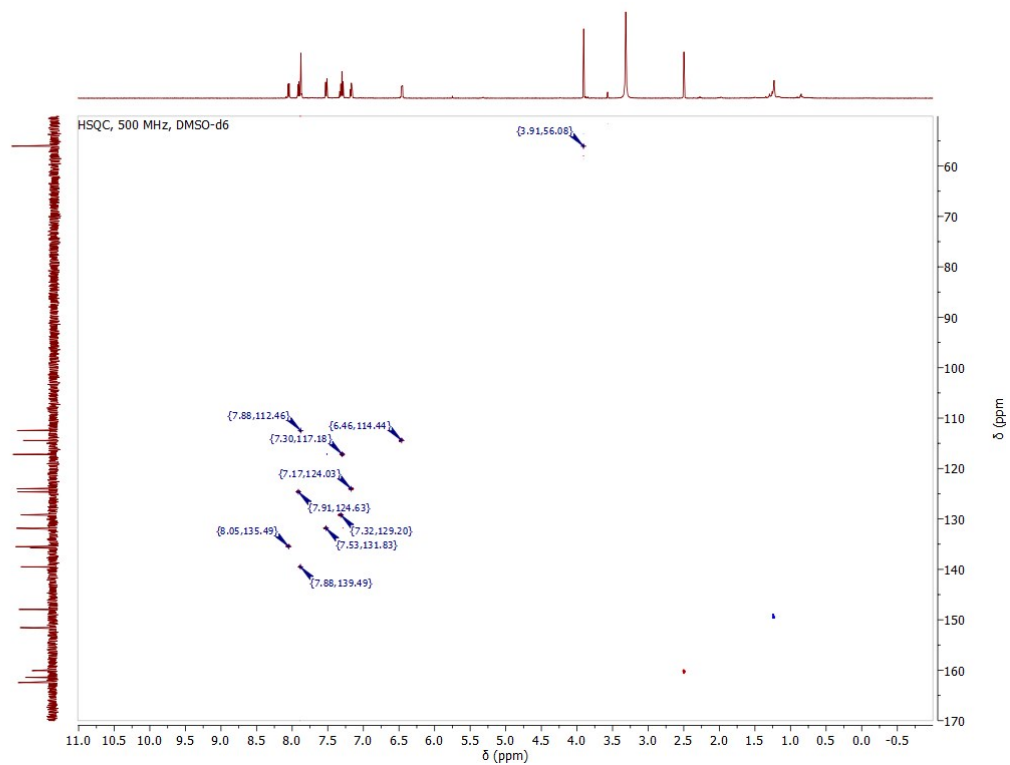


Figure S25. $^1\text{H}/^{13}\text{C}$ -gHSQC-NMR spectrum (600 MHz/150 MHz, DMSO-d₆) of PdLH.

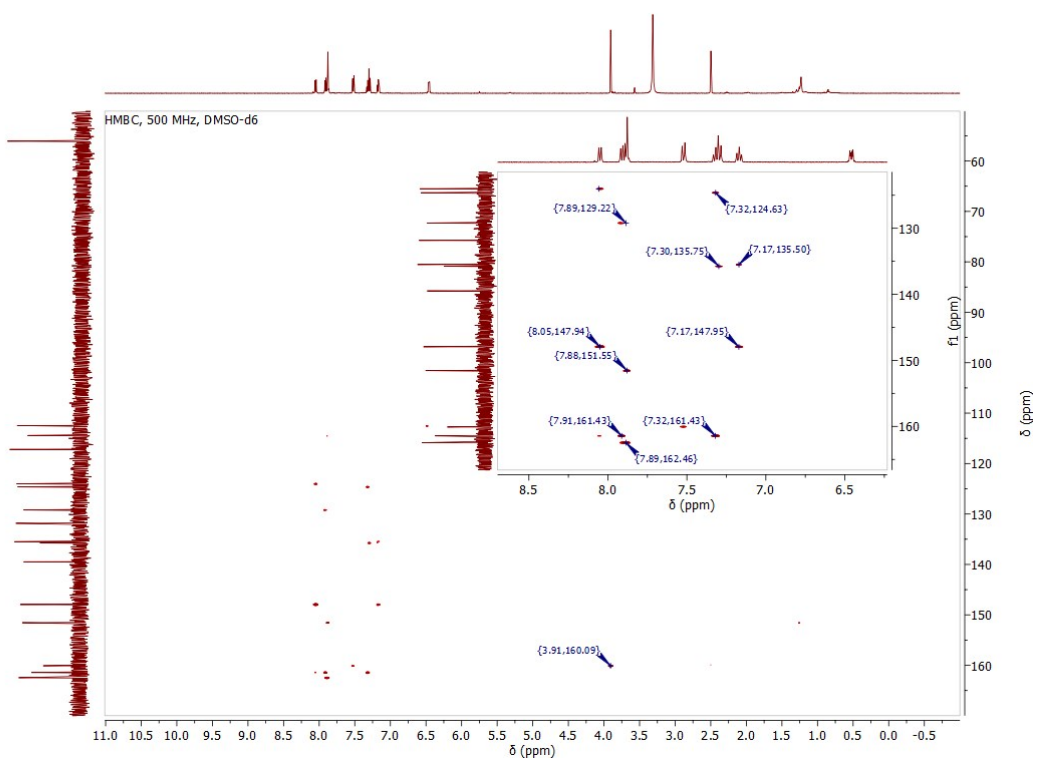


Figure S26. $^1\text{H}/^{13}\text{C}$ -gHMBC-NMR spectrum (600 MHz/150 MHz, DMSO-d₆) of PdLH.

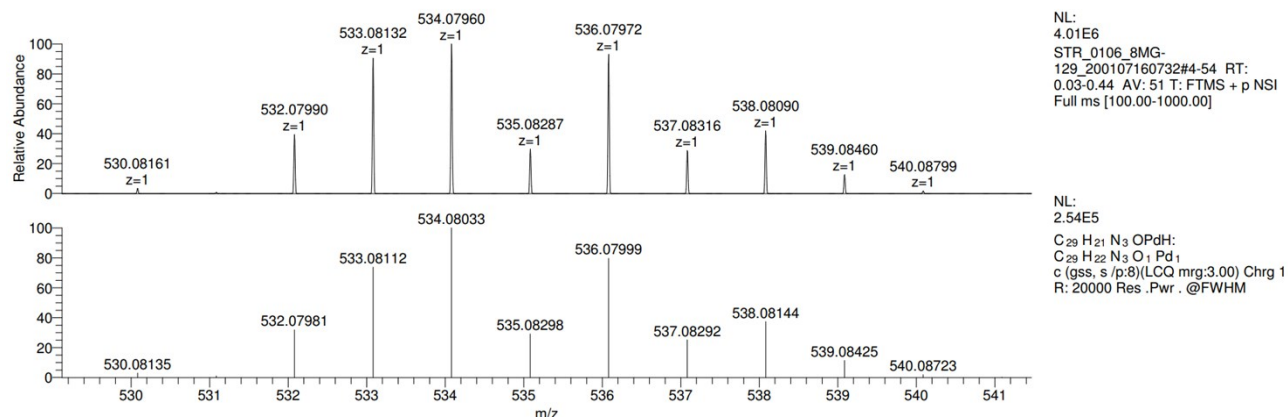


Figure S27. ESI+MS (MeOH) of PdLH.

Synthesis of PdLF: A mixture of the tetradentate ligand precursor **LF** (173 mg, 0.345 mmol) and palladium(II) acetate (78 mg, 0.047 mmol) were heated in glacial acetic acid (15 mL) for 72 h and refluxed afterwards at 130 °C for 12 h. After cooling down to room temperature, the solvent was removed. The crude product was loaded onto a column packed with silica gel to perform a column chromatography separation with CH₂Cl₂ as eluent to yield yellow solid (25 mg). Yield: 12 %

¹H NMR (500 MHz, DMSO-*d*₆): δ = 7.92 (t, *J* = 8.2 Hz, 2H), 7.86 (d, *J* = 7.9 Hz, 2H), 7.49 (d, *J* = 8.8 Hz, 2H), 7.40 (dd, *J* = 8.2, 2.4 Hz, 2H), 7.31 – 7.26 (m, 2H), 6.97 (ddd, *J* = 12.1, 9.1, 2.3 Hz, 2H), 6.53 (d, *J* = 8.7 Hz, 2H), 3.91 (s, 3H).

¹³C NMR (126 MHz, DMSO-*d*₆): δ = 167.1, 162.2, 159.8, 158.4, 151.7, 140.2, 135.7, 131.8, 117.3, 117.3, 116.0, 115.2, 100.5, 56.2.

¹⁹F NMR (470 MHz, DMSO-*d*₆): δ = -108.7 (d, *J* = 8.9 Hz), -108.8 (d, *J* = 8.9 Hz).

HRMS (ESI+, MeOH, *m/z*): calcd. for [M + H]⁺ 606.04205, found 606.04264.

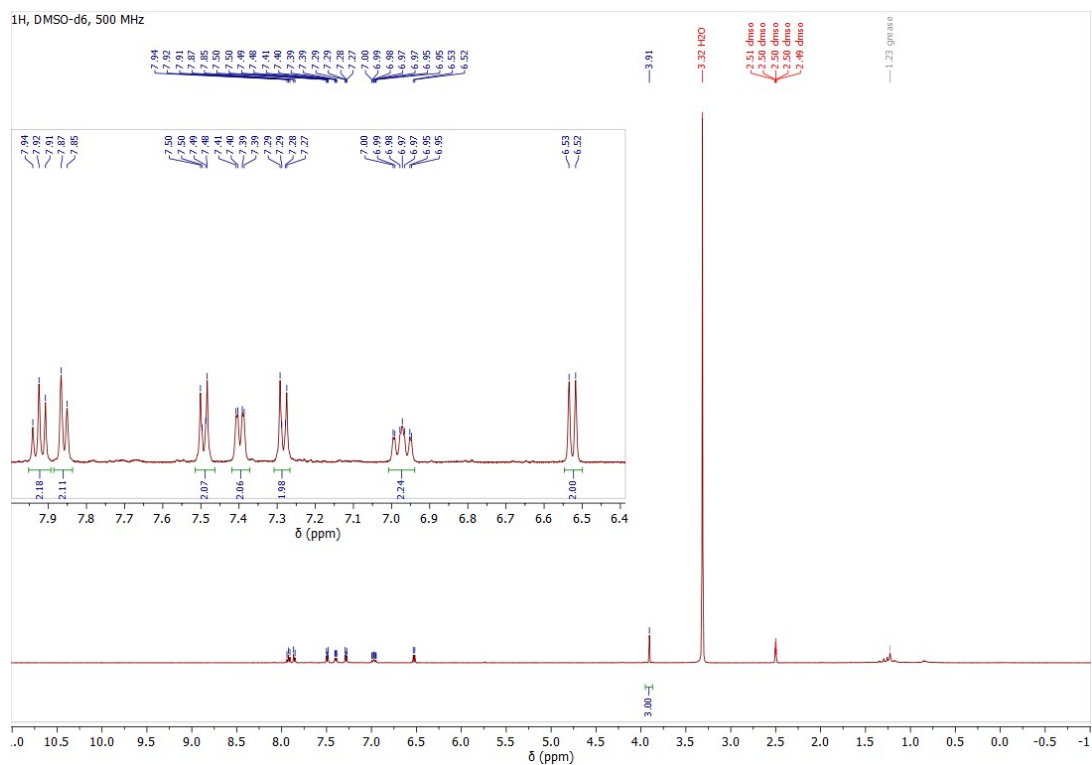


Figure S28. ¹H-NMR spectrum (500 MHz, DMSO-d₆) of PdLF.

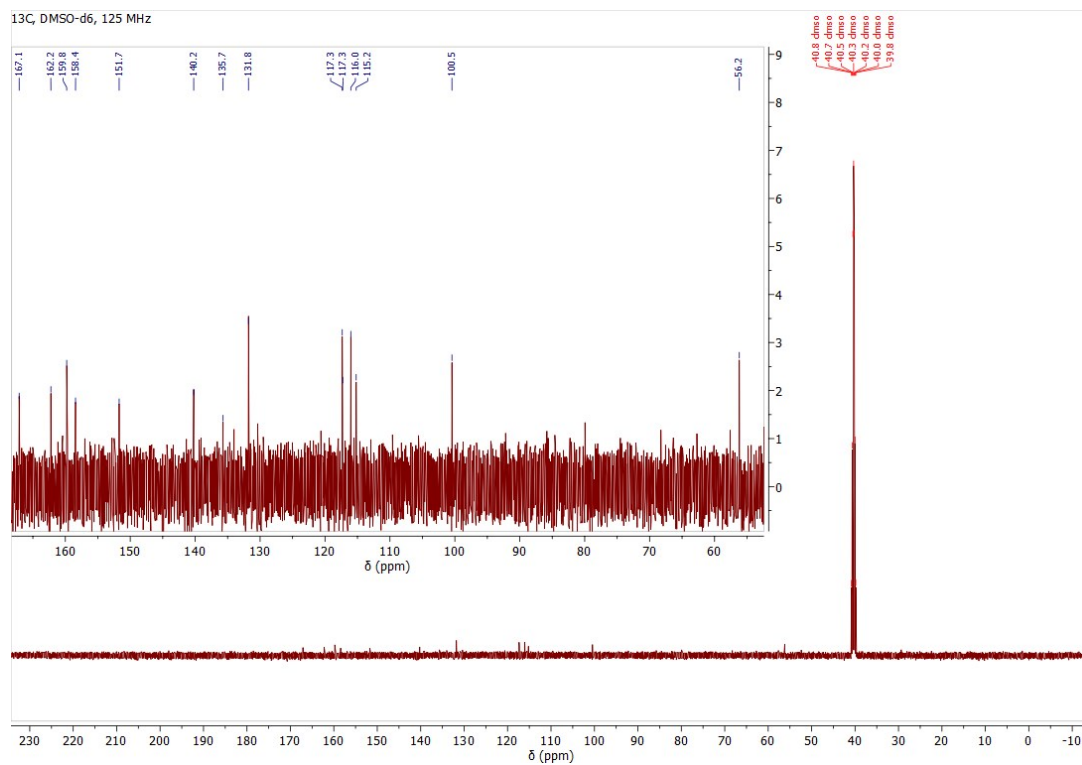


Figure S29. ¹³C-¹H-NMR spectrum (125 MHz, DMSO-d₆) of PdLF.

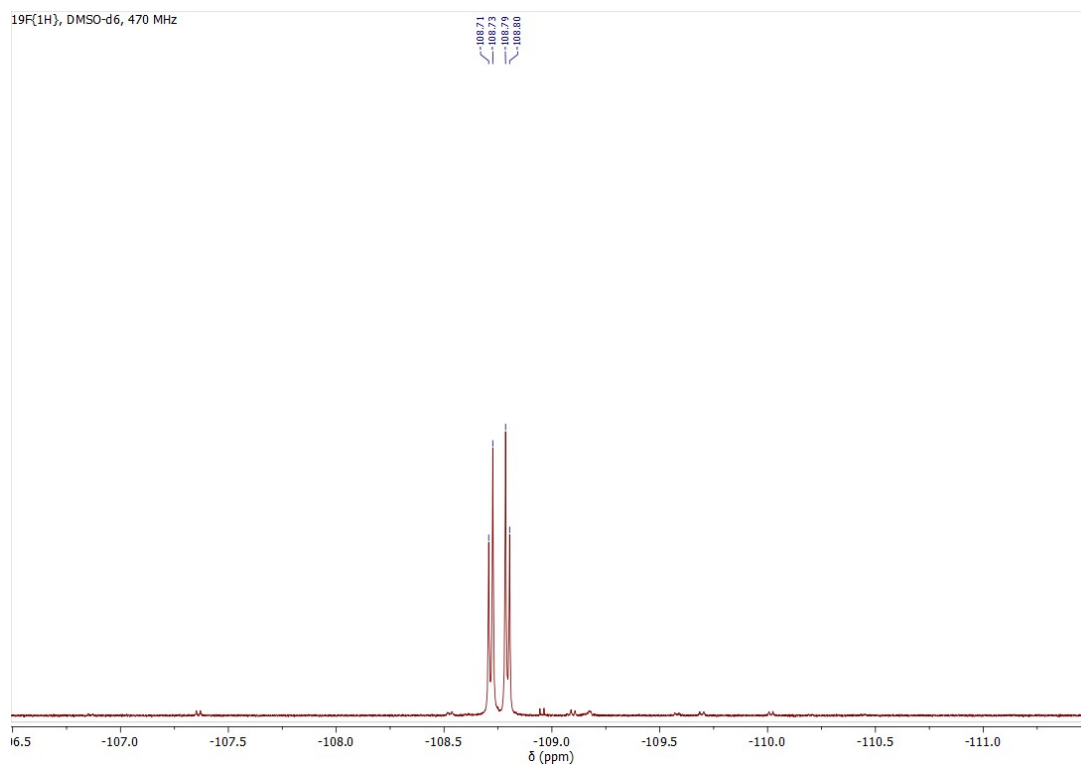


Figure S30. $^{19}\text{F}\{^1\text{H}\}$ -NMR spectrum (470 MHz, DMSO-d_6) of PdLF.

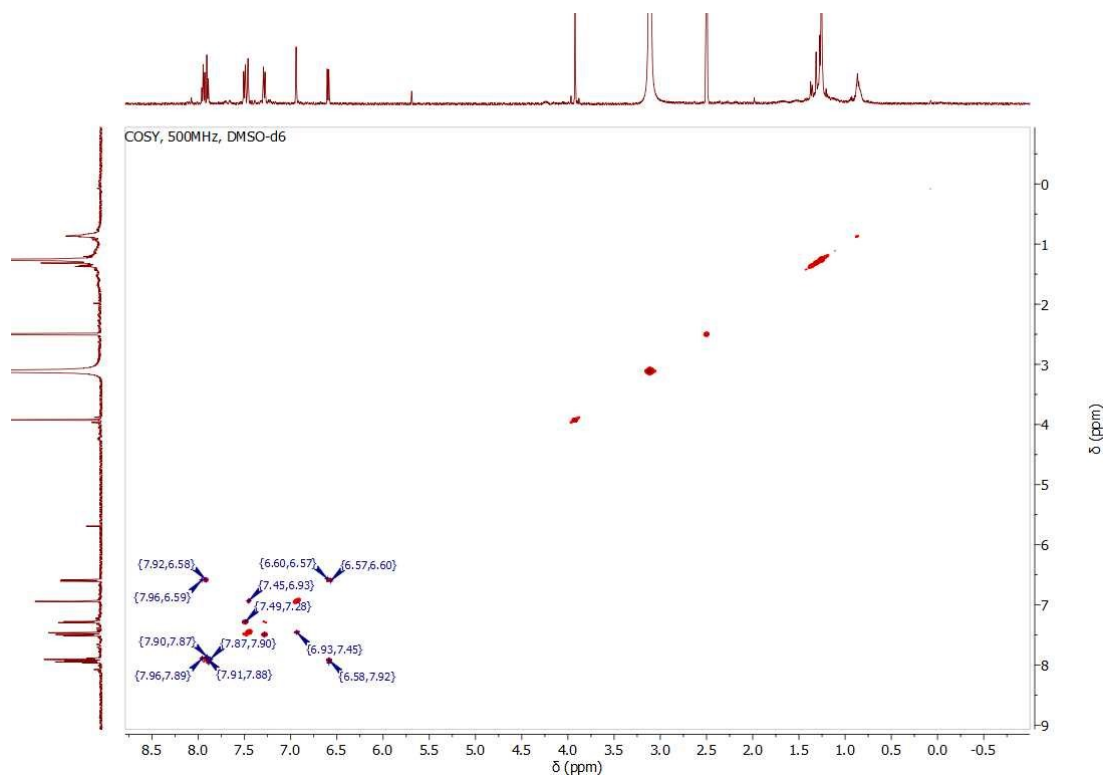


Figure S31. $^1\text{H}/^1\text{H}$ -COSY-NMR spectrum (500 MHz/500 MHz, DMSO-d_6) of PdLF.

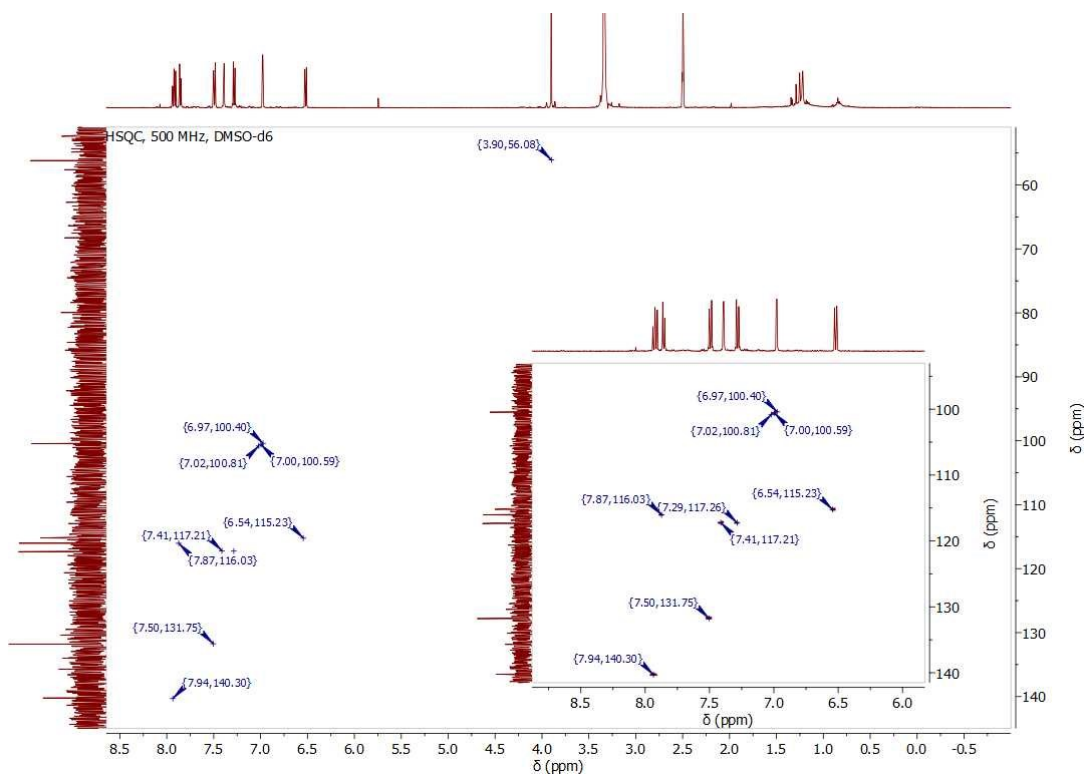


Figure S32. $^1\text{H}/^{13}\text{C}$ -gHSQC-NMR spectrum (500 MHz/125 MHz, DMSO-d_6) of PdLF.

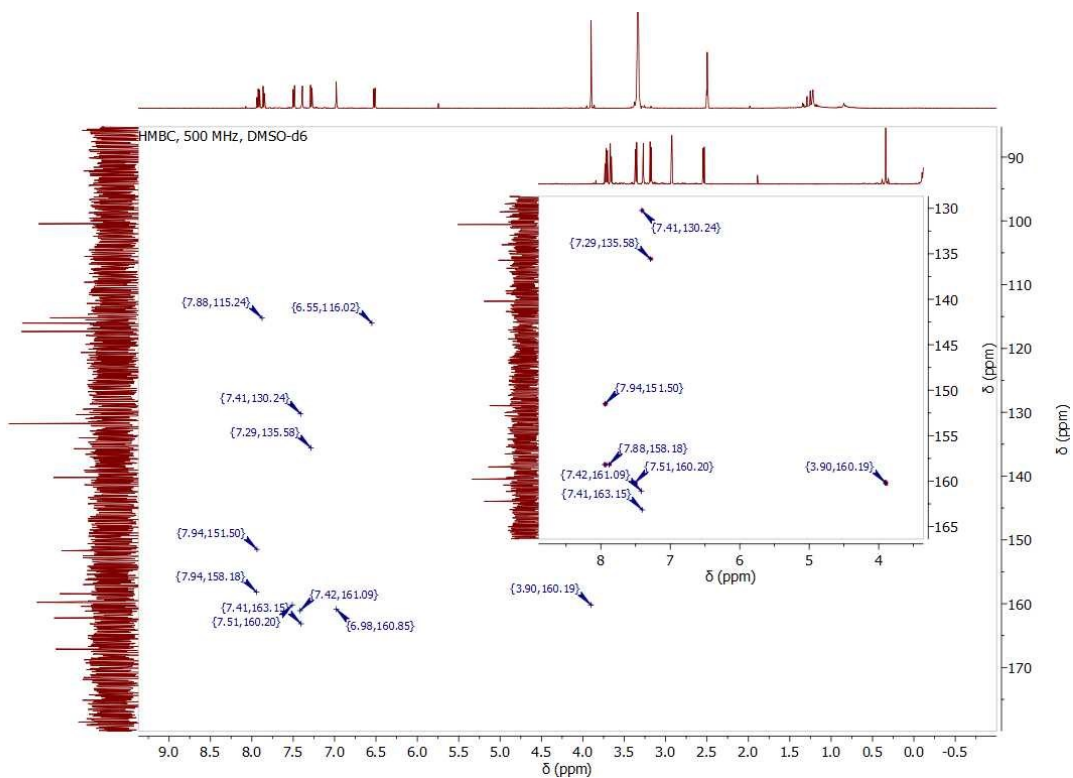


Figure S33. $^1\text{H}/^{13}\text{C}$ -gHMBC-NMR spectrum (500 MHz/125MHz, DMSO-d_6) of PdLF.

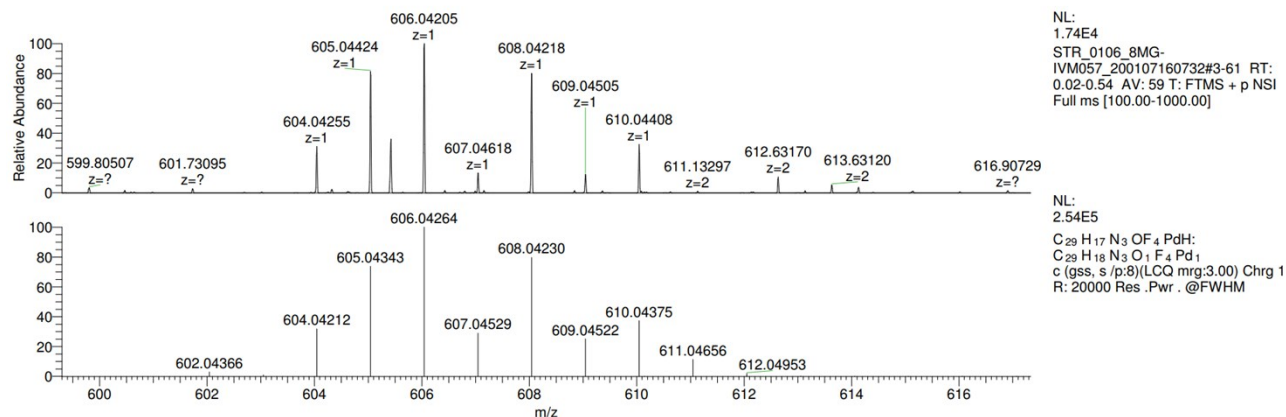


Figure S34. ESI-MS (MeOH) of PdLF.

Assignment of NMR signals for the complexes

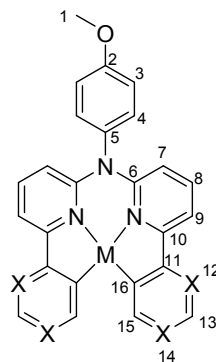


Table S1. Assignment of NMR signals for the complexes.

| Assignment | PtLH | | PtLF | | | PdLH | | PdLF | | |
|------------|----------------|-----------------|----------------|-----------------|-----------------|----------------|-----------------|----------------|-----------------|-----------------|
| | ¹ H | ¹³ C | ¹ H | ¹³ C | ¹⁹ F | ¹ H | ¹³ C | ¹ H | ¹³ C | ¹⁹ F |
| 1 | 3.92 | 56.1 | 3.94 | 56.1 | - | 3.91 | 56.1 | 3.90 | 56.2 | - |
| 2 | - | 160.2 | - | 160.3 | - | - | 160.1 | - | 159.8 | - |
| 3 | 7.56 | 131.8 | 7.53 | 116.8 | - | 7.52 | 131.8 | 7.49 | 131.8 | - |
| 4 | 7.32 | 117.2 | 7.31 | 117.3 | - | 7.32 | 117.2 | 7.28 | 117.3 | - |
| 5 | - | 135.8 | - | 130.2 | - | - | 135.7 | - | 135.7 | - |
| 6 | - | 163.2 | - | 162.7 | - | - | 162.5 | - | 162.2 | - |
| 7 | 6.62 | 112.6 | 6.96 | 99.3 | - | 6.46 | 114.4 | 6.54 | 115.2 | - |
| 8 | 8.02 | 138.3 | 8.07 | 139.3 | - | 7.91 | 139.5 | 7.92 | 140.2 | - |
| 9 | 7.92 | 114.8 | 7.97 | 116.1 | - | 7.90 | 112.4 | 7.86 | 116.0 | - |
| 10 | - | 149.0 | - | 154.8 | - | - | 147.9 | - | 151.7 | - |
| 11 | - | 149.6 | - | 158.9 | - | - | 151.6 | - | 158.4 | - |
| 12 | 7.96 | 124.5 | - | 149.2 | -109.4 | 7.88 | 124.6 | - | - | -108.7 |
| 13 | 7.17 | 123.3 | 6.75 | 115.4 | - | 7.17 | 124.3 | 6.97 | 100.5 | - |
| 14 | 7.36 | 129.3 | - | 160.3 | -108.4 | 7.29 | 129.2 | - | - | -108.8 |
| 15 | 8.20 | 135.3 | 7.59 | 131.7 | - | 8.05 | 135.5 | 7.40 | 117.3 | - |
| 16 | - | 147.4 | - | 135.9 | - | - | 161.4 | - | 167.1 | - |

Section S3: Single crystal X-ray diffractometric analysis of PtLH, PtLF, PdLH and PdLF

Suitable single crystals for X-ray diffractometric analysis were obtained from slow evaporation of DCM solutions of the four complexes. CCDC Nos. 2024154 - 2024158 contain the supplementary crystallographic data for the complexes. This material can be obtained free of charge via <http://www.ccdc.cam.ac.uk/conts/retrieving.html>, or from the Cambridge Crystallographic Data Centre, 12 Union Road, Cambridge CB2 1EZ, UK; fax: (+44) 1223-336-033; or E-mail: deposit@ccdc.cam.ac.uk.

Crystal structure analysis of PtLH: formula $C_{29}H_{21}N_3OPt$, $M = 622.58$, yellow crystal, $0.16 \times 0.09 \times 0.03$ mm, $a = 10.3090(2)$ Å, $b = 13.9097(2)$ Å, $c = 15.4326(3)$ Å, $\beta = 101.658(1)^\circ$, $V = 2167.31(7)$ Å³, $\rho_{\text{calc}} = 1.908$ g/cm³, $\mu = 6.504$ mm⁻¹, empirical absorption correction ($0.423 \leq T \leq 0.829$), $Z = 4$, monoclinic, space group $P2_1/n$ (No. 14), $\lambda = 0.71073$ Å, $T = 173(2)$ K, ω and φ scans, 13921 reflections collected ($\pm h$, $\pm k$, $\pm l$), 3775 independent ($R_{\text{int}} = 0.039$) and 3461 observed reflections [$I > 2\sigma(I)$], 308 refined parameters, $R = 0.030$, $wR^2 = 0.075$, max. (min.) residual electron density 1.81 (-0.87) e.Å⁻³, hydrogen atoms were calculated and refined as riding atoms.

Crystal structure analysis of PtLF (1): formula $C_{29}H_{17}F_4N_3OPt$, $M = 694.55$, yellow crystal, $0.20 \times 0.09 \times 0.04$ mm, $a = 9.6007(2)$ Å, $b = 11.7181(2)$ Å, $c = 12.0959(3)$ Å, $\alpha = 118.2830(1)^\circ$, $\beta = 95.325(1)^\circ$, $\gamma = 104.556(1)^\circ$, $V = 1123.48(4)$ Å³, $\rho_{\text{calc}} = 2.053$ g/cm³, $\mu = 6.309$ mm⁻¹, empirical absorption correction ($0.365 \leq T \leq 0.786$), $Z = 2$, triclinic, space group $P-1$ (No. 2), $\lambda = 0.71073$ Å, $T = 173(2)$ K, ω and φ scans, 11240 reflections collected ($\pm h$, $\pm k$, $\pm l$), 3910 independent ($R_{\text{int}} = 0.036$) and 3831 observed reflections [$I > 2\sigma(I)$], 344 refined parameters, $R = 0.024$, $wR^2 = 0.063$, max. (min.) residual electron density 0.67 (-1.88) e.Å⁻³, hydrogen atoms were calculated and refined as riding atoms.

Crystal structure analysis of PtLF (2): formula $C_{29}H_{17}F_4N_3OPt$, $M = 694.55$, yellow crystal, $0.07 \times 0.05 \times 0.03$ mm, $a = 22.8339(3)$ Å, $b = 9.8626(2)$ Å, $c = 22.7576(3)$ Å, $\beta = 117.704(1)^\circ$, $V = 4537.52(12)$ Å³, $\rho_{\text{calc}} = 2.033$ g/cm³, $\mu = 6.249$ mm⁻¹, empirical absorption correction ($0.669 \leq T \leq 0.835$), $Z = 8$, monoclinic, space group $P2/c$ (No. 2), $\lambda = 0.71073$ Å, $T = 173(2)$ K, ω and φ scans, 29814 reflections collected ($\pm h$, $\pm k$, $\pm l$), 7879 independent ($R_{\text{int}} = 0.063$) and 6114 observed reflections [$I > 2\sigma(I)$], 687 refined parameters, $R = 0.043$, $wR^2 = 0.094$, max. (min.) residual electron density 0.84 (-0.75) e.Å⁻³, hydrogen atoms were calculated and refined as riding atoms.

Crystal structure analysis of PdLH: formula $C_{29}H_{21}N_3OPd$, $M = 633.93$, yellow crystal, $0.030 \times 0.120 \times 0.200$ mm, $a = 9.2713(2)$ Å, $b = 11.5997(2)$ Å, $c = 11.9314(2)$ Å, $\alpha = 118.3680(10)^\circ$, $\beta = 92.8690(10)^\circ$, $\gamma = 106.8240(10)^\circ$, $V = 1053.60(4)$ Å³, $\rho_{\text{calc}} = 1.683$ g/cm³, $\mu = 7.336$ mm⁻¹, empirical absorption correction

($0.580 \leq T \leq 0.810$), $Z = 2$, triclinic, space group $P-1$ (No. 2), $\lambda = 1.54178 \text{ \AA}$, $T = 100(2) \text{ K}$, maximum θ angle of 66.74° (0.84 \AA resolution), 15777 reflections collected ($\pm h, \pm k, \pm l$), 3699 independent ($R_{int} = 0.0535$), and 3334 observed reflections [$I > 2\sigma(I)$], 308 refined parameters, $R = 0.032$, $wR^2 = 0.080$, max. (min.) residual electron density 0.49 (-0.61) e\AA^{-3} , hydrogen atoms were calculated and refined as riding atoms.

Crystal structure analysis of PdLF: formula $\text{C}_{29}\text{H}_{17}\text{F}_4\text{N}_3\text{OPd}$, $M = 605.85$, yellow crystal, $0.40 \times 0.10 \times 0.03 \text{ mm}$, $a = 11.8675(9) \text{ \AA}$, $b = 12.4514(10) \text{ \AA}$, $c = 17.2457(3) \text{ \AA}$, $\alpha = 94.655(2)^\circ$, $\beta = 96.279(2)^\circ$, $\gamma = 113.088(2)^\circ$, $V = 2308.6(3) \text{ \AA}^3$, $\rho_{\text{calc}} = 1.743 \text{ g/cm}^3$, $\mu = 0.867 \text{ mm}^{-1}$, empirical absorption correction ($0.6522 \leq T \leq 0.8878$), $Z = 4$, triclinic, space group $P-1$ (No. 2), $\lambda = 0.71073 \text{ \AA}$, $T = 240(2) \text{ K}$, ω scan, 29395 reflections collected ($\pm h, \pm k, \pm l$), 10852 independent ($R_{int} = 0.0406$) and 7766 observed reflections [$I > 2\sigma(I)$], 687 refined parameters, $R = 0.0546$, $wR^2 = 0.0942$, max. (min.) residual electron density 0.762 (-0.99) e\AA^{-3} , hydrogen atoms were calculated and refined as riding atoms.

Table S2. Cell parameters for the complexes.

| | PtLH | PtLF (1) | PtLF (2) | PdLH | PdLF |
|------------------------|--|--|--|--|--|
| Formula | $\text{C}_{29}\text{H}_{21}\text{N}_3\text{OPt}$ | $\text{C}_{29}\text{H}_{17}\text{F}_4\text{N}_3\text{OPt}$ | $\text{C}_{29}\text{H}_{17}\text{F}_4\text{N}_3\text{OPt}$ | $\text{C}_{29}\text{H}_{21}\text{N}_3\text{OPd}$ | $\text{C}_{29}\text{H}_{17}\text{F}_4\text{N}_3\text{OPd}$ |
| Formula Weight | 622.58 | 694.55 | 694.55 | 533.93 | 605.83 |
| Crystal System | Monoclinic | Triclinic | Monoclinic | Triclinic | Triclinic |
| Color | Yellow | Yellow | Yellow | Yellow | Yellow |
| Space Group | $P2_1/n$ | $P-1$ | $P2/c$ | $P-1$ | $P-1$ |
| Z | 4 | 2 | 8 | 2 | 4 |
| a (\AA) | 10.3090(2) | 9.6007(2) | 22.8339(3) | 9.2713(2) | 11.8675(9) |
| b (\AA) | 13.9097 (2) | 11.7181(2) | 9.8626(2) | 11.5997(2) | 12.4514(10) |
| c (\AA) | 15.4326 (3) | 12.0959(3) | 22.7576(3) | 11.9314(2) | 17.2457(14) |
| α ($^\circ$) | - | 118.283(1) | - | 118.3680(10) | 94.655(2) |
| β ($^\circ$) | 101.658(1) | 95.325(1) | 117.704(1) | 92.8690(10) | 96.279(2) |
| γ ($^\circ$) | - | 104.556(1) | - | 106.8240(10) | 113.088(2) |
| V (\AA^3) | 2167.31(7) | 1123.48 | 4537.52(13) | 1053.60(4) | 2308.63(30) |
| Temperature (K) | 173 | 173 | 173 | 100 | 240 |

Table S3. Most relevant crystallographic parameters from complexes PtLH, PtLF, PdLH and PdLF.

| | M...M (\AA) | C-H...F (\AA) | C-H...O (\AA) | N-M-N ($^\circ$) |
|----------|------------------------|---|---|--------------------|
| PtLH | 5.2538(1) | - | - | 92.838(1) |
| PtLF (1) | 4.2183(1) | 2.7391(1) (H24-F1) 2.5480(1) (H22-F2) 2.5296(1) (H2-F2) | 2.6902(1) (O1-H37B) | 93.354(1) |
| PtLF (2) | 3.5549(1) | 2.6565(0) (H2-F1) 2.6779(0) (H36-F1) 2.8556(0) (H37-F2) 2.9971(1) (H37-F1) | - | 93.228(1) |
| PdLH | 4.2964(1) | - | 3.0315(1) (O1-H18) 3.1931(1) (O1-H5) | 91.697(1) |
| PdLF | 3.7611(5) | 2.5461(27) (H44-F57) 2.760(3) (H54 - F57) | - | 92.81(14) |

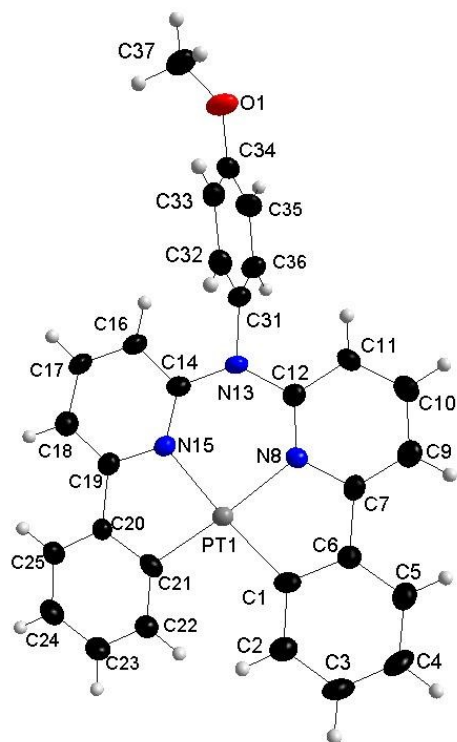


Figure S35. Molecular structure in the crystal of **PtLH**. Thermal displacement ellipsoids are shown at 50% probability.

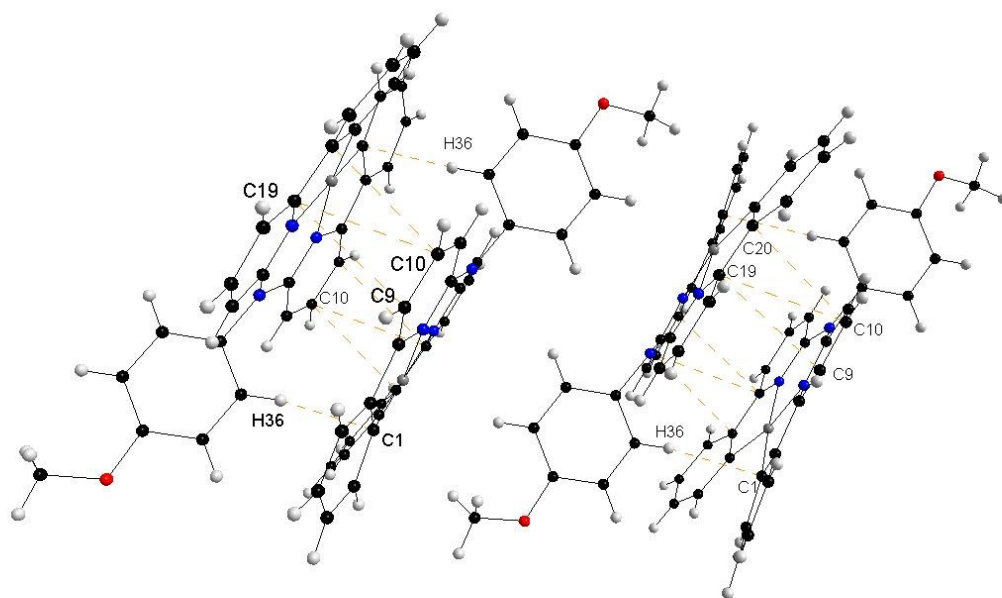


Figure S36. $\pi \cdots \pi$ and $C-H \cdots \pi$ interactions in **PtLH**.

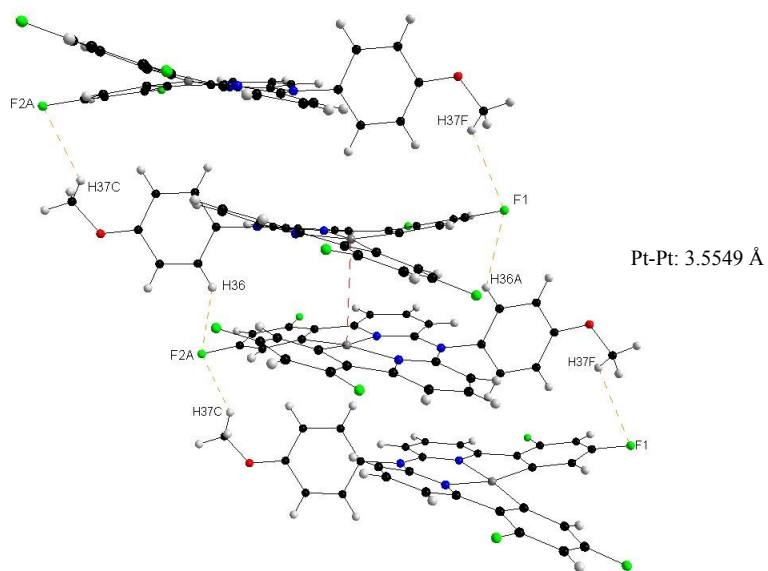


Figure S39. PtLF (2) dimers and their columnar arrangement.

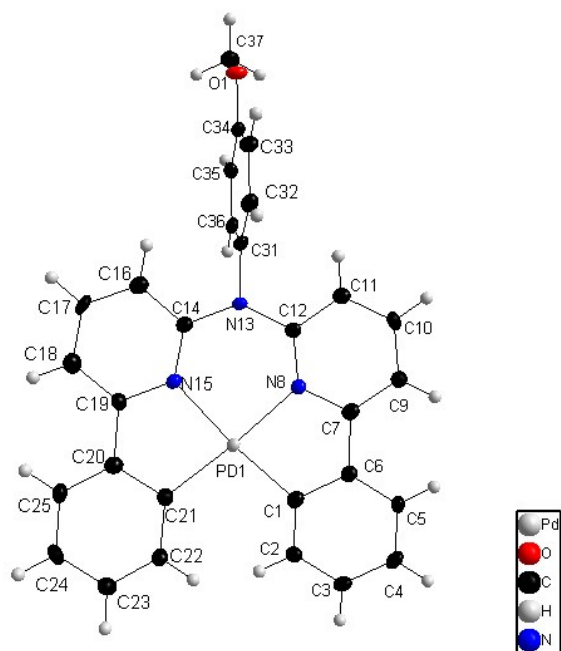


Figure S40. Molecular structure in the crystal of PdLH. Thermal displacement ellipsoids are shown at 50% probability.

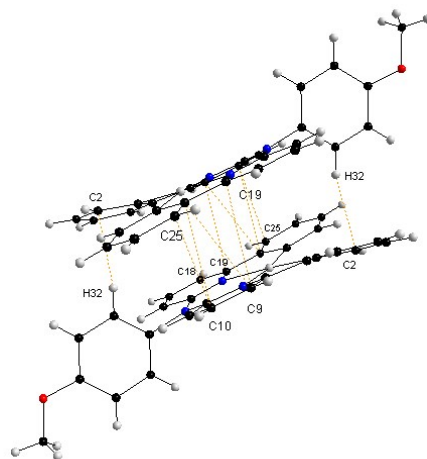


Figure S41. $\pi \cdots \pi$ and C-H $\cdots \pi$ interactions in PdLH.

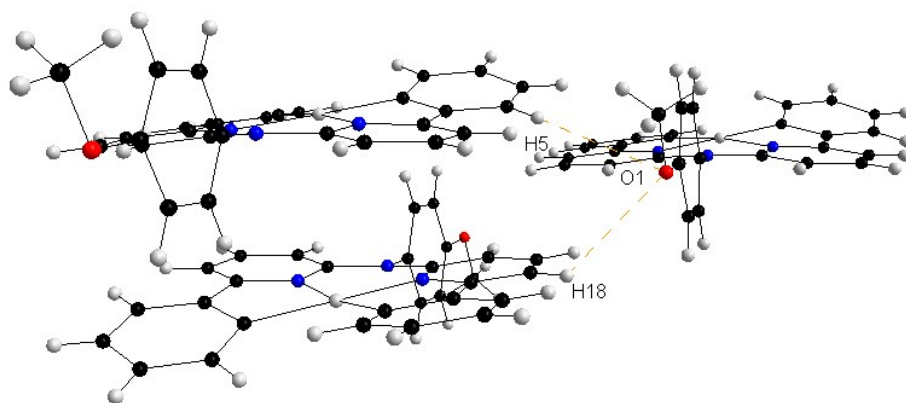


Figure S42. H-bond interactions in PdLH.

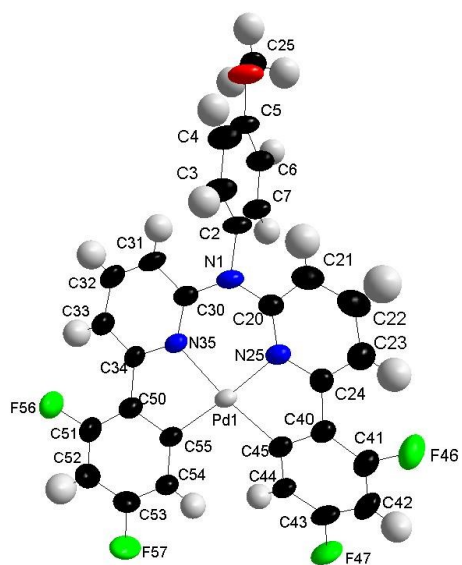


Figure S43. Molecular structure in the crystal of **PdLF**. Thermal displacement ellipsoids are shown at 50% probability.

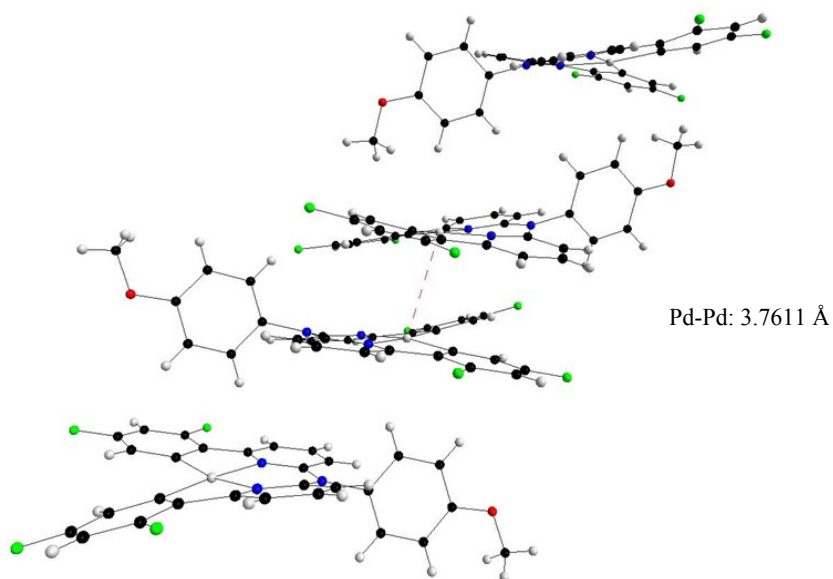


Figure S44. Pd...Pd interactions in **PdLF**.

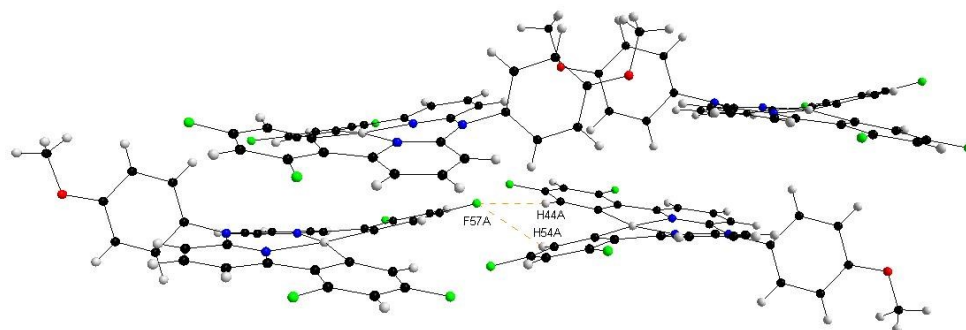


Figure S45. H-bond interactions in PdLF.

Table S4. Atomic parameters of PtLH.

| Atom | Wyck. | Site | x/a | y/b | z/c | U [Å ²] |
|------|-------|------|----------|----------|----------|---------------------|
| PT1 | 4e | 1 | 0.38503 | 0.16418 | 0.02214 | |
| C1 | 4e | 1 | 0.43077 | 0.25918 | -0.06425 | |
| C2 | 4e | 1 | 0.45782 | 0.35757 | -0.05854 | |
| H2 | 4e | 1 | 0.44774 | 0.39136 | -0.00681 | -1.2000 |
| C3 | 4e | 1 | 0.49891 | 0.40758 | -0.12585 | |
| H3 | 4e | 1 | 0.51644 | 0.47452 | -0.11939 | -1.2000 |
| C4 | 4e | 1 | 0.51456 | 0.36170 | -0.20154 | |
| H4 | 4e | 1 | 0.54808 | 0.39574 | -0.24566 | -1.2000 |
| C5 | 4e | 1 | 0.48149 | 0.26592 | -0.21348 | |
| H5 | 4e | 1 | 0.48846 | 0.23423 | -0.26688 | -1.2000 |
| C6 | 4e | 1 | 0.43762 | 0.21582 | -0.14632 | |
| C7 | 4e | 1 | 0.39252 | 0.11520 | -0.15909 | |
| N8 | 4e | 1 | 0.34654 | 0.07856 | -0.08768 | |
| C9 | 4e | 1 | 0.38428 | 0.06216 | -0.23529 | |
| H9 | 4e | 1 | 0.41596 | 0.08770 | -0.28421 | -1.2000 |
| C10 | 4e | 1 | 0.32887 | -0.02947 | -0.23968 | |
| H10 | 4e | 1 | 0.32171 | -0.06660 | -0.29210 | -1.2000 |
| C11 | 4e | 1 | 0.28466 | -0.06611 | -0.16842 | |
| H11 | 4e | 1 | 0.24642 | -0.12847 | -0.17148 | -1.2000 |
| C12 | 4e | 1 | 0.29601 | -0.01143 | -0.09121 | |
| N13 | 4e | 1 | 0.25027 | -0.05026 | -0.01829 | |
| C14 | 4e | 1 | 0.27472 | -0.02511 | 0.07206 | |
| N15 | 4e | 1 | 0.32926 | 0.06016 | 0.10086 | |
| C16 | 4e | 1 | 0.23799 | -0.08991 | 0.13290 | |
| H16 | 4e | 1 | 0.20189 | -0.15089 | 0.11353 | -1.2000 |
| C17 | 4e | 1 | 0.25459 | -0.06452 | 0.22011 | |
| H17 | 4e | 1 | 0.22902 | -0.10782 | 0.26123 | -1.2000 |
| C18 | 4e | 1 | 0.30838 | 0.02381 | 0.24875 | |
| H18 | 4e | 1 | 0.31781 | 0.04218 | 0.30899 | -1.2000 |
| C19 | 4e | 1 | 0.34755 | 0.08392 | 0.18958 | |
| C20 | 4e | 1 | 0.41297 | 0.17745 | 0.21087 | |
| C21 | 4e | 1 | 0.44259 | 0.23069 | 0.13965 | |
| C22 | 4e | 1 | 0.51881 | 0.31363 | 0.16261 | |
| H22 | 4e | 1 | 0.54214 | 0.35134 | 0.11676 | -1.2000 |
| C23 | 4e | 1 | 0.56132 | 0.34273 | 0.24903 | |
| H23 | 4e | 1 | 0.61246 | 0.39974 | 0.26139 | -1.2000 |
| C24 | 4e | 1 | 0.53053 | 0.29019 | 0.31750 | |
| H24 | 4e | 1 | 0.56006 | 0.31038 | 0.37703 | -1.2000 |
| C25 | 4e | 1 | 0.45526 | 0.20676 | 0.29825 | |
| H25 | 4e | 1 | 0.43279 | 0.16984 | 0.34488 | -1.2000 |
| C31 | 4e | 1 | 0.17279 | -0.13892 | -0.03740 | |
| C32 | 4e | 1 | 0.03664 | -0.13545 | -0.05115 | |
| H32 | 4e | 1 | -0.00767 | -0.07520 | -0.05713 | -1.2000 |
| C33 | 4e | 1 | -0.03578 | -0.22022 | -0.05627 | |
| H33 | 4e | 1 | -0.12964 | -0.21821 | -0.06505 | -1.2000 |
| C34 | 4e | 1 | 0.02979 | -0.30767 | -0.04849 | |
| C35 | 4e | 1 | 0.16686 | -0.31076 | -0.03861 | |
| H35 | 4e | 1 | 0.21110 | -0.37090 | -0.03635 | -1.2000 |
| C36 | 4e | 1 | 0.23882 | -0.22594 | -0.03208 | |
| H36 | 4e | 1 | 0.33262 | -0.22759 | -0.02402 | -1.2000 |
| C37 | 4e | 1 | -0.16208 | -0.39730 | -0.03251 | |
| H37A | 4e | 1 | -0.16316 | -0.36368 | 0.02315 | -1.5000 |
| H37B | 4e | 1 | -0.19025 | -0.46408 | -0.02795 | -1.5000 |
| H37C | 4e | 1 | -0.22276 | -0.36525 | -0.08098 | -1.5000 |
| O1 | 4e | 1 | -0.03067 | -0.39567 | -0.04968 | |

Table S5. Atomic parameter of PtLF (1).

| Atom | Wyck. | Site | x/a | y/b | z/c | U [Å ²] |
|------|-------|------|----------|----------|---------|---------------------|
| PT1 | 2i | 1 | 0.28833 | -0.51592 | 0.41572 | |
| F1 | 2i | 1 | -0.14482 | -0.96177 | 0.35135 | |

| | | | | | | |
|------|----|---|----------|----------|----------|---------|
| F2 | 2i | 1 | 0.07425 | -0.95692 | -0.07793 | |
| F3 | 2i | 1 | 0.00362 | -0.55607 | 0.75183 | |
| F4 | 2i | 1 | 0.54766 | -0.64709 | 0.03240 | |
| C1 | 2i | 1 | 0.12719 | -0.62806 | 0.45447 | |
| C2 | 2i | 1 | 0.03832 | -0.76672 | 0.37926 | |
| H2 | 2i | 1 | 0.04587 | -0.82084 | 0.29320 | -1.2000 |
| C3 | 2i | 1 | -0.05987 | -0.82546 | 0.42872 | |
| C4 | 2i | 1 | -0.07619 | -0.75672 | 0.55197 | |
| H4 | 2i | 1 | -0.14515 | -0.79948 | 0.58389 | -1.2000 |
| C5 | 2i | 1 | 0.01439 | -0.62095 | 0.62684 | |
| C6 | 2i | 1 | 0.11213 | -0.55340 | 0.58267 | |
| C7 | 2i | 1 | 0.20950 | -0.40874 | 0.66329 | |
| N8 | 2i | 1 | 0.30876 | -0.36898 | 0.60351 | |
| C9 | 2i | 1 | 0.20499 | -0.31724 | 0.78715 | |
| H9 | 2i | 1 | 0.13656 | -0.34587 | 0.82844 | -1.2000 |
| C10 | 2i | 1 | 0.30184 | -0.18332 | 0.84989 | |
| H10 | 2i | 1 | 0.29959 | -0.11906 | 0.93485 | -1.2000 |
| C11 | 2i | 1 | 0.40102 | -0.14262 | 0.79041 | |
| H11 | 2i | 1 | 0.46782 | -0.05062 | 0.83399 | -1.2000 |
| C12 | 2i | 1 | 0.40329 | -0.23866 | 0.66350 | |
| N13 | 2i | 1 | 0.50549 | -0.19317 | 0.60552 | |
| C14 | 2i | 1 | 0.54667 | -0.26274 | 0.48839 | |
| N15 | 2i | 1 | 0.46833 | -0.39500 | 0.39749 | |
| C16 | 2i | 1 | 0.67007 | -0.18923 | 0.46625 | |
| H16 | 2i | 1 | 0.72401 | -0.09551 | 0.52919 | -1.2000 |
| C17 | 2i | 1 | 0.71169 | -0.25391 | 0.35330 | |
| H17 | 2i | 1 | 0.79400 | -0.20467 | 0.33709 | -1.2000 |
| C18 | 2i | 1 | 0.63373 | -0.39139 | 0.26237 | |
| H18 | 2i | 1 | 0.66429 | -0.43767 | 0.18521 | -1.2000 |
| C19 | 2i | 1 | 0.51228 | -0.45946 | 0.28526 | |
| C20 | 2i | 1 | 0.40931 | -0.60009 | 0.19394 | |
| C21 | 2i | 1 | 0.27946 | -0.64439 | 0.23076 | |
| C22 | 2i | 1 | 0.16630 | -0.76522 | 0.13414 | |
| H22 | 2i | 1 | 0.07495 | -0.79495 | 0.15308 | -1.2000 |
| C23 | 2i | 1 | 0.18618 | -0.84051 | 0.01313 | |
| C24 | 2i | 1 | 0.31465 | -0.80588 | -0.02372 | |
| H24 | 2i | 1 | 0.32753 | -0.86229 | -0.10714 | -1.2000 |
| C25 | 2i | 1 | 0.42293 | -0.68380 | 0.06893 | |
| C31 | 2i | 1 | 0.59296 | -0.04704 | 0.68471 | |
| C32 | 2i | 1 | 0.72492 | -0.00445 | 0.77434 | |
| H32 | 2i | 1 | 0.75974 | -0.07039 | 0.78132 | -1.2000 |
| C33 | 2i | 1 | 0.80464 | 0.13423 | 0.85285 | |
| H33 | 2i | 1 | 0.89499 | 0.16355 | 0.91355 | -1.2000 |
| C34 | 2i | 1 | 0.75386 | 0.23107 | 0.84382 | |
| C35 | 2i | 1 | 0.62311 | 0.18836 | 0.75340 | |
| H35 | 2i | 1 | 0.58855 | 0.25404 | 0.74563 | -1.2000 |
| C36 | 2i | 1 | 0.54352 | 0.04865 | 0.67452 | |
| H36 | 2i | 1 | 0.45389 | 0.01899 | 0.61285 | -1.2000 |
| O1 | 2i | 1 | 0.83895 | 0.36433 | 0.92905 | |
| C37 | 2i | 1 | 0.79358 | 0.46959 | 0.92282 | |
| H37A | 2i | 1 | 0.79003 | 0.45705 | 0.83642 | -1.5000 |
| H37B | 2i | 1 | 0.86493 | 0.56026 | 0.98810 | -1.5000 |
| H37C | 2i | 1 | 0.69485 | 0.46316 | 0.93971 | -1.5000 |

Table S6. Atomic parameters of PtLF (2).

| Atom | Wyck. | Site | x/a | y/b | z/c | U [Å ²] |
|------|-------|------|---------|---------|----------|---------------------|
| Pt1 | 4g | 1 | 0.28296 | 0.40609 | 0.23518 | |
| F1 | 4g | 1 | 0.46423 | 0.20869 | 0.16732 | |
| F2 | 4g | 1 | 0.49157 | 0.15213 | 0.43585 | |
| F3 | 4g | 1 | 0.24792 | 0.26126 | 0.00048 | |
| F4 | 4g | 1 | 0.38903 | 0.50247 | 0.48929 | |
| C1 | 4g | 1 | 0.31855 | 0.32351 | 0.17873 | |
| C2 | 4g | 1 | 0.38383 | 0.28539 | 0.19594 | |
| H2 | 4g | 1 | 0.41681 | 0.28701 | 0.24105 | -1.2000 |
| C3 | 4g | 1 | 0.39977 | 0.24587 | 0.14741 | |
| C4 | 4g | 1 | 0.35487 | 0.23341 | 0.08229 | |
| H4 | 4g | 1 | 0.36699 | 0.19991 | 0.05032 | -1.2000 |
| C5 | 4g | 1 | 0.29127 | 0.27161 | 0.06515 | |
| C6 | 4g | 1 | 0.27215 | 0.32340 | 0.11031 | |
| C7 | 4g | 1 | 0.20814 | 0.38830 | 0.09212 | |
| N8 | 4g | 1 | 0.20456 | 0.44925 | 0.14446 | |
| C9 | 4g | 1 | 0.15545 | 0.39640 | 0.02926 | |
| H9 | 4g | 1 | 0.15719 | 0.35264 | -0.00709 | -1.2000 |
| C10 | 4g | 1 | 0.09989 | 0.46941 | 0.01990 | |
| H10 | 4g | 1 | 0.06314 | 0.47506 | -0.02315 | -1.2000 |
| C11 | 4g | 1 | 0.09747 | 0.53345 | 0.07212 | |
| H11 | 4g | 1 | 0.05985 | 0.58555 | 0.06535 | -1.2000 |
| C12 | 4g | 1 | 0.15143 | 0.52103 | 0.13592 | |
| N13 | 4g | 1 | 0.14774 | 0.58626 | 0.18880 | |
| C14 | 4g | 1 | 0.19477 | 0.60447 | 0.25642 | |
| N15 | 4g | 1 | 0.24809 | 0.52609 | 0.28530 | |
| C16 | 4g | 1 | 0.18205 | 0.70472 | 0.29365 | |
| H16 | 4g | 1 | 0.14405 | 0.76109 | 0.27342 | -1.2000 |
| C17 | 4g | 1 | 0.22504 | 0.71787 | 0.35810 | |
| H17 | 4g | 1 | 0.21693 | 0.78495 | 0.38340 | -1.2000 |
| C18 | 4g | 1 | 0.28095 | 0.63727 | 0.38931 | |
| H18 | 4g | 1 | 0.31040 | 0.64763 | 0.43527 | -1.2000 |
| C19 | 4g | 1 | 0.29261 | 0.54160 | 0.35174 | |
| C20 | 4g | 1 | 0.34769 | 0.44623 | 0.37567 | |
| C21 | 4g | 1 | 0.35274 | 0.36258 | 0.32634 | |

| | | | | | | |
|------|----|---|----------|----------|----------|---------|
| C22 | 4g | 1 | 0.40182 | 0.26280 | 0.34905 | |
| H22 | 4g | 1 | 0.40540 | 0.20283 | 0.31821 | -1.2000 |
| C23 | 4g | 1 | 0.44506 | 0.25049 | 0.41572 | |
| C24 | 4g | 1 | 0.44217 | 0.33073 | 0.46360 | |
| H24 | 4g | 1 | 0.47264 | 0.32120 | 0.50932 | -1.2000 |
| C25 | 4g | 1 | 0.39195 | 0.42663 | 0.44105 | |
| C31 | 4g | 1 | 0.08431 | 0.65183 | 0.17199 | |
| C32 | 4g | 1 | 0.07374 | 0.78695 | 0.15544 | |
| H32 | 4g | 1 | 0.10644 | 0.83756 | 0.15024 | -1.2000 |
| C33 | 4g | 1 | 0.01601 | 0.84986 | 0.14630 | |
| H33 | 4g | 1 | 0.01007 | 0.94426 | 0.13711 | -1.2000 |
| C34 | 4g | 1 | -0.03329 | 0.77465 | 0.15058 | |
| C35 | 4g | 1 | -0.02317 | 0.63764 | 0.16541 | |
| H35 | 4g | 1 | -0.05713 | 0.58580 | 0.16768 | -1.2000 |
| C36 | 4g | 1 | 0.03504 | 0.57525 | 0.17690 | |
| H36 | 4g | 1 | 0.04177 | 0.48170 | 0.18799 | -1.2000 |
| O1 | 4g | 1 | -0.09099 | 0.82806 | 0.14337 | |
| C37 | 4g | 1 | -0.09428 | 0.97105 | 0.15251 | |
| H37A | 4g | 1 | -0.05655 | 0.99871 | 0.19434 | -1.5000 |
| H37B | 4g | 1 | -0.13555 | 0.99253 | 0.15384 | -1.5000 |
| H37C | 4g | 1 | -0.09298 | 1.01972 | 0.11558 | -1.5000 |
| PT1A | 4g | 1 | 0.20375 | 0.10132 | 0.24298 | |
| F1A | 4g | 1 | 0.17551 | 0.43564 | 0.41747 | |
| F2A | 4g | 1 | -0.04539 | 0.28605 | 0.16298 | |
| F3A | 4g | 1 | 0.34422 | 0.11338 | 0.50206 | |
| F4A | 4g | 1 | 0.01316 | 0.15885 | 0.00019 | |
| C1A | 4g | 1 | 0.21879 | 0.18015 | 0.32969 | |
| C2A | 4g | 1 | 0.18749 | 0.28621 | 0.34320 | |
| H2A | 4g | 1 | 0.15118 | 0.32948 | 0.30754 | -1.2000 |
| C3A | 4g | 1 | 0.20719 | 0.33024 | 0.40598 | |
| C4A | 4g | 1 | 0.25895 | 0.27235 | 0.46017 | |
| H4A | 4g | 1 | 0.27130 | 0.30318 | 0.50392 | -1.2000 |
| C5A | 4g | 1 | 0.29202 | 0.16847 | 0.44858 | |
| C6A | 4g | 1 | 0.27501 | 0.12319 | 0.38489 | |
| C7A | 4g | 1 | 0.31382 | 0.02176 | 0.36841 | |
| N8A | 4g | 1 | 0.29119 | 0.00658 | 0.30152 | |
| C9A | 4g | 1 | 0.36866 | -0.04803 | 0.41353 | |
| H9A | 4g | 1 | 0.38449 | -0.03726 | 0.45994 | -1.2000 |
| C10A | 4g | 1 | 0.39970 | -0.13375 | 0.38914 | |
| H10A | 4g | 1 | 0.43756 | -0.18302 | 0.41927 | -1.2000 |
| C11A | 4g | 1 | 0.37741 | -0.14928 | 0.32320 | |
| H11A | 4g | 1 | 0.39899 | -0.21062 | 0.30742 | -1.2000 |
| C12A | 4g | 1 | 0.32292 | -0.07568 | 0.27833 | |
| N13A | 4g | 1 | 0.30350 | -0.08847 | 0.20954 | |
| C14A | 4g | 1 | 0.24759 | -0.04096 | 0.15310 | |
| N15A | 4g | 1 | 0.19919 | 0.02962 | 0.15688 | |
| C16A | 4g | 1 | 0.24354 | -0.06373 | 0.09053 | |
| H16A | 4g | 1 | 0.27858 | -0.10967 | 0.08745 | -1.2000 |
| C17A | 4g | 1 | 0.19087 | -0.02166 | 0.03475 | |
| H17A | 4g | 1 | 0.18863 | -0.04019 | -0.00721 | -1.2000 |
| C18A | 4g | 1 | 0.13979 | 0.04859 | 0.03801 | |
| H18A | 4g | 1 | 0.10272 | 0.07918 | -0.00124 | -1.2000 |
| C19A | 4g | 1 | 0.14415 | 0.07294 | 0.09962 | |
| C20A | 4g | 1 | 0.09492 | 0.14131 | 0.11345 | |
| C21A | 4g | 1 | 0.11217 | 0.16462 | 0.18173 | |
| C22A | 4g | 1 | 0.06254 | 0.21044 | 0.19638 | |
| H22A | 4g | 1 | 0.07169 | 0.22187 | 0.24129 | -1.2000 |
| C23A | 4g | 1 | 0.00133 | 0.23865 | 0.14671 | |
| C24A | 4g | 1 | -0.01660 | 0.22529 | 0.08073 | |
| H24A | 4g | 1 | -0.05929 | 0.24999 | 0.04704 | -1.2000 |
| C25A | 4g | 1 | 0.03125 | 0.17373 | 0.06632 | |
| C31A | 4g | 1 | 0.35138 | -0.15682 | 0.19468 | |
| C32A | 4g | 1 | 0.34865 | -0.29431 | 0.18252 | |
| H32A | 4g | 1 | 0.31600 | -0.34867 | 0.18591 | -1.2000 |
| C33A | 4g | 1 | 0.39328 | -0.35211 | 0.16552 | |
| H33A | 4g | 1 | 0.39214 | -0.44705 | 0.15800 | -1.2000 |
| C34A | 4g | 1 | 0.44013 | -0.27218 | 0.15927 | |
| C35A | 4g | 1 | 0.44271 | -0.13529 | 0.17089 | |
| H35A | 4g | 1 | 0.47460 | -0.08056 | 0.16635 | -1.2000 |
| C36A | 4g | 1 | 0.39824 | -0.07737 | 0.18939 | |
| H36A | 4g | 1 | 0.40020 | 0.01705 | 0.19839 | -1.2000 |
| O1A | 4g | 1 | 0.48662 | -0.32182 | 0.14264 | |
| C37A | 4g | 1 | 0.49694 | -0.46554 | 0.14559 | |
| H37D | 4g | 1 | 0.50907 | -0.49808 | 0.19049 | -1.5000 |
| H37E | 4g | 1 | 0.53264 | -0.48636 | 0.13454 | -1.5000 |
| H37F | 4g | 1 | 0.45617 | -0.51046 | 0.11377 | -1.5000 |

Table S7. Atomic parameters of PdLH.

| Atom | Wyck. | Site | x/a | y/b | z/c | U [Å ²] |
|------|-------|------|---------|---------|---------|---------------------|
| PD1 | 2i | 1 | 0.72277 | 1.03142 | 0.59471 | |
| O1 | 2i | 1 | 0.16003 | 0.12568 | 0.07089 | |
| C1 | 2i | 1 | 0.72726 | 1.16112 | 0.78285 | |
| C2 | 2i | 1 | 0.84080 | 1.28457 | 0.88209 | |
| H2 | 2i | 1 | 0.93787 | 1.31813 | 0.86420 | -1.2000 |
| C3 | 2i | 1 | 0.81570 | 1.36002 | 1.00678 | |
| H3 | 2i | 1 | 0.89525 | 1.44375 | 1.07201 | -1.2000 |
| C4 | 2i | 1 | 0.67534 | 1.31351 | 1.03603 | |
| H4 | 2i | 1 | 0.65613 | 1.36729 | 1.11939 | -1.2000 |
| C5 | 2i | 1 | 0.56310 | 1.18689 | 0.94143 | |
| H5 | 2i | 1 | 0.46762 | 1.15247 | 0.96102 | -1.2000 |

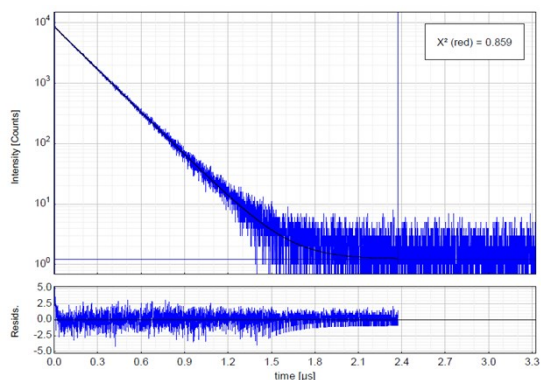
| | | | | | |
|------|----|---|---------|----------|-----------------|
| C6 | 2i | 1 | 0.59026 | 1.11017 | 0.81772 |
| C7 | 2i | 1 | 0.48353 | 0.96558 | 0.72288 |
| N8 | 2i | 1 | 0.53010 | 0.90043 | 0.60935 |
| C9 | 2i | 1 | 0.35337 | 0.89490 | 0.74780 |
| H9 | 2i | 1 | 0.32162 | 0.94088 | 0.82692 -1.2000 |
| C10 | 2i | 1 | 0.26978 | 0.75525 | 0.65487 |
| H10 | 2i | 1 | 0.18075 | 0.70449 | 0.67061 -1.2000 |
| C11 | 2i | 1 | 0.31637 | 0.69067 | 0.53996 |
| H11 | 2i | 1 | 0.25973 | 0.59524 | 0.47634 -1.2000 |
| C12 | 2i | 1 | 0.44800 | 0.76652 | 0.51721 |
| N13 | 2i | 1 | 0.49390 | 0.69824 | 0.39930 |
| C14 | 2i | 1 | 0.60257 | 0.74943 | 0.33962 |
| N15 | 2i | 1 | 0.70319 | 0.88227 | 0.40350 |
| C16 | 2i | 1 | 0.60688 | 0.65742 | 0.21140 |
| H16 | 2i | 1 | 0.53553 | 0.56360 | 0.16527 -1.2000 |
| C17 | 2i | 1 | 0.71454 | 0.70297 | 0.15225 |
| H17 | 2i | 1 | 0.71713 | 0.64072 | 0.06508 -1.2000 |
| C18 | 2i | 1 | 0.81849 | 0.83867 | 0.21927 |
| H18 | 2i | 1 | 0.89447 | 0.87039 | 0.17972 -1.2000 |
| C19 | 2i | 1 | 0.81042 | 0.92857 | 0.34587 |
| C20 | 2i | 1 | 0.91351 | 1.07650 | 0.42841 |
| C21 | 2i | 1 | 0.89420 | 1.15185 | 0.55765 |
| C22 | 2i | 1 | 0.98741 | 1.29336 | 0.63132 |
| H22 | 2i | 1 | 0.97742 | 1.34742 | 0.71823 -1.2000 |
| C23 | 2i | 1 | 1.09399 | 1.35817 | 0.58274 |
| H23 | 2i | 1 | 1.15420 | 1.45516 | 0.63584 -1.2000 |
| C24 | 2i | 1 | 1.11315 | 1.28200 | 0.45682 |
| H24 | 2i | 1 | 1.18743 | 1.32560 | 0.42365 -1.2000 |
| C25 | 2i | 1 | 1.02161 | 1.14053 | 0.37990 |
| H25 | 2i | 1 | 1.03328 | 1.08734 | 0.29338 -1.2000 |
| C31 | 2i | 1 | 0.40557 | 0.54864 | 0.31831 |
| C32 | 2i | 1 | 0.26959 | 0.50178 | 0.23074 |
| H32 | 2i | 1 | 0.23167 | 0.56742 | 0.22576 -1.2000 |
| C33 | 2i | 1 | 0.18868 | 0.35991 | 0.15048 |
| H33 | 2i | 1 | 0.09438 | 0.32787 | 0.09125 -1.2000 |
| C34 | 2i | 1 | 0.24580 | 0.26341 | 0.15654 |
| C35 | 2i | 1 | 0.38184 | 0.31036 | 0.24597 |
| H35 | 2i | 1 | 0.42002 | 0.24526 | 0.25179 -1.2000 |
| C36 | 2i | 1 | 0.46119 | 0.45422 | 0.32683 |
| H36 | 2i | 1 | 0.55408 | 0.48739 | 0.38813 -1.2000 |
| C37 | 2i | 1 | 0.20998 | 0.02354 | 0.07967 |
| H37A | 2i | 1 | 0.31477 | 0.03559 | 0.06435 -1.5000 |
| H37B | 2i | 1 | 0.13953 | -0.07086 | 0.01376 -1.5000 |
| H37C | 2i | 1 | 0.20973 | 0.03615 | 0.16691 -1.5000 |

Table S8. Atomic parameters of PdLF.

| Atom | Wyck. Site | x/a | y/b | z/c | U [Å ²] |
|------|------------|-----|------------|------------|---------------------|
| Pd1 | 2i | 1 | 0.18284(3) | 0.16913(3) | 0.78306(2) |
| N1 | 2i | 1 | 0.1767(4) | 0.2407(3) | 0.9699(2) |
| C2 | 2i | 1 | 0.1483(4) | 0.2520(4) | 1.0502(2) |
| C3 | 2i | 1 | 0.2342(5) | 0.3381(4) | 1.1075(3) |
| H3 | 2i | 1 | 0.30880 | 0.39210 | 1.09470 |
| C4 | 2i | 1 | 0.2094(5) | 0.3438(4) | 1.1833(3) |
| H4 | 2i | 1 | 0.26590 | 0.40340 | 1.22240 |
| C5 | 2i | 1 | 0.1007(5) | 0.2617(4) | 1.2022(3) |
| C6 | 2i | 1 | 0.0153(4) | 0.1764(4) | 1.1445(3) |
| H6 | 2i | 1 | -0.05880 | 0.12140 | 1.15720 |
| C7 | 2i | 1 | 0.0399(4) | 0.1728(4) | 1.0680(3) |
| H7 | 2i | 1 | -0.01820 | 0.11570 | 1.02820 |
| O8 | 2i | 1 | 0.0868(3) | 0.2716(3) | 1.27958(18) |
| C25 | 2i | 1 | -0.0068(5) | 0.1747(4) | 1.3053(3) |
| H25A | 2i | 1 | -0.08780 | 0.16730 | 1.28140 |
| H25B | 2i | 1 | 0.00010 | 0.18790 | 1.36210 |
| H25C | 2i | 1 | 0.00360 | 0.10290 | 1.28980 |
| C20 | 2i | 1 | 0.1369(4) | 0.3061(4) | 0.9193(3) |
| C21 | 2i | 1 | 0.1135(6) | 0.3998(5) | 0.9516(3) |
| H21 | 2i | 1 | 0.12980 | 0.42250 | 1.00640 |
| C22 | 2i | 1 | 0.0665(6) | 0.4586(5) | 0.9028(3) |
| H22 | 2i | 1 | 0.05030 | 0.52190 | 0.92430 |
| C23 | 2i | 1 | 0.0428(5) | 0.4262(5) | 0.8225(3) |
| H23 | 2i | 1 | 0.00840 | 0.46530 | 0.78920 |
| C24 | 2i | 1 | 0.0704(4) | 0.3358(4) | 0.7919(3) |
| N25 | 2i | 1 | 0.1180(3) | 0.2774(3) | 0.8405(2) |
| C30 | 2i | 1 | 0.2382(4) | 0.1663(4) | 0.9579(3) |
| C31 | 2i | 1 | 0.2776(5) | 0.1214(5) | 1.0231(3) |
| H31 | 2i | 1 | 0.26250 | 0.14100 | 1.07360 |
| C32 | 2i | 1 | 0.3373(5) | 0.0498(5) | 1.0124(3) |
| H32 | 2i | 1 | 0.36380 | 0.02000 | 1.05590 |
| C33 | 2i | 1 | 0.3601(5) | 0.0195(5) | 0.9386(3) |
| H33 | 2i | 1 | 0.40060 | -0.03110 | 0.93120 |
| C34 | 2i | 1 | 0.3216(4) | 0.0659(4) | 0.8762(3) |
| N35 | 2i | 1 | 0.2594(3) | 0.1362(3) | 0.88614(19) |
| C40 | 2i | 1 | 0.0479(4) | 0.2867(4) | 0.7081(3) |
| C41 | 2i | 1 | -0.0165(5) | 0.3177(5) | 0.6483(3) |
| C42 | 2i | 1 | -0.0471(5) | 0.2620(5) | 0.5716(3) |
| H42 | 2i | 1 | -0.09130 | 0.28420 | 0.53200 |
| C43 | 2i | 1 | -0.0099(5) | 0.1737(5) | 0.5569(3) |
| C44 | 2i | 1 | 0.0561(4) | 0.1396(4) | 0.6119(2) |
| H44 | 2i | 1 | 0.07850 | 0.07700 | 0.59810 |
| C45 | 2i | 1 | 0.0901(4) | 0.1977(4) | 0.6887(3) |

| | | | | | | |
|------|----|---|------------|------------|-------------|--------|
| F46 | 2i | 1 | -0.0538(3) | 0.4058(3) | 0.6626(2) | |
| F47 | 2i | 1 | -0.0429(3) | 0.1137(3) | 0.48241(16) | |
| C50 | 2i | 1 | 0.3361(4) | 0.0417(4) | 0.7937(3) | |
| C51 | 2i | 1 | 0.4114(5) | -0.0121(5) | 0.7701(3) | |
| C52 | 2i | 1 | 0.4216(6) | -0.0377(6) | 0.6932(3) | |
| H52 | 2i | 1 | 0.47160 | -0.07650 | 0.67880 | 0.0850 |
| C53 | 2i | 1 | 0.3546(5) | -0.0037(5) | 0.6385(3) | |
| C54 | 2i | 1 | 0.2843(4) | 0.0551(4) | 0.6569(3) | |
| H54 | 2i | 1 | 0.24440 | 0.08040 | 0.61680 | 0.0550 |
| C55 | 2i | 1 | 0.2707(4) | 0.0784(4) | 0.7348(2) | |
| F56 | 2i | 1 | 0.4802(3) | -0.0439(4) | 0.82395(19) | |
| F57 | 2i | 1 | 0.3609(3) | -0.0297(3) | 0.56094(18) | |
| Pd1A | 2i | 1 | 0.40601(3) | 0.41555(3) | 0.69293(2) | |
| N1A | 2i | 1 | 0.3811(3) | 0.3006(3) | 0.5095(2) | |
| C2A | 2i | 1 | 0.3543(4) | 0.2322(4) | 0.4314(2) | |
| C3A | 2i | 1 | 0.4164(4) | 0.2833(4) | 0.3712(3) | |
| H3A | 2i | 1 | 0.47920 | 0.36000 | 0.38110 | 0.0600 |
| C4A | 2i | 1 | 0.3849(4) | 0.2208(4) | 0.2971(3) | |
| H4A | 2i | 1 | 0.42720 | 0.25440 | 0.25620 | 0.0570 |
| C5A | 2i | 1 | 0.2912(4) | 0.1084(4) | 0.2823(2) | |
| C6A | 2i | 1 | 0.2323(4) | 0.0567(4) | 0.3424(2) | |
| H6A | 2i | 1 | 0.17130 | -0.02090 | 0.33320 | 0.0500 |
| C7A | 2i | 1 | 0.2646(4) | 0.1213(4) | 0.4172(3) | |
| H7A | 2i | 1 | 0.22350 | 0.08750 | 0.45840 | 0.0520 |
| O8A | 2i | 1 | 0.2651(3) | 0.0557(3) | 0.20608(17) | |
| C9A | 2i | 1 | 0.1636(5) | -0.0559(5) | 0.1865(3) | |
| H9A1 | 2i | 1 | 0.17950 | -0.11220 | 0.21680 | 0.0890 |
| H9A2 | 2i | 1 | 0.15350 | -0.08250 | 0.13080 | 0.0890 |
| H9A3 | 2i | 1 | 0.08860 | -0.04910 | 0.19880 | 0.0890 |
| C20A | 2i | 1 | 0.3170(4) | 0.3734(4) | 0.5174(3) | |
| C21A | 2i | 1 | 0.2455(5) | 0.3841(4) | 0.4502(3) | |
| H21A | 2i | 1 | 0.24190 | 0.34380 | 0.40090 | 0.0660 |
| C22A | 2i | 1 | 0.1818(5) | 0.4533(5) | 0.4571(3) | |
| H22A | 2i | 1 | 0.13460 | 0.46090 | 0.41210 | 0.0720 |
| C23A | 2i | 1 | 0.1850(5) | 0.5120(5) | 0.5283(3) | |
| H23A | 2i | 1 | 0.14000 | 0.55920 | 0.53280 | 0.0680 |
| C24A | 2i | 1 | 0.2558(4) | 0.5005(4) | 0.5937(3) | |
| N25A | 2i | 1 | 0.3209(3) | 0.4320(3) | 0.5874(2) | |
| C30A | 2i | 1 | 0.4739(4) | 0.2869(4) | 0.5624(3) | |
| C31A | 2i | 1 | 0.5465(5) | 0.2344(5) | 0.5323(3) | |
| H31A | 2i | 1 | 0.53620 | 0.21120 | 0.47780 | 0.0750 |
| C32A | 2i | 1 | 0.6329(5) | 0.2166(6) | 0.5824(3) | |
| H32A | 2i | 1 | 0.68290 | 0.18170 | 0.56220 | 0.0890 |
| C33A | 2i | 1 | 0.6477(5) | 0.2495(5) | 0.6625(3) | |
| H33A | 2i | 1 | 0.70730 | 0.23770 | 0.69710 | 0.0830 |
| C34A | 2i | 1 | 0.5733(4) | 0.3000(4) | 0.6904(3) | |
| N35A | 2i | 1 | 0.4876(3) | 0.3187(3) | 0.6402(2) | |
| C40A | 2i | 1 | 0.2704(4) | 0.5582(4) | 0.6743(3) | |
| C41A | 2i | 1 | 0.2218(5) | 0.6397(5) | 0.6944(3) | |
| C42A | 2i | 1 | 0.2409(6) | 0.6968(5) | 0.7696(3) | |
| H42A | 2i | 1 | 0.20490 | 0.74990 | 0.78200 | 0.0860 |
| C43A | 2i | 1 | 0.3148(6) | 0.6722(5) | 0.8248(3) | |
| C44A | 2i | 1 | 0.3660(5) | 0.5938(4) | 0.8099(3) | |
| H44A | 2i | 1 | 0.41710 | 0.58100 | 0.85050 | 0.0600 |
| C45A | 2i | 1 | 0.3431(4) | 0.5324(4) | 0.7350(2) | |
| F46A | 2i | 1 | 0.1509(4) | 0.6675(3) | 0.63897(19) | |
| F47A | 2i | 1 | 0.3370(4) | 0.7299(3) | 0.89964(18) | |
| C50A | 2i | 1 | 0.5695(4) | 0.3323(4) | 0.7744(3) | |
| C51A | 2i | 1 | 0.6314(5) | 0.3038(5) | 0.8370(3) | |
| C52A | 2i | 1 | 0.6146(5) | 0.3211(5) | 0.9142(3) | |
| H52A | 2i | 1 | 0.65860 | 0.30190 | 0.95560 | 0.0730 |
| C53A | 2i | 1 | 0.5309(5) | 0.3672(4) | 0.9270(3) | |
| C54A | 2i | 1 | 0.4673(4) | 0.3991(4) | 0.8682(2) | |
| H54A | 2i | 1 | 0.41020 | 0.43060 | 0.88030 | 0.0490 |
| C55A | 2i | 1 | 0.4874(4) | 0.3849(4) | 0.7907(3) | |
| F56A | 2i | 1 | 0.7135(4) | 0.2553(4) | 0.82454(19) | |
| F57A | 2i | 1 | 0.5073(3) | 0.3802(3) | 1.00185(16) | |

Section S4: Photophysical characterization of PtLH, PtLF, PdLH and PdLF



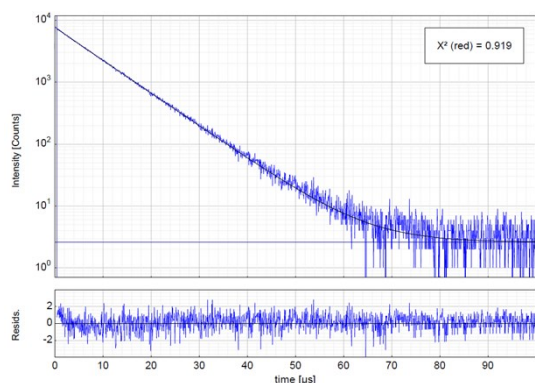
| Parameter | Value | Conf. Lower | Conf. Upper | Conf. Estimation |
|---------------------|----------|-------------|-------------|------------------|
| A_1 [Cnts] | 8384.3 | -48.1 | +48.1 | Fitting |
| τ_1 [μ s] | 0.184247 | -0.000762 | +0.000762 | Fitting |
| Bkgr. Dec [Cnts] | 1.235 | -0.387 | +0.387 | Fitting |

Average Lifetime:

$$\tau_{Av,1} = 0.184247 \mu\text{s (intensity weighted)}$$

$$\tau_{Av,2} = 0.184247 \mu\text{s (amplitude weighted)}$$

Figure S46. Left: Time-resolved photoluminescence decay of **PtLH** in aerated DCM at 298 K, including the residuals ($\lambda_{exc} = 376.7$ nm, $\lambda_{em} = 530$ nm). Right: Fitting parameters including pre-exponential factors and confidence limits.



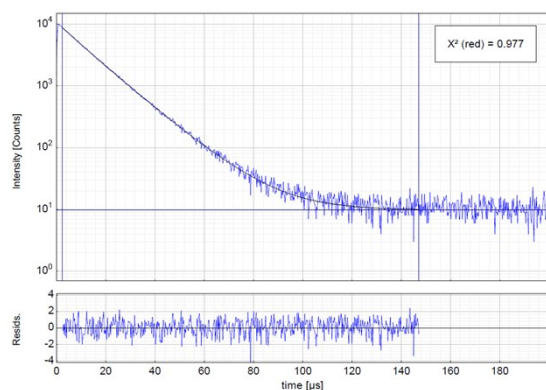
| Parameter | Value | Conf. Lower | Conf. Upper | Conf. Estimation |
|---------------------|--------|-------------|-------------|------------------|
| A_1 [Cnts] | 7272.4 | -45.1 | +45.1 | Fitting |
| τ_1 [μ s] | 8.1793 | -0.0368 | +0.0368 | Fitting |
| Bkgr. Dec [Cnts] | 2.621 | -0.489 | +0.489 | Fitting |

Average Lifetime:

$$\tau_{Av,1} = 8.1793 \mu\text{s (intensity weighted)}$$

$$\tau_{Av,2} = 8.1793 \mu\text{s (amplitude weighted)}$$

Figure S47. Left: Time-resolved photoluminescence decay of **PtLH** in deaerated DCM at 298 K, including the residuals ($\lambda_{exc} = 376.7$ nm, $\lambda_{em} = 530$ nm). Right: Fitting parameters including pre-exponential factors and confidence limits.



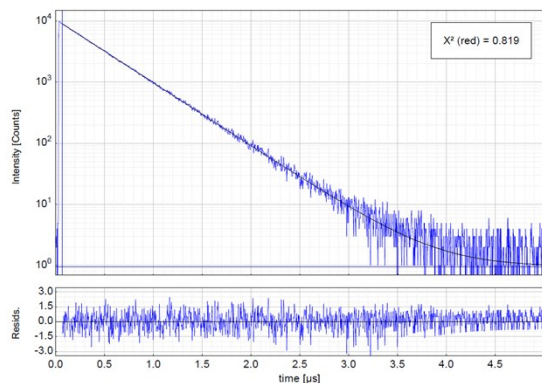
| Parameter | Value | Conf. Lower | Conf. Upper | Conf. Estimation |
|---------------------|---------|-------------|-------------|------------------|
| A_1 [Cnts] | 4439.1 | -42.1 | +42.1 | Fitting |
| τ_1 [μ s] | 14.4664 | -0.0938 | +0.0938 | Fitting |
| A_2 [Cnts] | 4187.5 | -58.2 | +58.2 | Fitting |
| τ_2 [μ s] | 10.248 | -0.120 | +0.120 | Fitting |
| Bkgr. Dec [Cnts] | 9.921 | -0.849 | +0.849 | Fitting |

Average Lifetime:

$$\tau_{Av,1} = 12.7765 \mu\text{s (intensity weighted)}$$

$$\tau_{Av,2} = 12.4185 \mu\text{s (amplitude weighted)}$$

Figure S48. Left: Time-resolved photoluminescence decay of **PtLH** in a frozen glassy matrix of DCM/MeOH (V:V = 1:1) at 77 K, including the residuals ($\lambda_{exc} = 376.7$ nm, $\lambda_{em} = 530$ nm). Right: Fitting parameters including pre-exponential factors and confidence limits.



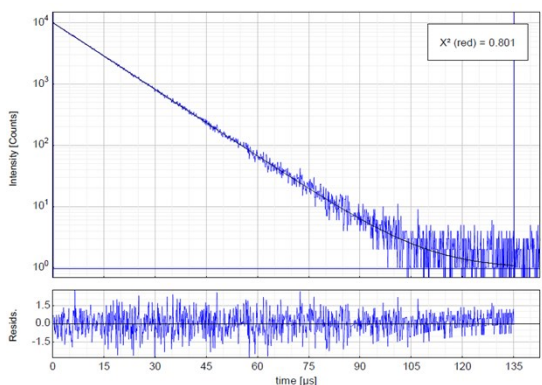
| Parameter | Value | Conf. Lower | Conf. Upper | Conf. Estimation |
|---------------------|---------|-------------|-------------|------------------|
| A_1 [Cnts] | 8923.6 | -46.2 | +46.2 | Fitting |
| τ_1 [μ s] | 0.42034 | -0.00157 | +0.00157 | Fitting |
| Bkgr. Dec [Cnts] | 0.958 | -0.403 | +0.403 | Fitting |

Average Lifetime:

$$\tau_{Av,1} = 0.42034 \mu\text{s (intensity weighted)}$$

$$\tau_{Av,2} = 0.42034 \mu\text{s (amplitude weighted)}$$

Figure S49. Left: Time-resolved photoluminescence decay of PtLF in aerated DCM at 298 K, including the residuals ($\lambda_{exc} = 376.7$ nm, $\lambda_{em} = 500$ nm). Right: Fitting parameters including pre-exponential factors and confidence limits.



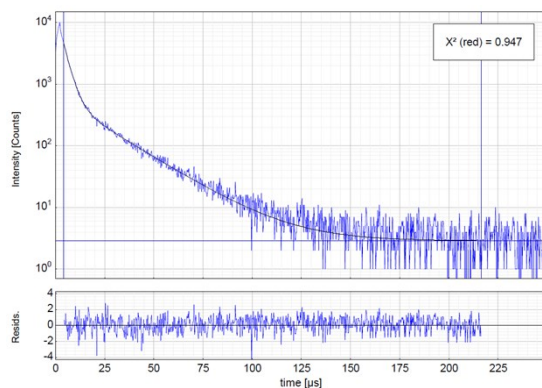
| Parameter | Value | Conf. Lower | Conf. Upper | Conf. Estimation |
|---------------------|---------|-------------|-------------|------------------|
| A_1 [Cnts] | 9895.1 | -47.2 | +47.2 | Fitting |
| τ_1 [μ s] | 11.9304 | -0.0409 | +0.0409 | Fitting |
| Bkgr. Dec [Cnts] | 0.968 | -0.420 | +0.420 | Fitting |

Average Lifetime:

$$\tau_{Av,1} = 11.9304 \mu\text{s (intensity weighted)}$$

$$\tau_{Av,2} = 11.9304 \mu\text{s (amplitude weighted)}$$

Figure S50. Left: Time-resolved photoluminescence decay of PtLF in deaerated DCM at 298 K, including the residuals ($\lambda_{exc} = 376.7$ nm, $\lambda_{em} = 500$ nm). Right: Fitting parameters including pre-exponential factors and confidence limits.



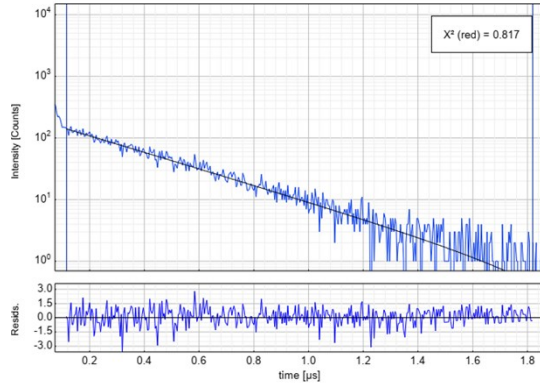
| Parameter | Value | Conf. Lower | Conf. Upper | Conf. Estimation |
|---------------------|--------|-------------|-------------|------------------|
| A_1 [Cnts] | 515.8 | -13.1 | +13.1 | Fitting |
| τ_1 [μ s] | 21.805 | -0.373 | +0.373 | Fitting |
| A_2 [Cnts] | 3843.2 | -88.9 | +88.9 | Fitting |
| τ_2 [μ s] | 3.1249 | -0.0698 | +0.0698 | Fitting |
| Bkgr. Dec [Cnts] | 2.869 | -0.448 | +0.448 | Fitting |

Average Lifetime:

$$\tau_{Av,1} = 12.159 \mu\text{s (intensity weighted)}$$

$$\tau_{Av,2} = 5.336 \mu\text{s (amplitude weighted)}$$

Figure S51. Left: Time-resolved photoluminescence decay of PtLF in a frozen glassy matrix of DCM/MeOH (V:V = 1:1) at 77 K, including the residuals ($\lambda_{exc} = 376.7$ nm, $\lambda_{em} = 500$ nm). Right: Fitting parameters including pre-exponential factors and confidence limits.



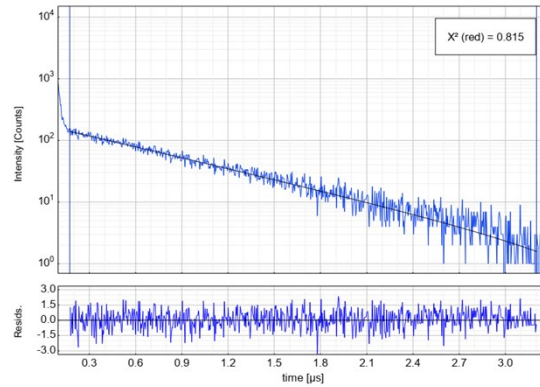
| Parameter | Value | Conf. Lower | Conf. Upper | Conf. Estimation |
|-----------------------|---------|-------------|-------------|------------------|
| A ₁ [Cnts] | 140.50 | -3.95 | +3.95 | Fitting |
| τ ₁ [μs] | 0.32556 | -0.00728 | +0.00728 | Fitting |
| Bkgr. Dec [Cnts] | -0.324 | -0.365 | +0.365 | Fitting |

Average Lifetime:

$$\tau_{Av,1} = 0.32556 \mu\text{s (intensity weighted)}$$

$$\tau_{Av,2} = 0.32556 \mu\text{s (amplitude weighted)}$$

Figure S52. Left: Time-resolved photoluminescence decay of PdLH in aerated DCM at 298 K, including the residuals ($\lambda_{exc} = 376.7$ nm, $\lambda_{em} = 500$ nm). Right: Fitting parameters including pre-exponential factors and confidence limits.



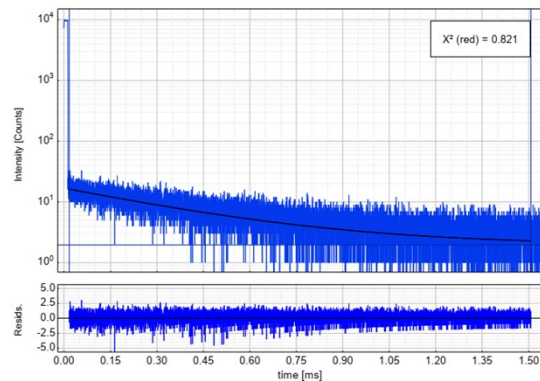
| Parameter | Value | Conf. Lower | Conf. Upper | Conf. Estimation |
|-----------------------|--------|-------------|-------------|------------------|
| A ₁ [Cnts] | 140.25 | -3.47 | +3.47 | Fitting |
| τ ₁ [μs] | 0.7459 | -0.0152 | +0.0152 | Fitting |
| Bkgr. Dec [Cnts] | -0.843 | -0.477 | +0.477 | Fitting |

Average Lifetime:

$$\tau_{Av,1} = 0.7459 \mu\text{s (intensity weighted)}$$

$$\tau_{Av,2} = 0.7459 \mu\text{s (amplitude weighted)}$$

Figure S53. Left: Time-resolved photoluminescence decay of PdLH in deaerated DCM at 298 K, including the residuals ($\lambda_{exc} = 376.7$ nm, $\lambda_{em} = 500$ nm). Right: Fitting parameters including pre-exponential factors and confidence limits.



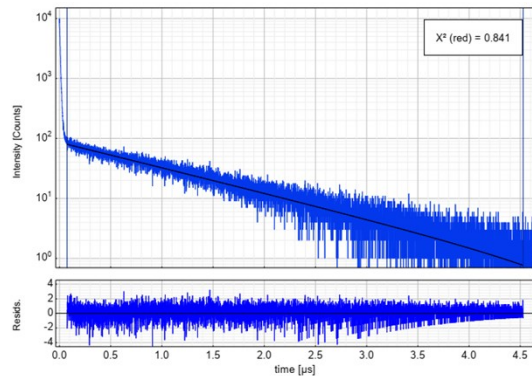
| Parameter | Value | Conf. Lower | Conf. Upper | Conf. Estimation |
|-----------------------|--------|-------------|-------------|------------------|
| A ₁ [Cnts] | 14.25 | -1.38 | +1.38 | Fitting |
| τ ₁ [ms] | 0.3953 | -0.0409 | +0.0409 | Fitting |
| Bkgr. Dec [Cnts] | 1.962 | -0.347 | +0.347 | Fitting |

Average Lifetime:

$$\tau_{Av,1} = 0.3953 \text{ ms (intensity weighted)}$$

$$\tau_{Av,2} = 0.3953 \text{ ms (amplitude weighted)}$$

Figure S54. Left: Time-resolved photoluminescence decay of PdLH in a frozen glassy matrix of DCM/MeOH (V:V = 1:1) at 77 K, including the residuals ($\lambda_{exc} = 376.7$ nm, $\lambda_{em} = 525$ nm). Right: Fitting parameters including pre-exponential factors and confidence limits.



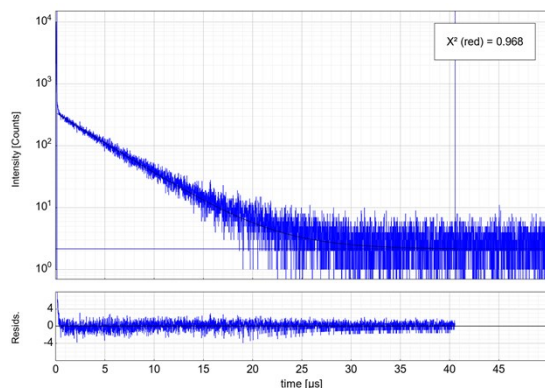
| Parameter | Value | Conf. Lower | Conf. Upper | Conf. Estimation |
|---------------------|--------|-------------|-------------|------------------|
| A_1 [Cnts] | 79.99 | -2.81 | +2.81 | Fitting |
| τ_1 [μ s] | 1.0327 | -0.0315 | +0.0315 | Fitting |
| Bkgr. Dec. [Cnts] | -0.305 | -0.380 | +0.380 | Fitting |

Average Lifetime:

$$\tau_{Av,1} = 1.0327 \mu\text{s (intensity weighted)}$$

$$\tau_{Av,2} = 1.0327 \mu\text{s (amplitude weighted)}$$

Figure S55. Left: Time-resolved photoluminescence decay of PdLF in aerated DCM at 298 K, including the residuals ($\lambda_{exc} = 376.7$ nm, $\lambda_{em} = 500$ nm). Right: Fitting parameters including pre-exponential factors and confidence limits.



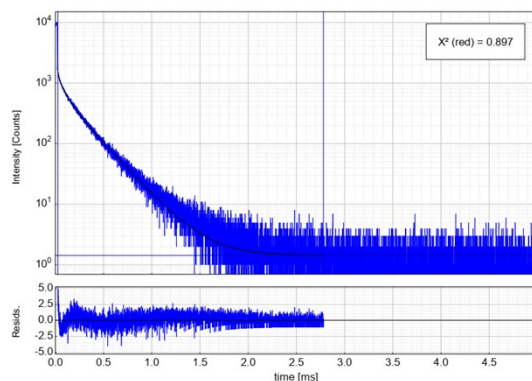
| Parameter | Value | Conf. Lower | Conf. Upper | Conf. Estimation |
|---------------------|--------|-------------|-------------|------------------|
| A_1 [Cnts] | 329.24 | -8.80 | +8.80 | Fitting |
| τ_1 [μ s] | 4.3855 | -0.0946 | +0.0946 | Fitting |
| Bkgr. Dec. [Cnts] | 2.157 | -0.411 | +0.411 | Fitting |

Average Lifetime:

$$\tau_{Av,1} = 4.3855 \mu\text{s (intensity weighted)}$$

$$\tau_{Av,2} = 4.3855 \mu\text{s (amplitude weighted)}$$

Figure S56. Left: Time-resolved photoluminescence decay of PdLF in deaerated DCM at 298 K, including the residuals ($\lambda_{exc} = 376.7$ nm, $\lambda_{em} = 500$ nm). Right: Fitting parameters including pre-exponential factors and confidence limits.



| Parameter | Value | Conf. Lower | Conf. Upper | Conf. Estimation |
|-------------------|---------|-------------|-------------|------------------|
| A_1 [Cnts] | 702.3 | -14.5 | +14.5 | Fitting |
| τ_1 [ms] | 0.24875 | -0.00364 | +0.00364 | Fitting |
| A_2 [Cnts] | 669.4 | -45.7 | +45.7 | Fitting |
| τ_2 [ms] | 0.05918 | -0.00453 | +0.00453 | Fitting |
| Bkgr. Dec. [Cnts] | 1.442 | -0.349 | +0.349 | Fitting |

Average Lifetime:

$$\tau_{Av,1} = 0.21371 \text{ ms (intensity weighted)}$$

$$\tau_{Av,2} = 0.15623 \text{ ms (amplitude weighted)}$$

Figure S57. Left: Time-resolved photoluminescence decay of PdLF in a frozen glassy matrix of DCM/MeOH (V:V = 1:1) at 77 K, including the residuals ($\lambda_{exc} = 376.7$ nm, $\lambda_{em} = 500$ nm). Right: Fitting parameters including pre-exponential factors and confidence limits.

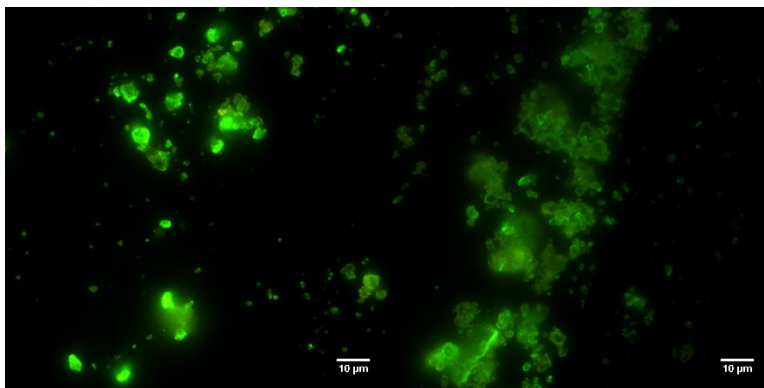


Figure S58. Luminescence micrographs of **PtLH** crystals. Excitation filter BP360 – 370, emission filter BA420.

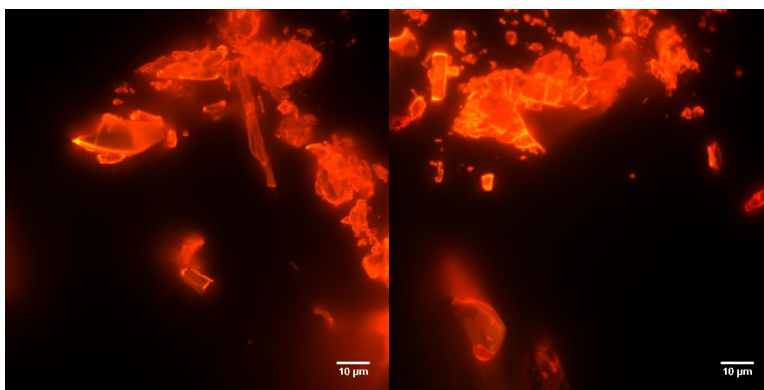


Figure S59. Luminescence micrographs of **PtLF** crystals. Excitation filter BP360 – 370, emission filter BA420

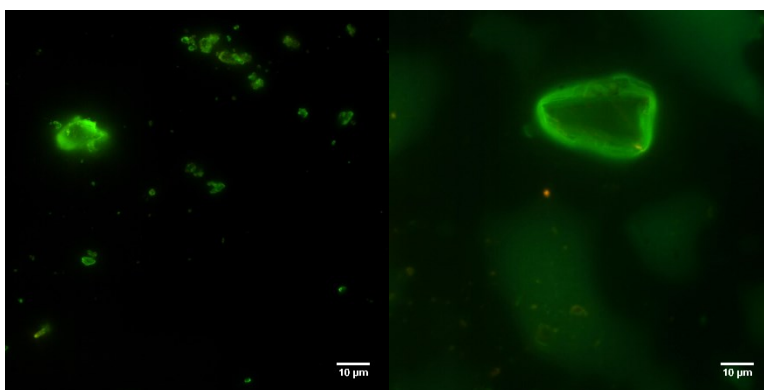


Figure S60. Luminescence micrographs of **PdLH** crystals. Excitation filter BP360 – 370, emission filter BA420

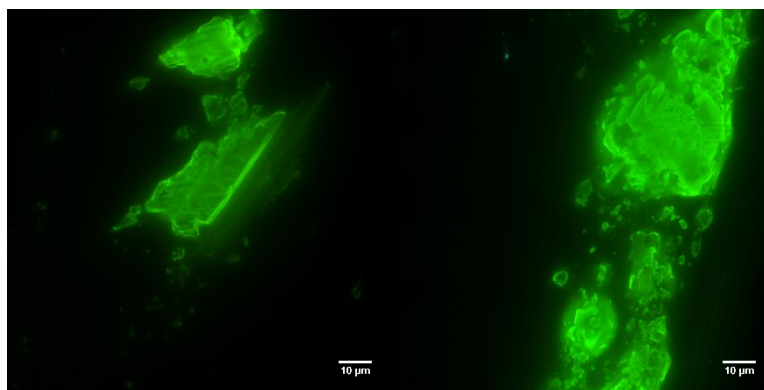


Figure S61. Luminescence micrographs of **PdLF** crystals. Excitation filter BP360 – 370, emission filter BA420-

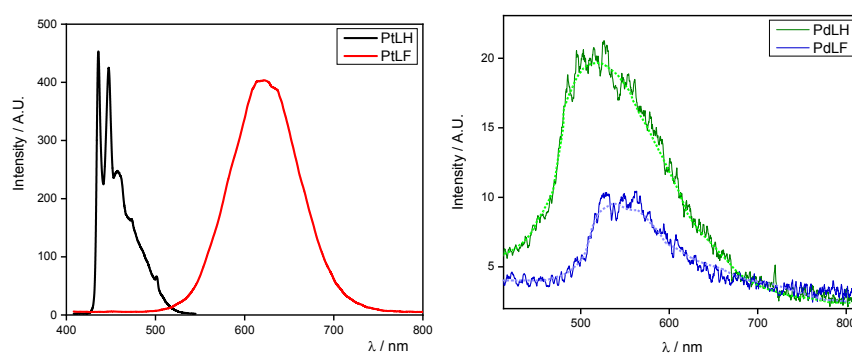


Figure S62. Emission spectra of the complexes as single crystals ($\lambda_{exc} = 376.6$ nm) at 298 K. Normalized to the highest intensity. Black PtLH; red PtLF; green PdLH and blue PdLF. Measured using a spectrograph coupled to a confocal microscope.

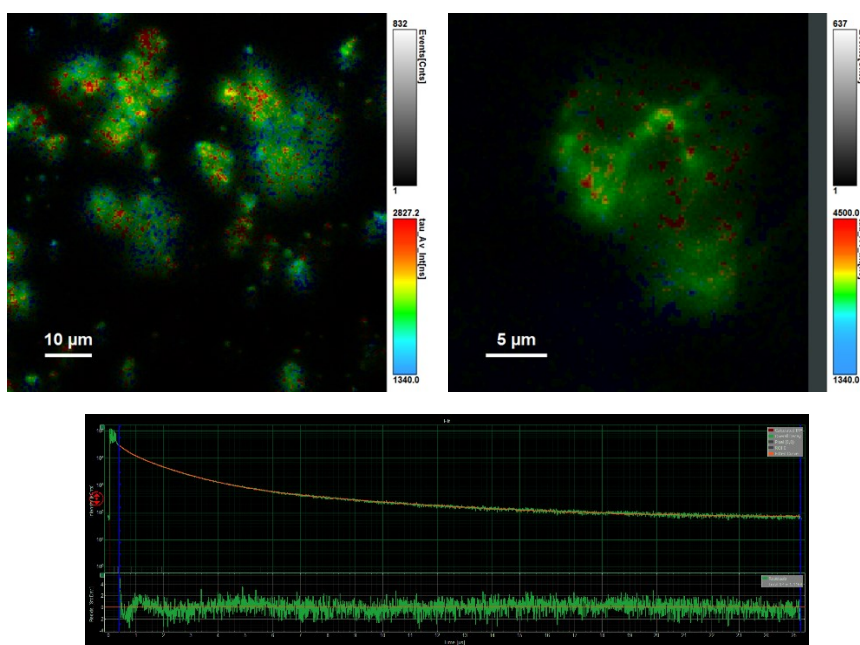


Figure S63. Phosphorescence lifetime maps and photoluminescence decay obtained by time-resolved confocal microscopy of **PtLH** as single crystals at 298 K ($\lambda_{exc} = 376.6$ nm).

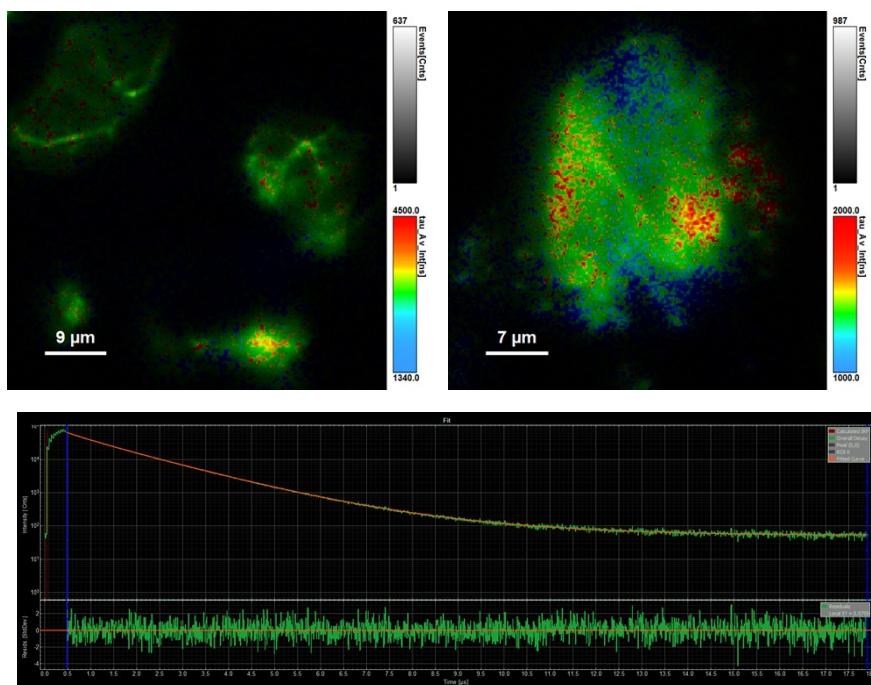


Figure S64. Phosphorescence lifetime maps and photoluminescence decay obtained by time-resolved confocal microscopy of **PtLF** as single crystals at 298 K ($\lambda_{\text{exc}} = 376.6$ nm).

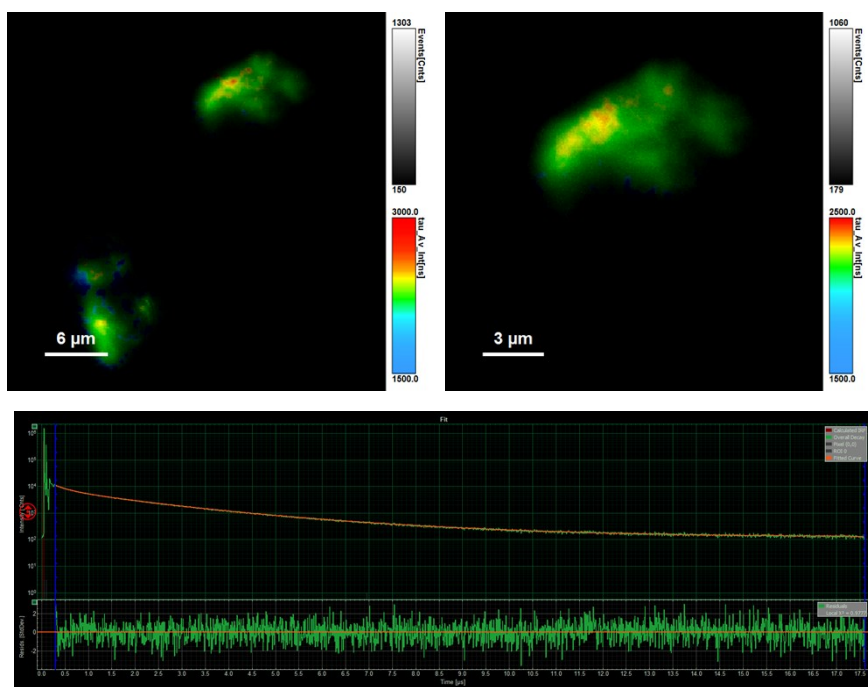


Figure S65. Phosphorescence lifetime maps and photoluminescence decay obtained by time-resolved confocal microscopy of **PdLH** as single crystals at 298 K ($\lambda_{\text{exc}} = 376.6$ nm).

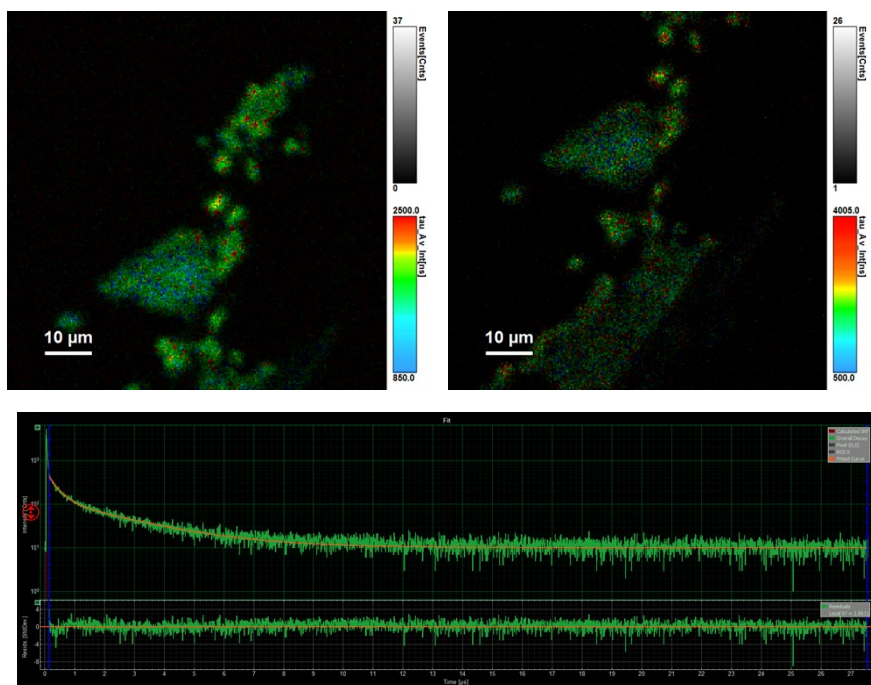


Figure S66. Phosphorescence lifetime maps and photoluminescence decay obtained by time-resolved confocal microscopy of PdLF as crystals at 298 K ($\lambda_{\text{exc}} = 376.6$ nm).

Table S9. Measured and average lifetimes of the single crystal of the complexes. $\tau_{\text{av_amp}}$: Amplitude-weighted average lifetime.

| Complex | Lifetime components (μs) | Average Lifetime (μs) |
|-------------|--|---|
| PdLH | $\tau_1 = 2.88 \pm 0.01$ (28%); $\tau_2 = 1.38 \pm 0.01$ (47%); $\tau_3 = 0.25 \pm 0.01$ (25%) | $\tau_{\text{av_amp}} = 1.51 \pm 0.01$ |
| PdLF | $\tau_1 = 2.08 \pm 0.08$ (29%); $\tau_2 = 0.28 \pm 0.04$ (71%) | $\tau_{\text{av_amp}} = 0.80 \pm 0.06$ |
| PtLH | $\tau_1 = 4.49 \pm 0.06$ (5%); $\tau_2 = 1.08 \pm 0.06$ (56%); $\tau_3 = 0.30 \pm 0.01$ (39%) | $\tau_{\text{av_amp}} = 0.94 \pm 0.01$ |
| PtLF | $\tau_1 = 1.13 \pm 0.03$ (81%); $\tau_2 = 2.32 \pm 0.02$ (5%); $\tau_3 = 0.43 \pm 0.06$ (14%) | $\tau_{\text{av_amp}} = 1.09 \pm 0.01$ |

Section S5: Quantum chemistry of PtLH, PtLF, PdLH and PdLF

Vibrationally resolved emission spectra. All calculations of vibrational Franck-Condon spectra and optimized geometries were carried out using the quantum chemistry package Gaussian 09 Rev. D.01⁵. The PBE0 functional⁶ was used along with Grimme's D3 dispersion correction with Becke-Johnson damping (BJ)⁷ and the SDD basis set, which applies an effective core potential for the Pt and Pd atoms⁸ and the D95 basis set for H, C, N, F and O atoms⁹. Vibrational Franck-Condon spectra were computed according to the method of Barone *et al.*^{10,11} with Kohn-Sham DFT-based geometry optimizations of the S_0 and T_1 state followed by frequency analysis calculations.

The energies were corrected by zero-point vibrational energies and thermal free energy contributions. In order to calculate the overlap integrals for the vibronic spectra, the transitions are divided into classes C_n where n is the number of the excited normal modes in the final electronic state. The maximum number of quanta per mode was set to 100, the maximum number of quanta for combinations of two modes to 65. The number of integrals calculated was limited to 1.5×10^8 . A maximum of 20 classes were computed. The line spectrum was broadened by Gaussian functions with a half-width at half-maximum of 400 cm^{-1} . The solvent dichloromethane (DCM) was described by the polarizable continuum model (PCM) in an integral equation formalism framework¹² with atomic radii from the universal force field model (UFF).¹³

Character of T_1 state. The character of the emissive T_1 state is determined by TD-DFT calculations including 20 excited singlet and triplet states at the T_1 geometry optimized with Kohn-Sham DFT with multiplicity 3.

Absorption spectra. To obtain the UV-Vis absorption spectrum of the complexes, TDDFT calculations of the 70 lowest excited singlet states were performed with the PBE0 functional and the SDD basis set. A Lorentzian broadening with a half-width at half-maximum (HWHM) of 10 nm was used for each transition.

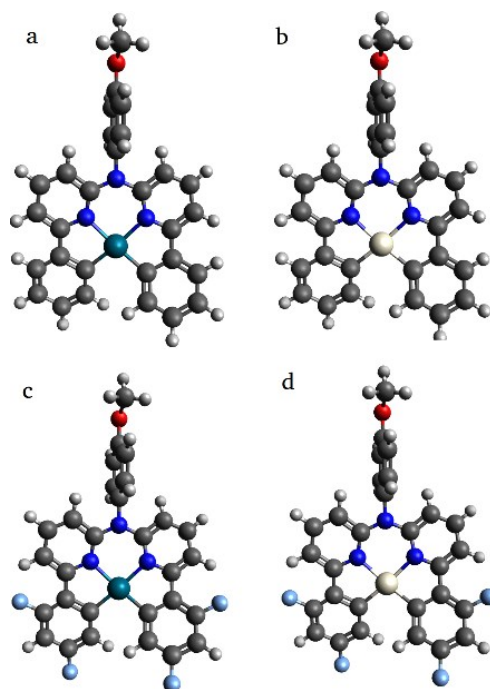


Figure S67. Geometry-optimized ground state monomer structures of (a) **PdLH**, (b) **PtLH**, (c) **PdLF** and (d) **PtLF**.

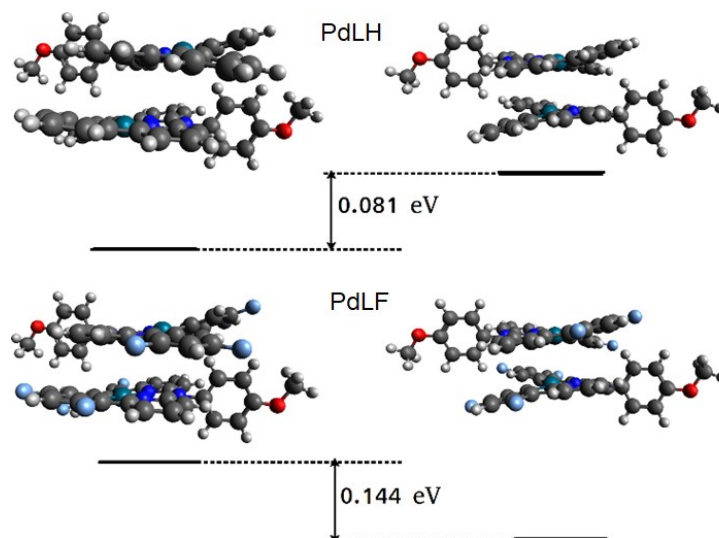


Figure S68. Comparison in energy of different kinds of stacking modes for geometry-optimized ground state dimer structures.

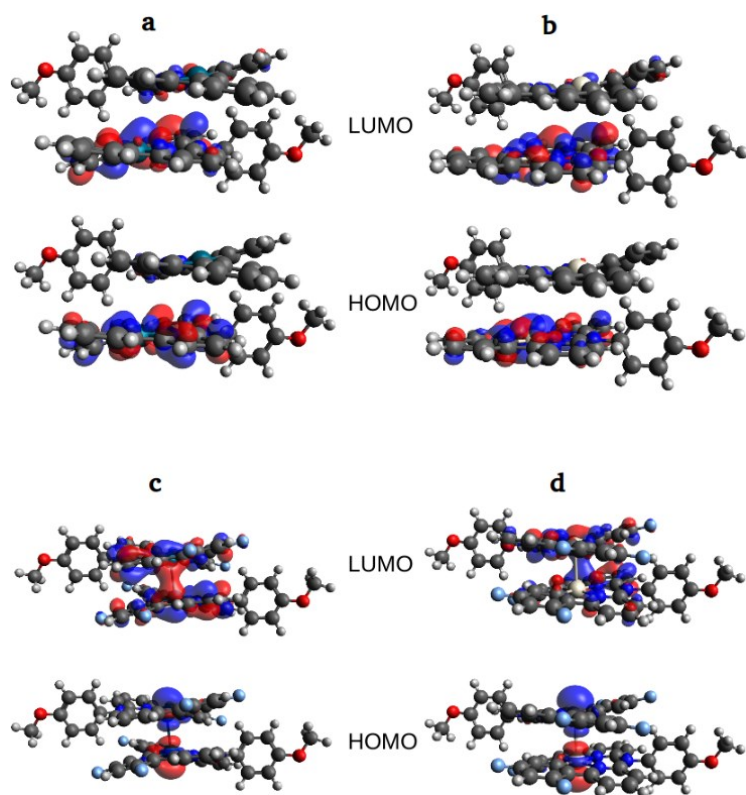


Figure S69. Frontier orbitals at the optimized T_1 dimer geometry of (a) **PdLH**, (b) **PtLH**, (c) **PdLF** and (d) **PtLF**.

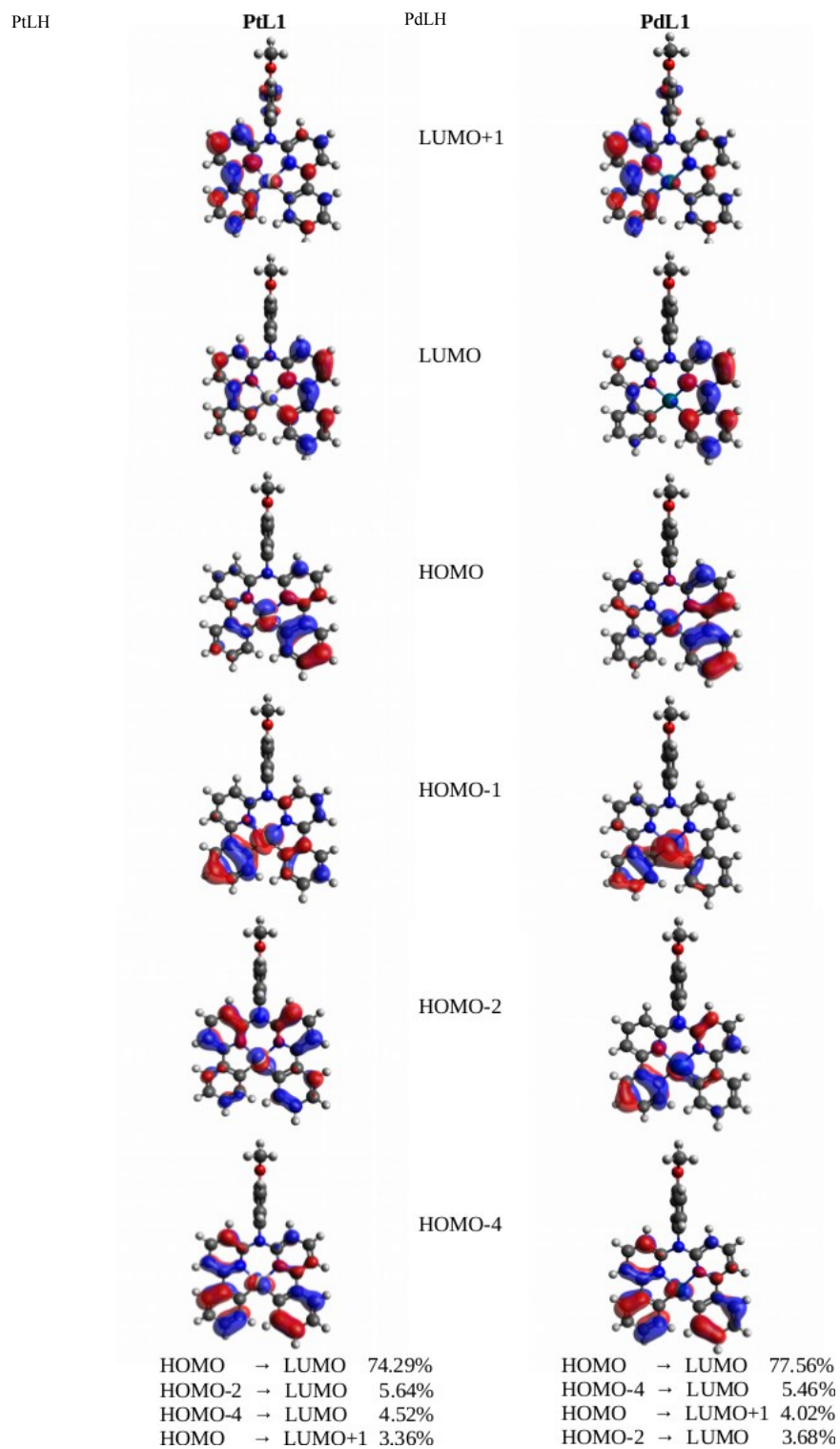


Figure S70: Frontier orbitals of complexes **PtLH** and **PdLH** at the optimized T_1 geometry together with the highest contributions to the emitting T_1 state as obtained from TD-DFT calculations at the optimized T_1 geometry.

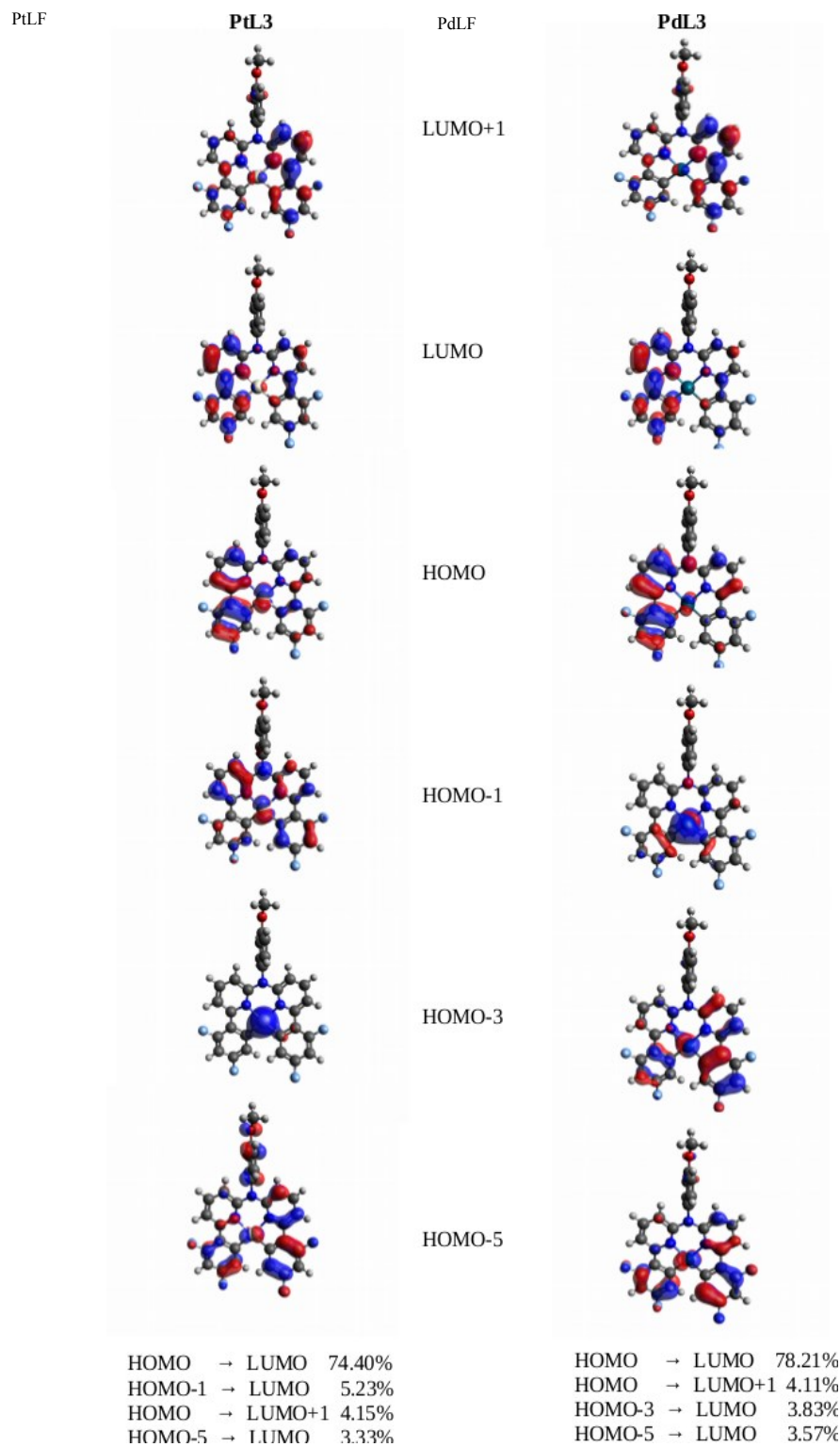


Figure S71: Frontier orbitals of complexes **PtLF** and **PdLF** at the optimized T_1 geometry together with the highest contributions to the emitting T_1 state as obtained from TDDFT calculations at the optimized T_1 geometry.

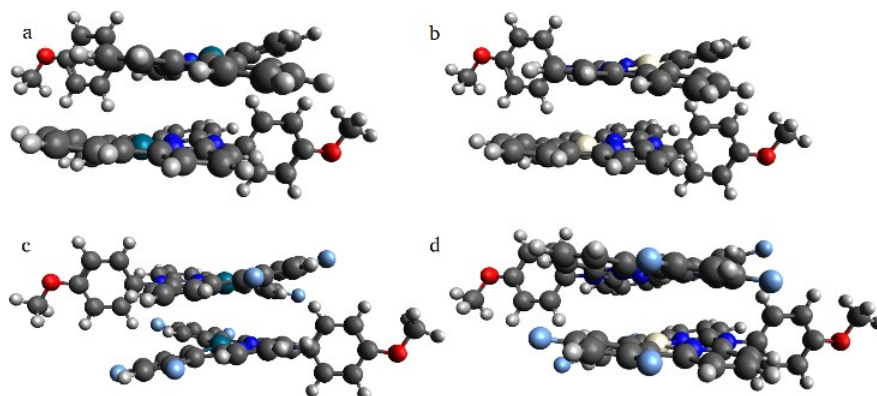


Figure S72: Geometry-optimized ground state dimer structures of (a) PdLH, (b) PtLH, (c) PdLF and (d) PtLF.

Table S10. Dimer energy differences ($E_{LH}-E_{LF}$) between stacked (LH-minimum) and displaced (LF-minimum) dimer geometries in the S_0 and T_1 state (a negative sign corresponds to an energetically favourable LH geometry).

| | PdLH | PdLF | PtLH | PtLF |
|----------------------|----------|----------|----------|----------|
| $E_{LH}-E_{LF}(S_0)$ | -0.14 eV | +0.08 eV | -0.16 eV | +0.07 eV |
| $E_{LH}-E_{LF}(T_1)$ | +0.40 eV | +0.51 eV | +0.58 eV | +0.81 eV |

Table S11. Electrostatic interaction energies (U) in eV for the S_0 geometry calculated between all atoms of one monomer to each one of the other monomer, based on partial atomic charges for stacked (LH-minimum) and displaced (LF-minimum) dimer geometries.

| Energies (eV) | PdLH | PdLF | PtLH | PtLF |
|------------------------|--------|--------|--------|--------|
| LH minimum (stacked) | -1.290 | -0.869 | -1.962 | -0.897 |
| LF minimum (displaced) | -0.064 | -0.259 | -0.477 | -0.255 |
| $U_{LH}-U_{LF}(S_0)$ | -1.226 | -0.61 | -1.485 | -0.642 |

Table S12. Electrostatic interaction energies (U) in eV for the T_1 geometry calculated between all atoms of one monomer to each one of the other monomer, based on partial atomic charges.

| Energies (eV) | PdLH | PdLF | PtLH | PtLF |
|------------------------|-------|-------|-------|-------|
| LH minimum (stacked) | -1.52 | -1.05 | -1.75 | -1.79 |
| LF minimum (displaced) | 0.21 | -0.15 | 0.10 | -0.18 |
| $U_{LH}-U_{LF}(T_1)$ | -1.73 | -0.90 | -1.85 | -1.61 |

Table S13. Contributions (> 3%) of mono-electronic excitations to the T_1 dimer state as obtained from TD-DFT calculations at the optimized T_1 geometry.

| | PdLH | PtLH | PdLF | PtLF |
|---------------------------|--------|--------|--------|--------|
| HOMO \rightarrow LUMO | 71.36% | 68.93% | 98.02% | 98.00% |
| HOMO \rightarrow LUMO+1 | 5.26% | 5.55% | - | - |
| HOMO-8 \rightarrow LUMO | 3.09% | 4.64% | - | - |
| HOMO-4 \rightarrow LUMO | - | 4.07% | - | - |

Table S14. HOMO-LUMO gap of all monomer S_0 and T_1 geometries obtained from TD-DFT calculations.

| Monomer | | PdLH | PdLF | PtLH | PtLF |
|---------|---------------|-------------|-------------|-------------|-------------|
| S_0 | LUMO | -0.065 | -0.075 | -0.069 | -0.078 |
| | HOMO | -0.224 | -0.237 | -0.216 | -0.233 |
| | gap [Hartree] | 0.159 | 0.162 | 0.147 | 0.155 |
| | gap [eV] | 4.327 | 4.408 | 4.000 | 4.218 |
| T_1 | LUMO | -0.157 | -0.168 | -0.157 | -0.170 |
| | HOMO | -0.225 | -0.238 | -0.221 | -0.231 |
| | gap [Hartree] | 0.068 | 0.070 | 0.064 | 0.061 |
| | gap [eV] | 1.850 | 1.905 | 1.742 | 1.660 |

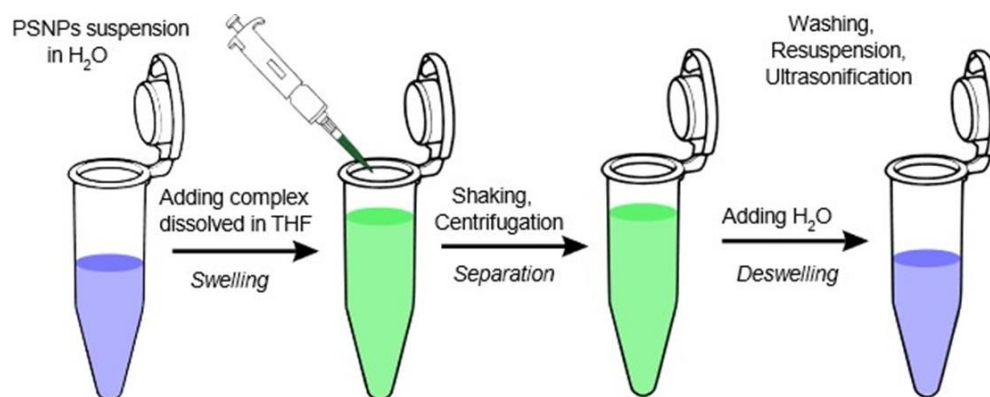
Table S15. HOMO-LUMO gap of all dimer S_0 and T_1 geometries obtained from TD-DFT calculations.

| Dimer | | PdLH | PdLF | PtLH | PtLF |
|-------|---------------|-------------|-------------|-------------|-------------|
| S_0 | LUMO | -0.067 | -0.077 | -0.069 | -0.081 |
| | HOMO | -0.220 | -0.216 | -0.213 | -0.211 |
| | gap [Hartree] | 0.153 | 0.139 | 0.144 | 0.130 |
| | gap [eV] | 4.163 | 3.782 | 3.918 | 3.537 |
| T_1 | LUMO | -0.077 | -0.087 | -0.076 | -0.090 |
| | HOMO | -0.214 | -0.195 | -0.208 | -0.187 |
| | gap [Hartree] | 0.137 | 0.108 | 0.132 | 0.097 |
| | gap [eV] | 3.728 | 2.939 | 3.592 | 2.640 |

Section S6: Synthesis and characterization of the loaded nanoparticles (PS)

S6.1 Preparation of the Pt(II)- and Pd(II)-complex-loaded nanoparticles

100 nm-sized aminated polystyrene nanoparticles (PS) were bought from Micromod GmbH (Germany).



Scheme S1: Schematic illustration of one-step staining procedure using 100 nm polystyrene nanoparticles (PSNPs).

The preparation of the nanoparticles loaded with Pt(II)- or Pd(II)-complex is illustrated in **Scheme S1**. The highly hydrophobic complexes **PtLH**, **PtLF**, **PdLH** and **PdLF** were encapsulated into 100 nm-sized aminated polystyrene nanoparticles (PS) via a simple one-step staining procedure. 3 mg of PS nanoparticles were dispersed in deionized water to 2.5 mg/mL (1.2 mL). The Pt(II)- or Pd(II)-complex was dissolved in tetrahydrofuran (THF) with the initial loading concentration c_L ranging from 0.1 mM to 2.0 mM and eventually to 4.0 mM. 200 μ L of metal complex solution in THF was then added to the PS dispersion and the sample was subsequently shaken for 40 minutes. Shrinking of the particles was induced by adding 200 μ L deionized water to the dispersion, thereby encapsulating the complex molecules in the nanoparticles. The particles were then centrifuged at 16,000 rcf for 60 minutes (Centrifuge 5415D from *Eppendorf*, Germany). The precipitate was washed three times with ethanol/water mixtures (volume ratios of 40/60, 30/70, and 20/80) and once with deionized water to remove excess dye adsorbed onto the particle surface. Finally the PS loaded with the Pt(II)- or Pd(II)-complex were diluted to 5 mg/mL (600 μ L).

S6.2 Surface and structure characterization of nanoparticles

Table S16: Size distribution of PS(PtLF-series), dispersed in H₂O with particle concentration of 1 mg/mL.

| Samples | Averaged hydrodynamic diameter (nm) | Polydispersity index (PDI) |
|------------------------|-------------------------------------|----------------------------|
| Blank PS nanoparticles | 131.1 | 0.007 |
| PS(PtLF-0.1 mM) | 132.3 | 0.003 |
| PS(PtLF-0.5 mM) | 136.6 | 0.020 |
| PS(PtLF-1.0 mM) | 140.8 | 0.049 |
| PS(PtLF-2.0 mM) | 146.0 | 0.063 |
| PS(PtLF-3.0 mM) | 142.6 | 0.062 |
| PS(PtLF-4.0 mM) | 153.4 | 0.095 |

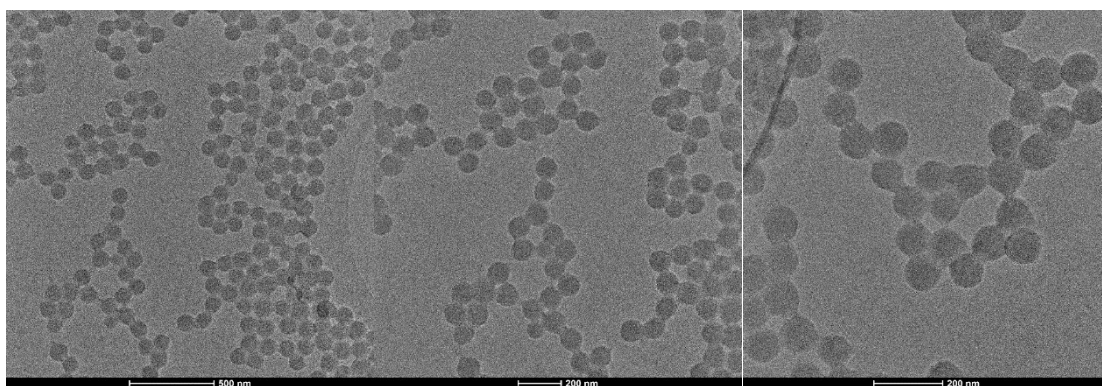


Figure S73. HRTEM images of blank polystyrene nanoparticles (PS).

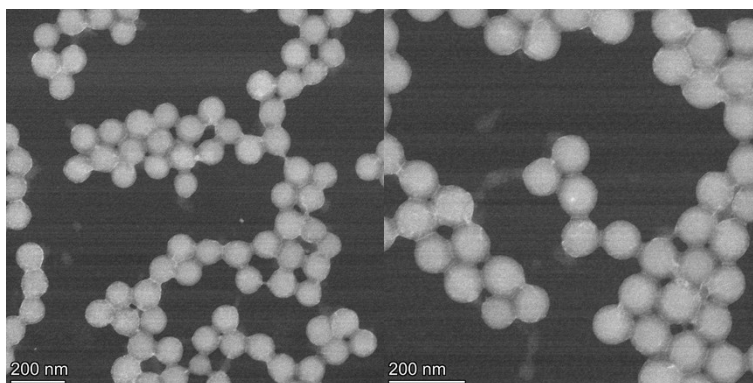


Figure S74. HAADF image of blank polystyrene nanoparticles (PS).

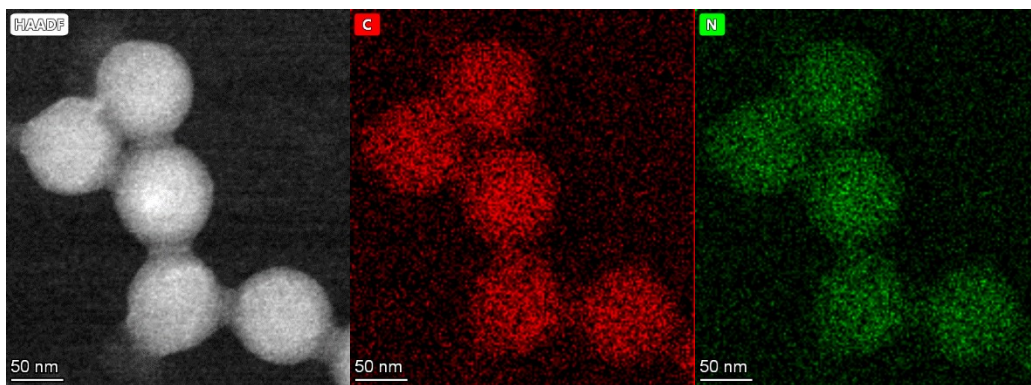


Figure S75. HAADF image and corresponding EDX maps of blank polystyrene nanoparticles (PS).

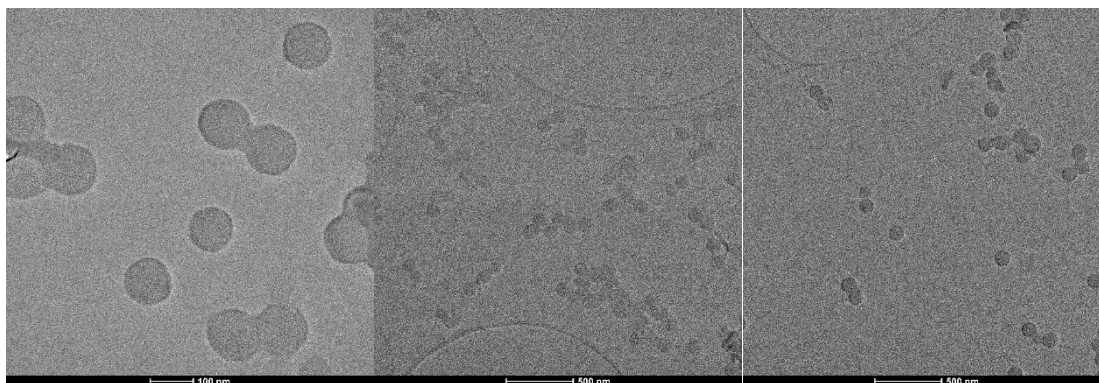


Figure S76. HRTEM images of polystyrene nanoparticles loaded with PtLH, i.e. PS(PtLH-0.5 mM).

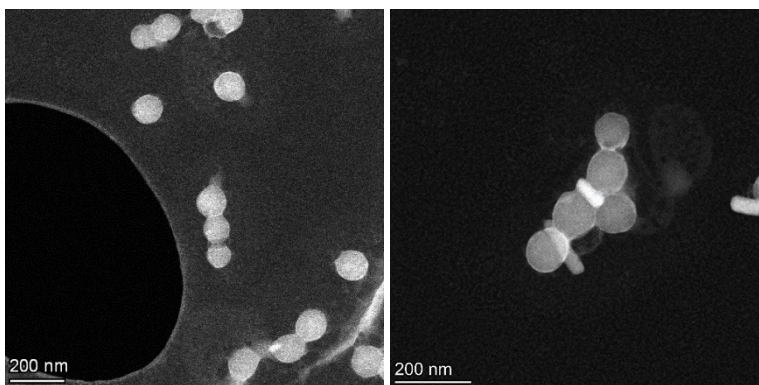


Figure S77. HAADF image of polystyrene nanoparticles loaded with PtLH, i.e. PS(PtLH-0.5 mM).

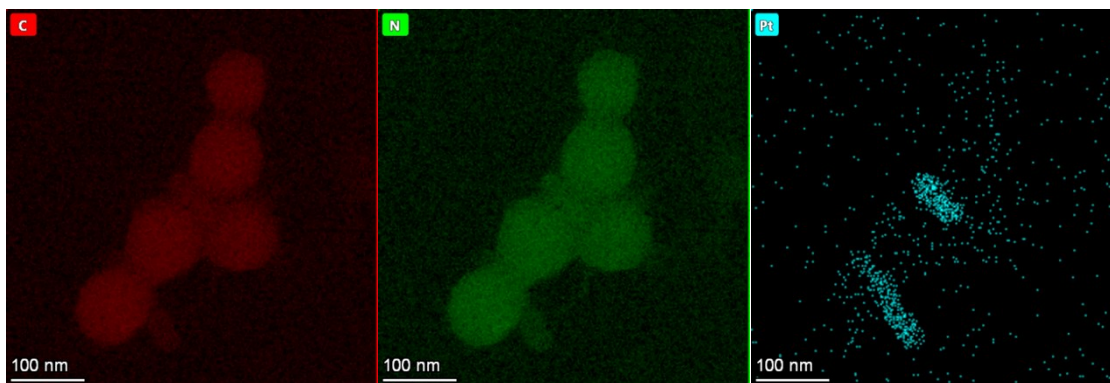


Figure S78. EDX maps of polystyrene nanoparticles loaded with **PtLH**, i.e. **PS(PtLH-0.5 mM)**.

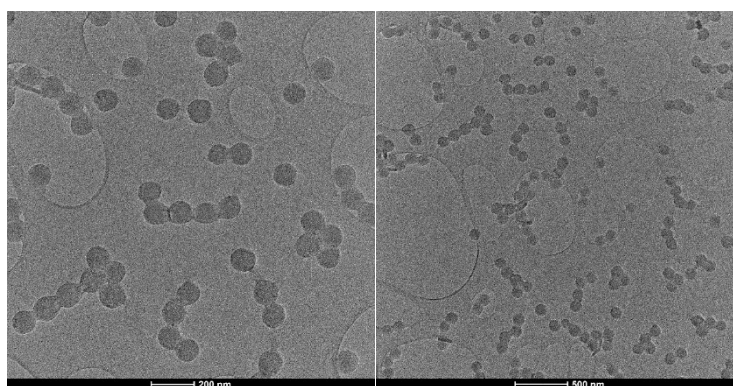


Figure S79. HRTEM images of polystyrene nanoparticles loaded with **PtLF**, i.e. **PS(PtLF-0.5 mM)**.

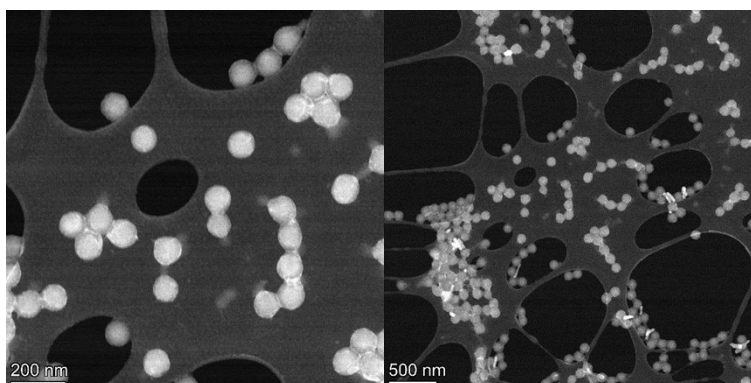


Figure S80. HAADF image of polystyrene nanoparticles loaded with **PtLF**, i.e. **PS(PtLF-0.5 mM)**.

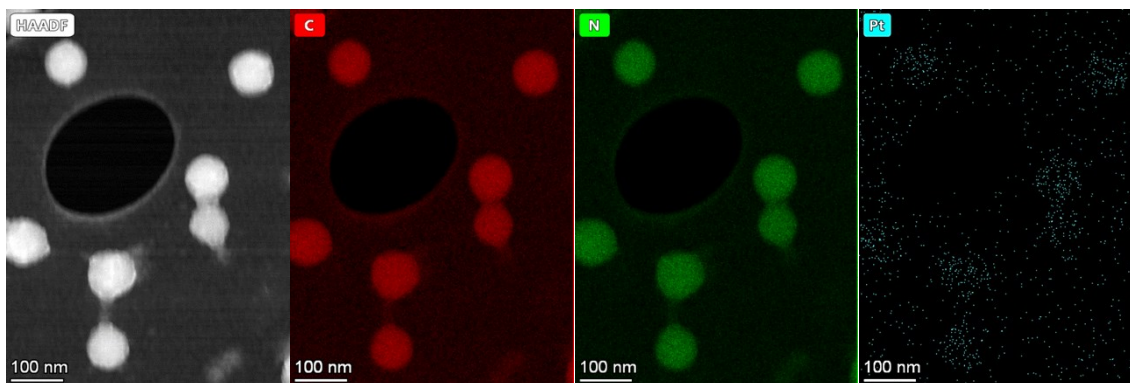


Figure S81. HAADF image and corresponding EDX maps of polystyrene nanoparticles loaded with **PtLF**, i.e. **PS(PtLF-0.5 mM)**.

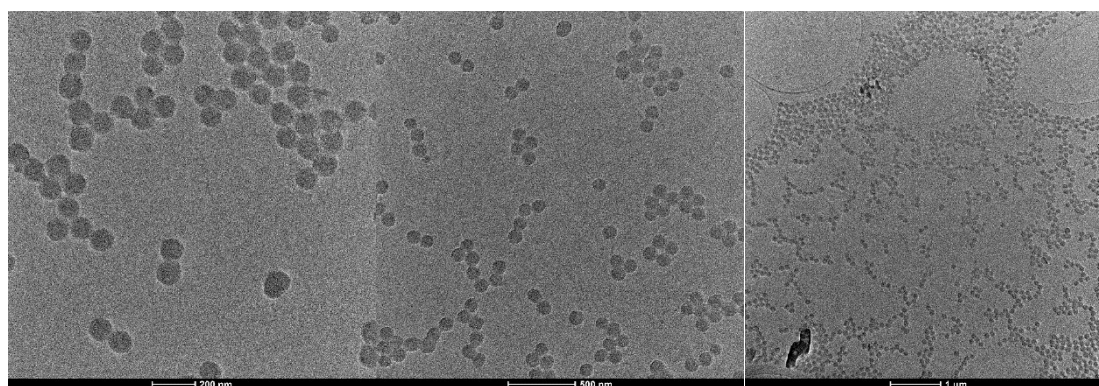


Figure S82. HRTEM images of polystyrene nanoparticles loaded with **PdLH**, i.e. **PS(PdLH-0.5 mM)**.

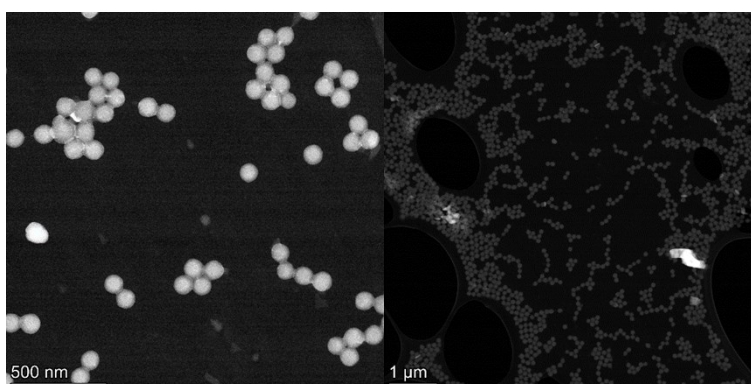


Figure S83. HAADF image of polystyrene nanoparticles loaded with **PdLH**, i.e. **PS(PdLH-0.5 mM)**.

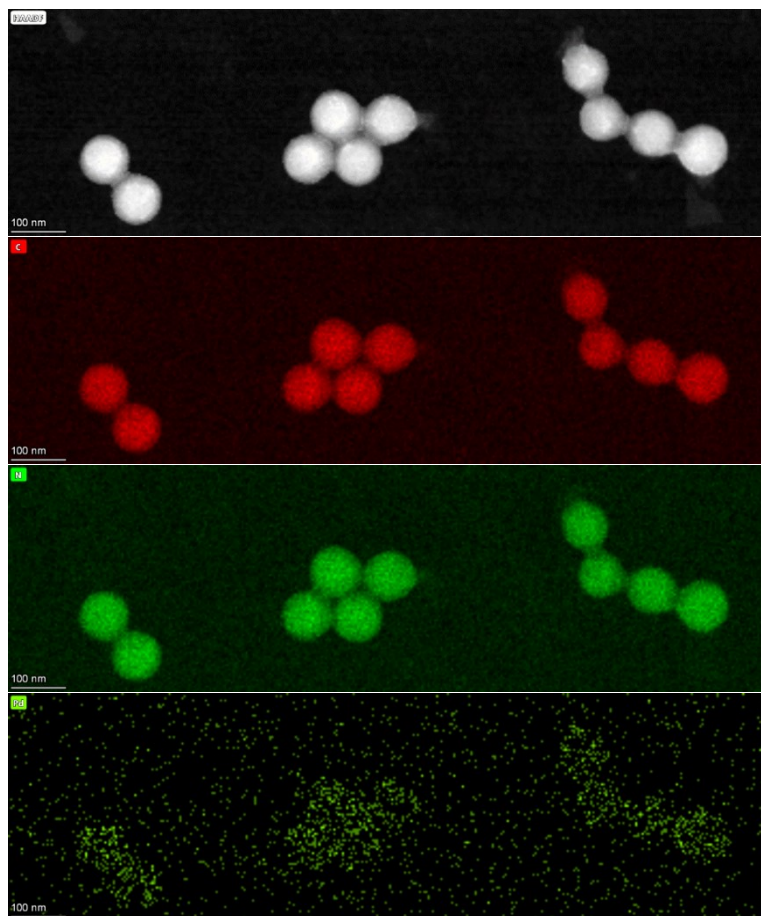


Figure S84. HAADF image and corresponding EDX maps of polystyrene nanoparticles loaded with **PdLH**, i.e. **PS(PdLH-0.5 mM)**.

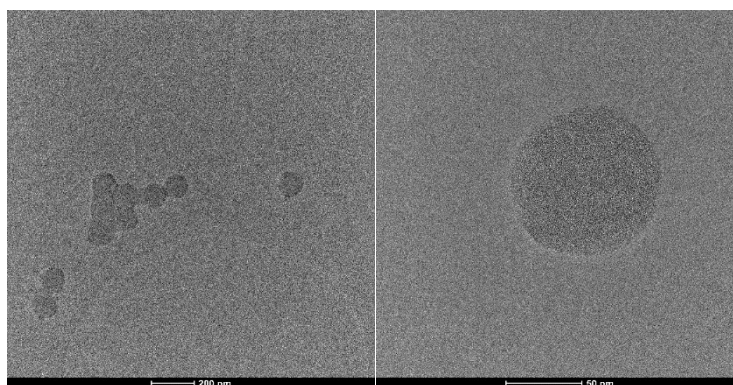


Figure S85. HRTEM images of polystyrene nanoparticles loaded with **PdLF**, i.e. **PS(PdLF-0.5 mM)**.

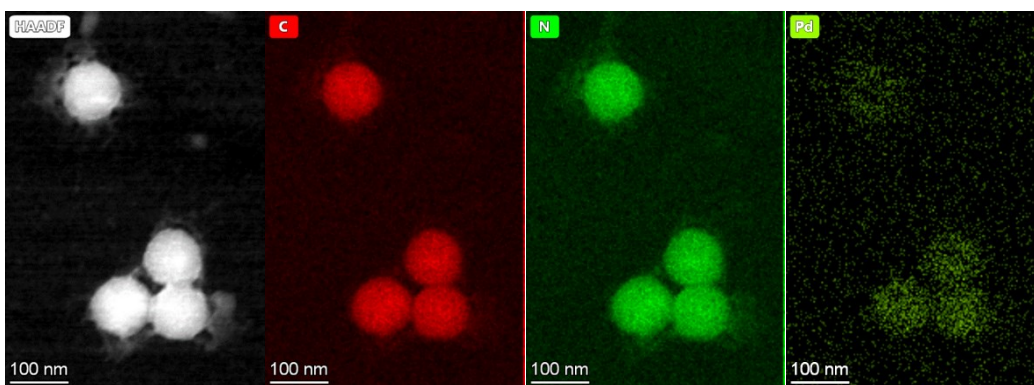


Figure S86. HAADF image and corresponding EDX maps of polystyrene nanoparticles loaded with **PdLH**, i.e. **PS(PdLH-0.5 mM)**.

S6.3 Leaking experiments

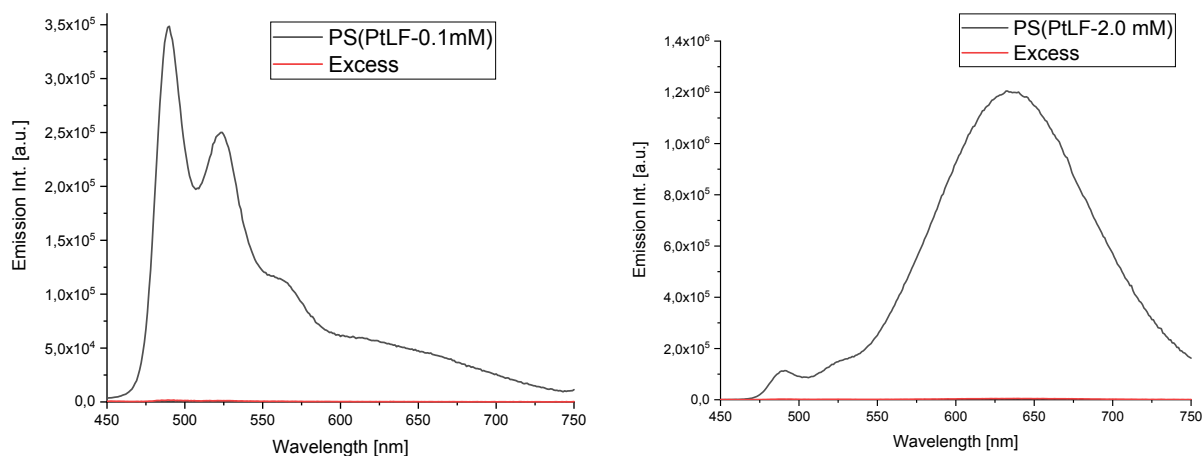


Figure S87. Emission spectra of freshly prepared **PtLF**-loaded PS nanoparticles and of the corresponding supernatant after centrifugation after 2 days storage. Left: fresh **PS(PtLF-0.1 mM)** in H_2O (black) and its supernatant in excess (red). Right: fresh **PS(PtLF-2.0 mM)** in H_2O (black) and its supernatant in excess (red).

S6.4 Determination of loading with PtLF

To estimate the loading with complex of the PS, the absorption coefficient had to be determined firstly. DMF containing dissolved PS nanoparticles (0.1 mg/mL) was taken as the solvent. **PtLF** calibration samples in the DMF-PS were prepared with known concentrations. Their respective absorbances were measured and plotted as a function of the **PtLF** concentration (**Figure S88**). The fitted linear function acted as the calibration curve, whose slope value contains the information about the molar absorption coefficient and the optical path length through the sample.

The samples **PS(PtLF-series)** were dissolved in pure DMF to give the final particle concentration of 0.1 mg/mL. By measuring the absorbance, the **PtLF** concentrations were calculated according to the generated

linear calibration function as shown in **Figure S88**. Knowing the mass/particle $m = 5.39307 \cdot 10^{-16}$ g/particle (data from the manufacturer) and the particle mass concentration (recorded in the preparation protocol), the particle number can be calculated. The obtained loading of **PtLF** molecules per particle of PS(**PtLF**-series) are listed in **Table S17**.

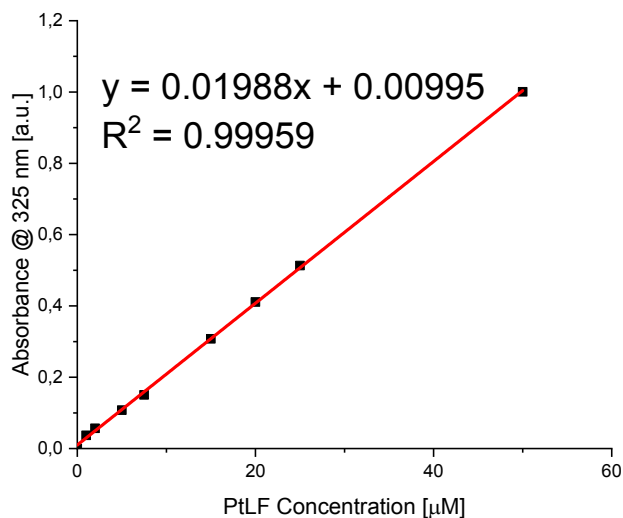


Figure S88. Absorbance of **PtLF** in DMF-PS (0.1 mg/mL) as a function of **PtLF** concentration.

Table S17: Number of **PtLF** molecules loaded on each PS nanoparticle and the corresponding parameters (c_L).

| PS(PtLF-series) | Absorbance | PtLF concentration in 0.1 mg/mL PS, μM) | Number of PtLF molecules per PS nanoparticle |
|------------------------|------------|--|---|
| $c_L = 0.1$ mM | 0.02508 | 0.7610664 | 2472 |
| $c_L = 0.2$ mM | 0.04670 | 1.84859155 | 6004 |
| $c_L = 0.5$ mM | 0.09594 | 4.32545272 | 14048 |
| $c_L = 1.0$ mM | 0.13119 | 6.09859155 | 19806 |
| $c_L = 2.0$ mM | 0.26685 | 12.9225352 | 41969 |

S6.5 Photophysical studies of nanoparticles loaded with the complexes

Table S18: Photoluminescence quantum yield Φ_L and decay lifetimes data of **PtLH**- and **PtLF**-stained nanoparticles.^[a]

| Medium (RT) | PtLH ($\lambda_{\text{exc}} = 405$ nm) | | | | PtLF ($\lambda_{\text{exc}} = 388$ nm) | | | | | |
|----------------------|--|----------------|--------------------------------------|----------------|--|----------------|--------------------------------------|----------------|--------------------------------------|---------------|
| | Φ_L [%] | | $\tau_{510}^{[c]}$ [μs] | | Φ_L [%] | | $\tau_{490}^{[c]}$ [μs] | | $\tau_{635}^{[c]}$ [μs] | |
| | Air | Ar | Air | Ar | Air | Ar | Air | Ar | Air | Ar |
| $c_L^{[b]} = 0.1$ mM | 36.0 ± 1.0 | 55.1 ± 0.7 | 9.0 ± 0.8 | 12.6 ± 0.5 | 47.3 ± 0.4 | 79.3 ± 0.5 | 10.9 ± 0.6 | 15.7 ± 0.3 | 8 ± 2 | 9.9 ± 1.7 |
| $c_L^{[b]} = 0.5$ mM | 23.4 ± 0.2 | 32.7 ± 0.2 | 9.0 ± 0.9 | 12.8 ± 0.5 | 61.5 ± 0.2 | 72.1 ± 0.1 | 10.8 ± 0.8 | 15.3 ± 0.4 | 6.7 ± 1.1 | 6.6 ± 1.1 |
| $c_L^{[b]} = 1.0$ mM | 14.5 ± 0.1 | 19.8 ± 0.2 | 9.7 ± 0.8 | 11.8 ± 0.6 | 59.1 ± 0.2 | 66.2 ± 0.2 | 9.8 ± 0.7 | 14.6 ± 0.4 | 6.7 ± 1.5 | 6.8 ± 1.5 |
| $c_L^{[b]} = 2.0$ mM | 7.9 ± 0.1 | 10.9 ± 0.2 | 8.9 ± 0.9 | 12.1 ± 0.6 | 64.6 ± 0.4 | 70.3 ± 0.1 | 10.5 ± 0.7 | 14.3 ± 0.4 | 7.9 ± 1.5 | 8.0 ± 1.2 |

[a] The stained PS nanoparticles were dispersed in deionized water with a particle concentration of 0.25 mg/mL. [b] Loading concentration of metal complex in the PS. [c] Lifetimes τ_{510} and τ_{490} were fitted monoexponentially, while lifetime τ_{635} were fitted biexponentially. The averaged lifetimes were calculated as intensity-weighted.

Table S19: Photoluminescence quantum yield Φ_L of the monomer and aggregate emission of PS(**PtLF**-series).

| PS(PtLF -series) | Φ_L [%] | | | |
|--------------------------|------------------|--------------------|------------------|--------------------|
| | Air | | Ar | |
| | Monomer (490 nm) | Aggregate (635 nm) | Monomer (490 nm) | Aggregate (635 nm) |
| $c_L = 0.1$ mM | 28.1 ± 1.4 | 19.2 ± 0.9 | 49 ± 2 | 29.9 ± 1.5 |
| $c_L = 0.25$ mM | 17.3 ± 0.8 | 32.4 ± 1.6 | 28.9 ± 1.4 | 41 ± 2 |
| $c_L = 0.5$ mM | 8.0 ± 0.4 | 54 ± 3 | 12.5 ± 0.6 | 60 ± 3 |
| $c_L = 1.0$ mM | 4.5 ± 0.3 | 55 ± 3 | 7.1 ± 0.3 | 59 ± 3 |
| $c_L = 2.0$ mM | 2.9 ± 0.1 | 61 ± 3 | 4.3 ± 0.2 | 66 ± 3 |

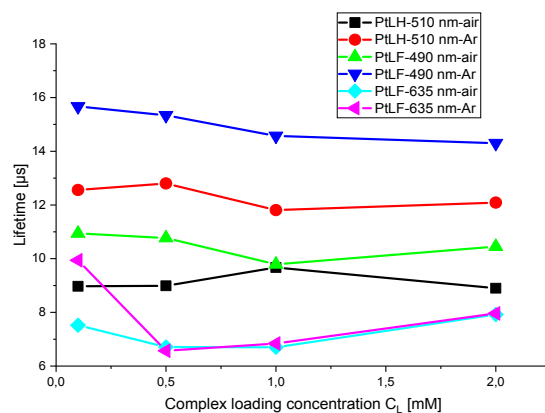


Figure S89. Photoluminescence lifetimes vs. loading with **PtLH** ($\lambda_{exc.} = 405$ nm) and **PtLF** ($\lambda_{exc.} = 388$ nm) in PS nanoparticles under different conditions

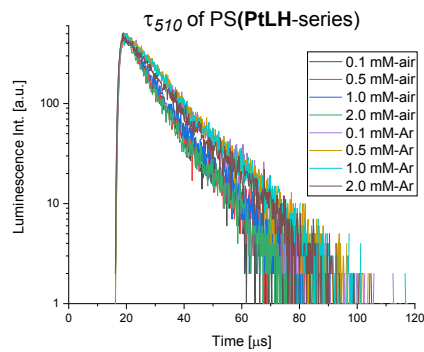


Figure S90. Time-resolved photoluminescence decays of PS(**PtLH**-series) in air-equilibrated and Ar-purged H_2O ($\lambda_{exc.} = 405$ nm).

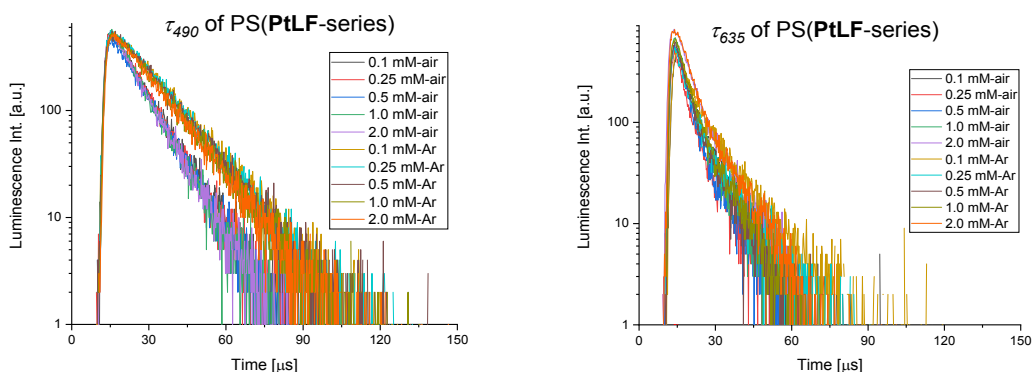


Figure S91. Time-resolved photoluminescence decays of PS(PtLF-series) in air-equilibrated and in Ar-purged H₂O ($\lambda_{\text{exc.}} = 388$ nm).

Table S20: Photoluminescence quantum yield Φ_L of Pd(II)-complexes and stained PS nanoparticles. [a] The stained PS nanoparticles were dispersed in deionized water with a particle mass concentration of 0.25 mg/mL. [b] Loading concentration of metal complex in the PS nanoparticles. [c] Lifetimes of PdLH and of PdLF were fitted triexponentially and calculated as intensity-weighted. [d] The decay signal was too weak to be measured.

| Medium (RT) | PdLH ($\lambda_{\text{exc.}} 335$ nm) | | | | | | | | PdLF ($\lambda_{\text{exc.}} 368$ nm) | | | | | | | |
|--------------------|--|----|--------------------------------------|--------------|--------------------------------------|--------------|--------------------------------------|--------------|--|----|--------------------------------------|------------|--------------------------------------|-------------|--------------------------------------|-------------|
| | $\Phi_L \pm 2$ [%] | | $\tau_{488}^{[c]}$ [μs] | | $\tau_{520}^{[c]}$ [μs] | | $\tau_{561}^{[c]}$ [μs] | | $\Phi_L \pm 2$ [%] | | $\tau_{480}^{[c]}$ [μs] | | $\tau_{530}^{[c]}$ [μs] | | $\tau_{565}^{[c]}$ [μs] | |
| | Air | Ar | Air | Ar | Air | Ar | Air | Ar | Air | Ar | Air | Ar | Air | Ar | Air | Ar |
| [b] $c_L = 0.1$ mM | 2 | 12 | 20 \pm 4 | 113 \pm 8 | 20 \pm 5 | 112 \pm 10 | 20 \pm 7 | 108 \pm 14 | 2 | 5 | 11 \pm 3 | 85 \pm 6 | 16 \pm 3 | 90 \pm 10 | 18 \pm 3 | 106 \pm 9 |
| [b] $c_L = 0.5$ mM | 3 | 9 | 33 \pm 5 | 113 \pm 10 | 32 \pm 7 | 116 \pm 11 | 32 \pm 7 | 118 \pm 13 | 2 | 6 | 15 \pm 2 | 78 \pm 7 | 15.3 \pm 1.6 | 87 \pm 7 | 20 \pm 7 | 79 \pm 7 |
| [b] $c_L = 1.0$ mM | 1 | 3 | 45 \pm 4 | 119 \pm 5 | 45 \pm 5 | 113 \pm 7 | 41 \pm 3 | 114 \pm 8 | 3 | 6 | 14 \pm 2 | 71 \pm 8 | 16.2 \pm 1.7 | 77 \pm 8 | 17 \pm 1 | 73 \pm 7 |
| [b] $c_L = 2.0$ mM | 1 | 2 | 21 \pm 5 | 119 \pm 6 | 24 \pm 6 | 116 \pm 11 | 21 \pm 4 | 108 \pm 9 | 3 | 6 | 13 \pm 2 | 61 \pm 8 | 16.9 \pm 1.5 | 67 \pm 7 | 20 \pm 4 | 71 \pm 7 |
| [b] $c_L = 3.0$ mM | 1 | 2 | 26 \pm 4 | 121 \pm 7 | 24 \pm 4 | 114 \pm 7 | 21 \pm 4 | 109 \pm 6 | 4 | 6 | 15 \pm 2 | 48 \pm 7 | 19 \pm 2 | 63 \pm 6 | 23 \pm 6 | 64 \pm 7 |
| [b] $c_L = 4.0$ mM | 1 | 2 | 23 \pm 3 | 108 \pm 7 | 22 \pm 4 | 107 \pm 9 | 20 \pm 6 | 112 \pm 10 | 4 | 6 | 16 \pm 2 | 45 \pm 9 | 22.9 \pm 1.2 | 51 \pm 6 | 24 \pm 7 | 50 \pm 7 |

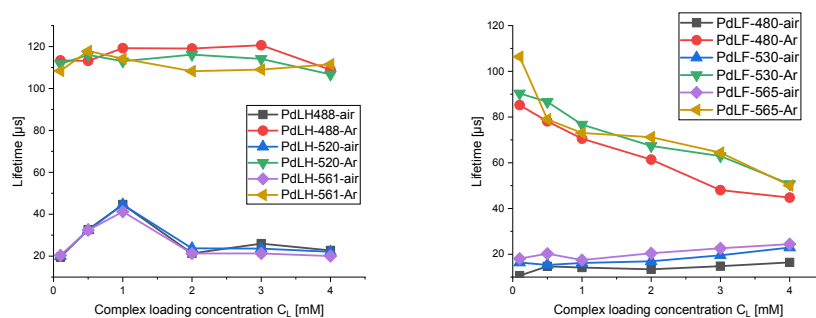


Figure S92. Photoluminescence lifetimes vs. loading concentration of PdLH ($\lambda_{\text{exc.}} = 335$ nm) (left) and PdLF ($\lambda_{\text{exc.}} = 368$ nm) (right) in PS nanoparticles under different conditions.

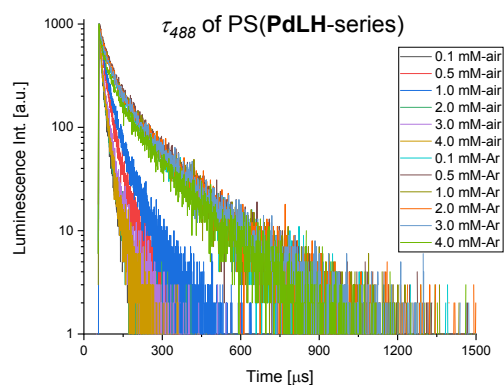


Figure S93. Time-resolved photoluminescence decays of PS(**PdLH**-series) in air-equilibrated and in Ar-purged H₂O ($\lambda_{\text{exc}} = 335$, $\lambda_{\text{em}} 488$ nm).

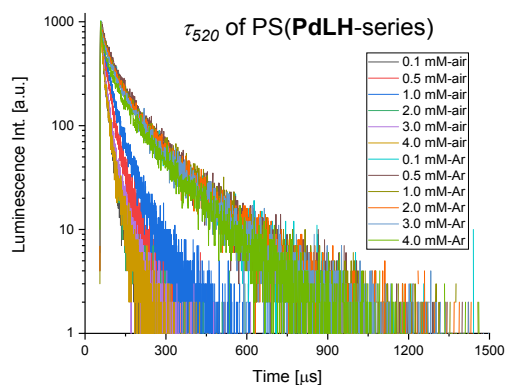


Figure S94. Time-resolved photoluminescence decays of PS(**PdLH**-series) in air-equilibrated and in Ar-purged H₂O ($\lambda_{\text{exc}} = 335$ nm, $\lambda_{\text{em}} = 520$ nm).

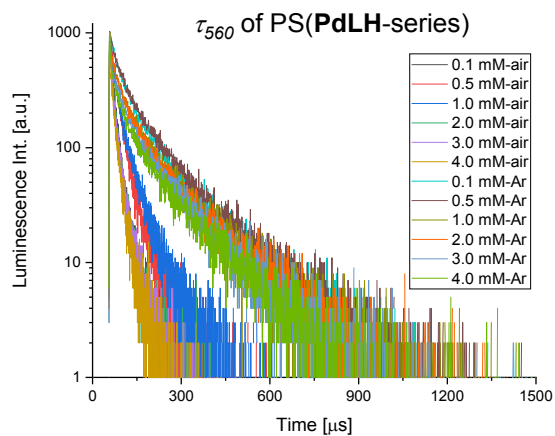


Figure S95. Time-resolved photoluminescence decays of PS(**PdLH**-series) in air-equilibrated and in Ar-purged H₂O ($\lambda_{\text{exc}} = 335$ nm, $\lambda_{\text{em}} = 560$ nm).

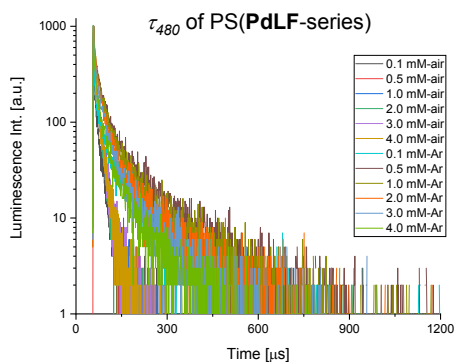


Figure S96. Time-resolved photoluminescence decays of PS(PdLF-series) in air-equilibrated and in Ar-purged H₂O ($\lambda_{\text{exc}} = 368$ nm, $\lambda_{\text{em}} = 480$ nm).

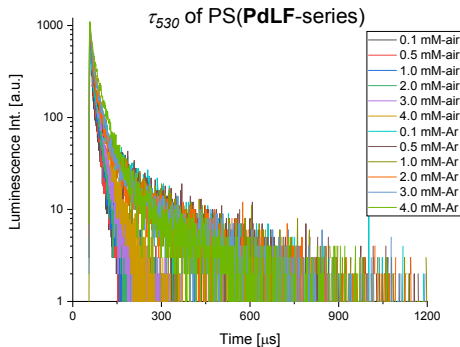


Figure S97. Time-resolved photoluminescence decays of PS(PdLF-series) in air-equilibrated and in Ar-purged H₂O ($\lambda_{\text{exc}} = 368$ nm, $\lambda_{\text{em}} = 530$ nm).

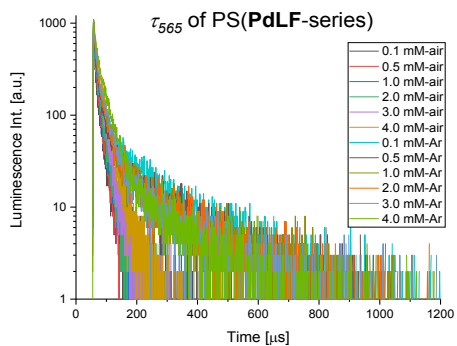


Figure S98. Time-resolved photoluminescence decays of PS(PdLF-series) in air-equilibrated and in Ar-purged H₂O ($\lambda_{\text{exc}} = 368$ nm, $\lambda_{\text{em}} = 565$ nm).

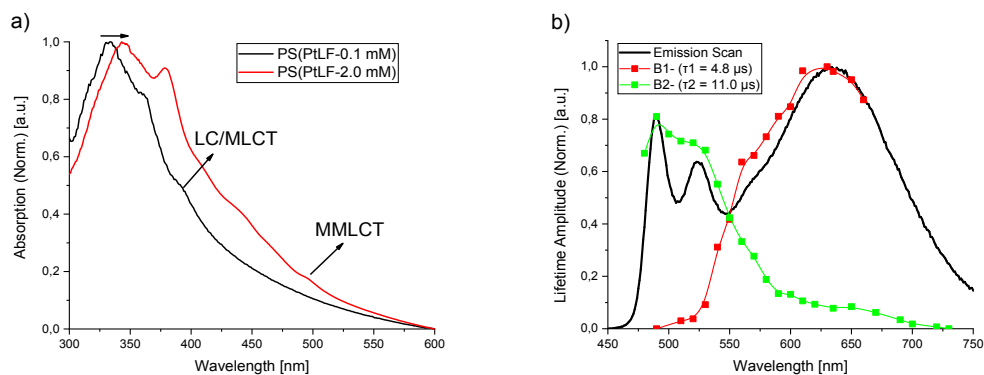


Figure S99. a) Absorption spectra of PS(PtLF-series) with loading concentrations of 0.1 mM (black) and 2.0 mM (red). b) Lifetime amplitudes of PS(PtLF-0.5 mM) plotted as a function of the emission wavelength, together with the emission spectrum (solid line). Amplitude *B1* (red dotted line) corresponds to the aggregate lifetime of $\tau_1 = 4.8 \mu\text{s}$ and amplitude *B2* (green dotted line) describes the monomer distribution with a lifetime of $\tau_2 = 11.0 \mu\text{s}$.

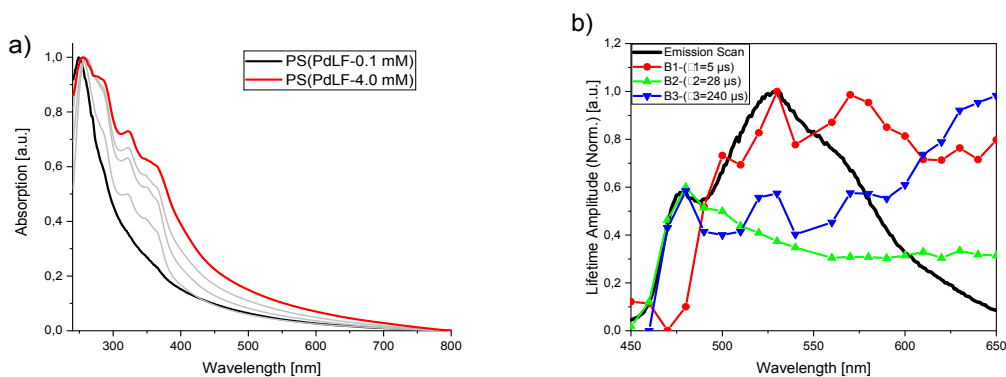


Figure S100. a) Absorption spectra of PS(PdLF-series) with PdLF loading concentration c_L from 0.1 mM (black) to 4.0 mM (red) with growing c_L (grey). b) Lifetime amplitudes of degassed PS(PdLH-0.5 mM) plotted as a function of the emission wavelength, together with the emission spectrum (solid line). Amplitude *B1* (red dotted line) corresponds to the fixed lifetime of $\tau_1 = 5 \mu\text{s}$, *B2* (green dotted line) describes the lifetime component $\tau_2 = 28 \mu\text{s}$, while *B3* (blue dotted line) is assigned to the component with lifetime of $240 \mu\text{s}$.

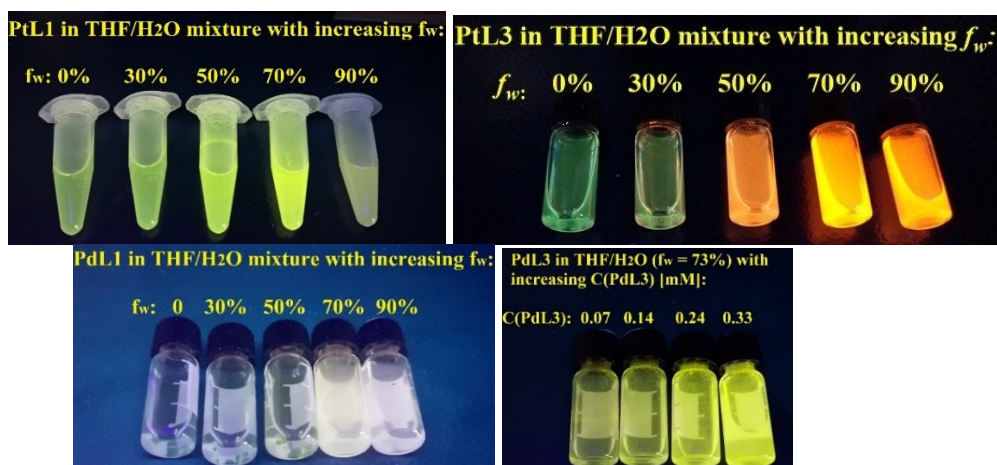


Figure S101. Pt(II)- and Pd(II)-complexes in THF/H₂O mixtures with different water fractions f_w . Top left: **PtLH** complex in THF/H₂O mixtures with water fractions f_w of 0, 30%, 50%, 70%, 90%. Top right: **PtLF** complex in THF/H₂O mixtures with different water fraction f_w of 0, 30%, 50%, 70%, 90%. Bottom left: **PdLH** complex in THF/H₂O mixtures with water fraction f_w of 0, 30%, 50%, 70%, 90%. Bottom right: **PdLF** complex in THF/H₂O ($f_w = 73%$) with various **PdLF** concentration of 0.07 mM, 0.14 mM, 0.24 mM and 0.33 mM. The sample pictures were taken under 365 nm UV lamp illumination under air saturation.

S6.6 Stern-Volmer studies of PSNPs loaded with complexes

Table S21. Stern-Volmer constant (K_{SV}) and quenching rate constant (K_q) values of PS(**PtLF**-series) ($K_q = K_{SV} / \tau_{max}$).

| Loading concentration | K_{SV} [hPa ⁻¹] | | K_q [hPa ⁻¹ s ⁻¹] | |
|-----------------------|-------------------------------|-------------------------|--|----------------------|
| | Emission-based K_{SV} | Lifetime-based K_{SV} | Emission-based K_q | Lifetime-based K_q |
| $c_L = 0.1$ mM | 0.0039 ± 0.0004 | 0.0026 ± 0.0003 | 250 ± 30 | 166 ± 19 |
| $c_L = 0.25$ mM | 0.0022 ± 0.0004 | 0.0025 ± 0.0003 | 150 ± 30 | 170 ± 20 |
| $c_L = 0.5$ mM | 0.0032 ± 0.0004 | 0.0026 ± 0.0003 | 210 ± 30 | 170 ± 20 |
| $c_L = 1.0$ mM | 0.0030 ± 0.0004 | 0.0026 ± 0.0003 | 210 ± 30 | 180 ± 20 |
| $c_L = 2.0$ mM | 0.0030 ± 0.0004 | 0.0026 ± 0.0003 | 210 ± 30 | 180 ± 20 |

Table S22. Stern-Volmer constant (K_{SV}) and quenching rate constant (K_q) values of PS(**PtLH**-series) ($K_q = K_{SV} / \tau_{max}$).

| Samples | K_{SV} [hPa ⁻¹] | | K_q [hPa ⁻¹ s ⁻¹] | |
|----------------|-------------------------------|-------------------------|--|----------------------|
| | Emission-based K_{SV} | Lifetime-based K_{SV} | Emission-based K_q | Lifetime-based K_q |
| $c_L = 0.1$ mM | 0.0028 ± 0.0004 | 0.0021 ± 0.0003 | 220 ± 30 | 170 ± 20 |
| $c_L = 0.5$ mM | 0.0029 ± 0.0004 | 0.0021 ± 0.0003 | 230 ± 30 | 160 ± 20 |
| $c_L = 1.0$ mM | 0.0029 ± 0.0004 | 0.0023 ± 0.0003 | 230 ± 30 | 180 ± 20 |
| $c_L = 2.0$ mM | 0.0026 ± 0.0004 | 0.0021 ± 0.0003 | 220 ± 30 | 170 ± 30 |

To explore the oxygen response of the Pd(II) complexes loaded into PS nanoparticles, we completed the Stern-Volmer studies of PS(**PdLH**-series) and PS(**PdLF**-series). It was noticed that the Stern-Volmer plots of both complexes cannot be simply described with a linear fit, especially with high loading concentration. This is due to the multi-exponential contribution for each complex, which demonstrates different responses to oxygen. According to the luminescence decay curves of Pd(II) complexes dissolved in THF, the lifetimes were fitted triexponentially. Different lifetime components might demonstrate various oxygen responses, thus the overall Stern-Volmer plots could be dominated by different components in various oxygen partial pressure ranges. On the other hand, with increasing complex loading concentration c_L , aggregates are formed in the PS nanoparticles. This might lead to different quenching sites with various oxygen accessibilities in the nanomatrices.¹⁴ Despite these influencing factors, we fitted the Stern-Volmer plots of

both PS(**PdLH**-series) and PS(**PdLF**-series) with two linear sections, aiming to exploiting more dynamic quenching information of the systems.

For PS(**PdLH**-series), regardless ACQ, no spectral change was observed, and the lifetimes showed independence on c_L or aggregation, indicating similar optical properties to the **PdLH** monomer. As a result, the K_{SV} and K_q of **PdLH** showed basically bare dependence on the c_L and aggregation (Table S23). On the contrary, in terms of PS(**PdLF**-series), Stern-Volmer plots showed significant difference with increasing c_L . With lower c_L , e.g. PS(**PdLF**-0.5 mM), monitoring oxygen partial pressure from 0.1 hPa to 201.0 hPa, oxygen response can be achieved by emission intensity and lifetime, as shown in Figure S102 a) and inset in c). Stern-Volmer plots based on I_{475} (or τ_{475}) and I_{530} (and τ_{530}) have essentially the same K_{SV} and K_q value, as shown in Figure S102 b) and c). Nevertheless, for PS(**PdLF**-4.0 mM), when increasing the pO_2 from 0.1 hPa to 187.0 hPa, the Stern-Volmer plots based on I_{480} (or τ_{480}) and I_{530} (and τ_{530}) differ clearly from each other (Figure S102 d), e), f) and inset). The K_{SV} values derived from I_{530} (or τ_{530}) showed a high tendency to decrease with increasing c_L (Table S24). This can be probably explained by the increased contribution of the **PdLF** aggregate state, which possesses lower oxygen sensitivity, demonstrating again that the emission band at around 530 nm is supported by both monomeric and aggregated states. Moreover, the K_{SV} values of the second section derived from $I_{475/480}$ (or $\tau_{475/480}$) becomes smaller. Possibly, one or more oxygen-sensitive components of monomeric **PdLF** are influenced by formation of the aggregates.

Table S23. Stern-Volmer constant (K_{SV}) and quenching rate constant (K_q) values of PS(**PdLH**-series).

| Loading concentration | λ_{em} [nm] | Emission-based K_{SV} [hpa ⁻¹] | Lifetime-based K_{SV} [hpa ⁻¹] | | K_q [hpa ⁻¹ s ⁻¹] | |
|-----------------------|---------------------|--|--|-----------------|--|-----------|
| | | | Section 1 | Section 2 | Section 1 | Section 2 |
| $c_L = 0.1$ mM | 488 | 0.0166 ± 0.0009 | 0.031 ± 0.003 | 0.0173 ± 0.0006 | 270 ± 20 | 153 ± 5 |
| $c_L = 0.5$ mM | 488 | 0.0190 ± 0.0006 | 0.029 ± 0.003 | 0.0182 ± 0.0013 | 250 ± 20 | 161 ± 11 |
| | 520 | 0.0186 ± 0.0006 | 0.030 ± 0.002 | 0.014 ± 0.002 | 258 ± 10 | 120 ± 20 |
| $c_L = 1.0$ mM | 488 | 0.0176 ± 0.0004 | 0.0301 ± 0.0018 | 0.0168 ± 0.0008 | 253 ± 10 | 141 ± 7 |
| | 520 | 0.0174 ± 0.0003 | 0.030 ± 0.002 | 0.0166 ± 0.0005 | 270 ± 20 | 147 ± 4 |
| $c_L = 2.0$ mM | 488 | 0.0183 ± 0.0004 | 0.030 ± 0.003 | 0.0171 ± 0.0006 | 250 ± 20 | 144 ± 5 |
| | 520 | 0.0182 ± 0.0004 | 0.0279 ± 0.0019 | 0.0175 ± 0.0003 | 240 ± 20 | 151 ± 3 |
| $c_L = 3.0$ mM | 488 | 0.0168 ± 0.0011 | 0.032 ± 0.002 | 0.0169 ± 0.0012 | 270 ± 20 | 140 ± 10 |
| | 520 | 0.0164 ± 0.0010 | 0.0299 ± 0.0015 | 0.0153 ± 0.0004 | 262 ± 10 | 134 ± 4 |
| $c_L = 4.0$ mM | 488 | 0.0135 ± 0.0006 | 0.032 ± 0.002 | 0.0175 ± 0.0004 | 290 ± 20 | 162 ± 4 |
| | 520 | 0.0132 ± 0.0006 | 0.0267 ± 0.0015 | 0.0148 ± 0.0006 | 250 ± 10 | 139 ± 6 |

Table S24. Stern-Volmer constant (K_{SV}) and quenching rate constant (K_q) values of PS(**PdLF**-series).

| Loading concentration | λ_{em} [nm] | Emission-based K_{SV} [hpa ⁻¹] | | Lifetime-based K_{SV} [hpa ⁻¹] | | K_q [hpa ⁻¹ s ⁻¹] | |
|-----------------------|---------------------|--|-----------------|--|-----------------|--|-----------|
| | | Section 1 | Section 2 | Section 1 | Section 2 | Section 1 | Section 2 |
| $c_L = 0.1$ mM | 475 | 0.0068 ± 0.0003 | 0.0022 ± 0.0002 | 0.0191 ± 0.0007 | 0.0121 ± 0.0011 | 224 ± 8 | 142 ± 13 |
| | 510 | 0.0120 ± 0.0003 | 0.0044 ± 0.0004 | 0.0240 ± 0.0008 | 0.0131 ± 0.0004 | 266 ± 9 | 145 ± 4 |
| $c_L = 0.5$ mM | 475 | 0.0101 ± 0.0015 | 0.0060 ± 0.0003 | 0.0153 ± 0.0005 | 0.0125 ± 0.0014 | 196 ± 6 | 160 ± 18 |
| | 530 | 0.0106 ± 0.0010 | 0.0062 ± 0.0002 | 0.0168 ± 0.0019 | 0.0124 ± 0.0007 | 190 ± 20 | 143 ± 8 |
| $c_L = 1.0$ mM | 480 | 0.011 ± 0.002 | 0.0044 ± 0.0003 | 0.022 ± 0.002 | 0.0127 ± 0.0005 | 310 ± 30 | 180 ± 7 |
| | 530 | 0.009 ± 0.002 | 0.0036 ± 0.0002 | 0.0211 ± 0.0014 | 0.0061 ± 0.0007 | 276 ± 18 | 80 ± 9 |
| $c_L = 2.0$ mM | 480 | 0.0105 ± 0.0005 | 0.0049 ± 0.0003 | 0.0171 ± 0.0003 | 0.0083 ± 0.0007 | 279 ± 5 | 135 ± 11 |
| | 530 | 0.0094 ± 0.0007 | 0.0029 ± 0.0001 | 0.0090 ± 0.0011 | 0.0029 ± 0.0001 | 134 ± 16 | 43 ± 2 |
| $c_L = 3.0$ mM | 475 | 0.0083 ± 0.0005 | 0.0015 ± 0.0003 | 0.0174 ± 0.0016 | 0.0046 ± 0.0003 | 360 ± 30 | 96 ± 6 |
| | 530 | 0.0065 ± 0.0009 | 0.0008 ± 0.0003 | 0.0076 ± 0.0003 | 0.0006 ± 0.0004 | 121 ± 5 | 9 ± 6 |
| $c_L = 4.0$ mM | 480 | 0.0056 ± 0.0010 | 0.0019 ± 0.0003 | 0.0143 ± 0.0017 | 0.0049 ± 0.0005 | 320 ± 40 | 109 ± 11 |
| | 530 | 0.0034 ± 0.0009 | 0.0012 ± 0.0007 | 0.0041 ± 0.0004 | 0.0014 ± 0.0002 | 81 ± 8 | 28 ± 4 |

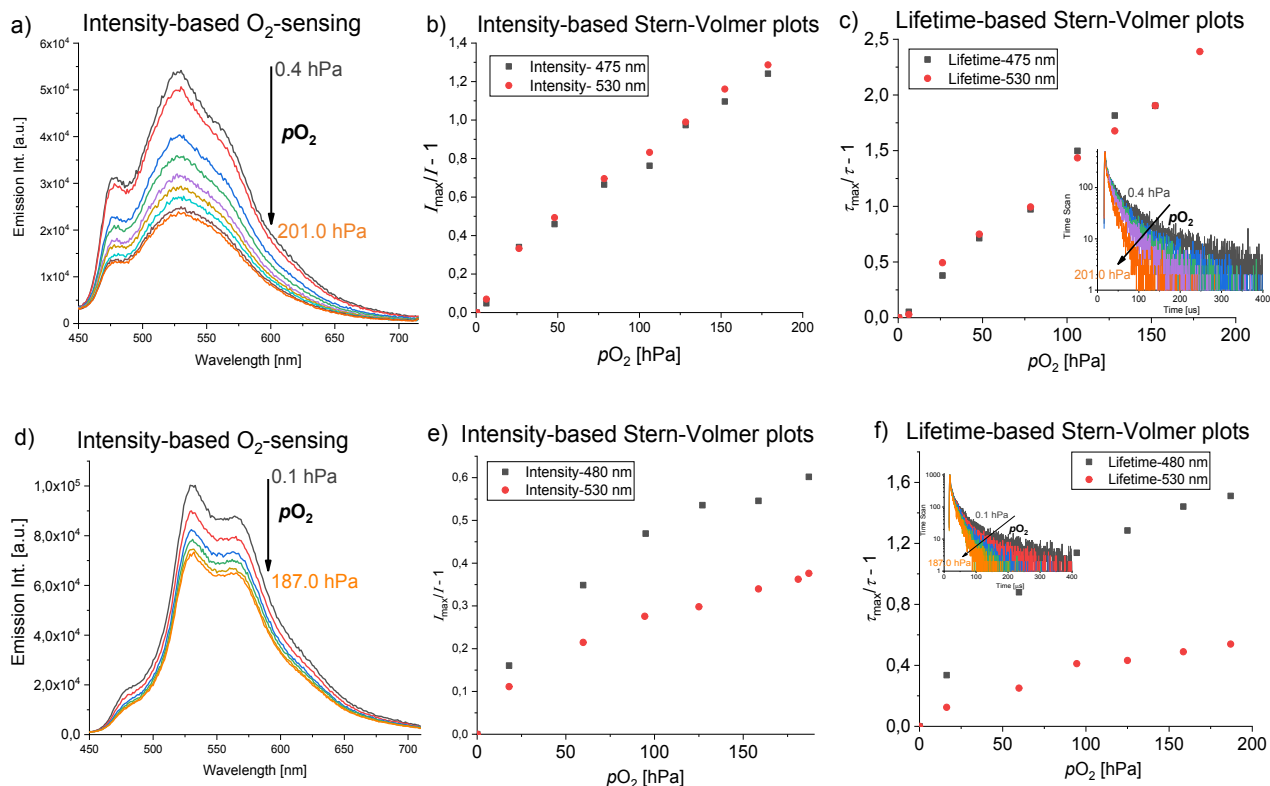


Figure S102. Stern-Volmer analysis of PS(PdLF-0.5 mM) and PS(PdLF-4.0 mM). a) Emission intensity of PS(PdLF-0.5 mM) at different oxygen partial pressures. b) Emission intensity (I_{475} and I_{530})-based Stern-Volmer plots. c) Lifetime (τ_{475} and τ_{530})-based Stern-Volmer plots; inset: lifetime (τ_{475}) at different oxygen partial pressures. d) Emission intensity of PS(PdLF-4.0 mM) at different oxygen partial pressures. e) Emission intensity (I_{480} and I_{530})-based Stern-Volmer plots. f) Lifetime (τ_{480} and τ_{530})-based Stern-Volmer plots; inset: lifetime (τ_{480}) at different oxygen partial pressures.

References

- 1 Saint+, Bruker AXS INC., 6.02, (includes Xprep Sadabs).
- 2 G. M. Sheldrick, *SADABS*, Univ. Göttingen, Ger. 1996.
- 3 G. M. Sheldrick, *SHELXL-97 SHELXL-2013*, *Progr. Refinement Struct. Univ. Göttingen, Ger.*
- 4 G. M. Sheldrick, *Acta Crystallogr. Sect. C Struct. Chem.*, 2015, **71**, 3–8.
- 5 G. A. et al. Frisch, M. J.; Trucks, G. W.; Schlegel, H. B.; Scuseria, G. E.; Robb, M. A.; Cheeseman, J. R.; Scalmani, G.; Barone, V.; Mennucci, B.; Petersson, *Gaussian Inc. Wallingford CT.*
- 6 C. Adamo and V. Barone, *J. Chem. Phys.*, 1999, **110**, 6158–6170.
- 7 S. Grimme, S. Ehrlich and L. Goerigk, *J. Comput. Chem.*, 2011, **32**, 1456–1465.
- 8 D. Andrae, U. Häußermann, M. Dolg, H. Stoll and H. Preuß, *Theor. Chim. Acta*, 1990, **77**, 123–141.
- 9 T. H. Dunning Jr. and P. J. Hay, *Modern Theoretical Chemistry*, vol. 3, Plenum, New York, 1977.
- 10 V. Barone, J. Bloino and M. Biczysko, *MRS Bull.*, 2013, **37**, 1–20.
- 11 V. Barone, J. Bloino, M. Biczysko and F. Santoro, *J. Chem. Theory Comput.*, 2009, **5**, 540–554.
- 12 J. Tomasi, B. Mennucci and R. Cammi, *Chem. Rev.*, 2005, **105**, 2999–3094.
- 13 A. K. Rappe, C. J. Casewit, K. S. Colwell, W. A. Goddard and W. M. Skiff, *J. Am. Chem. Soc.*, 1992, **114**, 10024–10035.
- 14 M. H. Gehlen, *J. Photochem. Photobiol. C Photochem. Rev.*, 2020, **42**, 100338.